DESIGN OF A MAGNETICALLY TUNED VIBRATION ABSORBER

A THESIS SUBMITTED TO
THE GRADUATE SCHOOL OF NATURAL AND APPLIED SCIENCES
OF
MIDDLE EAST TECHNICAL UNIVERSITY

BY

HALIT ERDEM NAKKAŞ

IN PARTIAL FULFILLMENT OF THE REQUIREMENTS
FOR
THE DEGREE OF MASTER OF SCIENCE
IN
MECHANICAL ENGINEERING

NOVEMBER 2019

Approval of the thesis:

DESIGN OF A MAGNETICALLY TUNED VIBRATION ABSORBER

submitted by **HALIT ERDEM NAKKAŞ** in partial fulfillment of the requirements for the degree of **Master of Science in Mechanical Engineering Department, Middle East Technical University** by,

Prof. Dr. Halil Kalıpçılar
Dean, Graduate School of **Natural and Applied Sciences**   _____

Prof. Dr. M.A. Sahir Arıkan
Head of Department, **Mechanical Engineering**   _____

Assist. Prof. Dr. Gökhan O. Özgen
Supervisor, **Mechanical Engineering, METU**   _____

Examining Committee Members:

Assoc. Prof. Dr. M. Bülent Özer
Mechanical Engineering, METU   _____

Assist. Prof. Dr. Gökhan O. Özgen
Mechanical Engineering, METU   _____

Prof. Dr. Ender Ciğeroğlu
Mechanical Engineering, METU   _____

Assoc. Prof. Dr. Yiğit Yazıcıoğlu
Mechanical Engineering, METU   _____

Assoc. Prof. Dr. S. Çağlar Başlamışlı
Mechanical Engineering, Hacettepe University   _____

Date: 28.11.2019

I hereby declare that all information in this document has been obtained and presented in accordance with academic rules and ethical conduct. I also declare that, as required by these rules and conduct, I have fully cited and referenced all material and results that are not original to this work.

Name, Surname: Halit Erdem Nakkaş

Signature:

ABSTRACT

DESIGN OF A MAGNETICALLY TUNED VIBRATION ABSORBER

Nakkaş, Halit Erdem
Master of Science, Mechanical Engineering
Supervisor: Assist. Prof. Dr. Gökhan O. Özgen

November 2019, 132 pages

In this thesis, a TVA is designed, manufactured and validated experimentally. The TVA uses eddy current effect as the damping mechanism with adjustable damping through changing distance between magnets and the conductors. In order to tune the damping level of the absorber to the desired range, magnetic analyzes are conducted and selection of conductor and magnets are made accordingly. Physical design of the TVA consists of a mass element, a spring element and a damping element. Compression helical spring is used as a spring element. A design procedure is developed and demonstrated for the spring that will satisfy the design criteria of the TVA. A procedure to estimate the fatigue life the spring element was also developed and demonstrated. Structural design of the TVA is done such that the natural frequency of the structural assembly should larger compared to tuning frequency of the vibration absorber. Modal analyses are conducted to ensure that. Finally, absorber parameters are extracted through vibration experiments validating the final design.

Keywords: Tuned vibration absorber, eddy current damping, vibration control, spring design, design for fatigue

ÖZ

MANYETİK SÖNÜMLÜ AYARLI KÜTLE SÖNÜMLEYİCİSİ TASARIMI

Nakkaş, Halit Erdem
Yüksek Lisans, Makina Mühendisliği
Tez Danışmanı: Dr. Öğr. Üyesi Gökhan O. Özgen

Kasım 2019, 132 sayfa

Bu tezde, bir ayarlı kütle sönümleyici tasarlanmış üretilmiş ve testler ile doğrulanmıştır. Tasarlanan sönümleyici, sönümleme mekanizması olarak girdap akımı efektini kullanmaktadır ve sönüm miktarı mıknatıslar ve karşı iletken malzemesi arasındaki mesafe değiştirilerek ayarlanabilmektedir. Sönümleyici seviyesinin istenen aralıkta olmasını sağlamak için çeşitli manyetik analizler yapılmış, mıknatıs ve karşı iletken malzeme seçimi yapılmıştır. Ayarlı kütle sönümleyici, kütle, yay ve sönüm elemanından oluşmaktadır. Yay elemanı olarak helisal baskı yayı kullanılmıştır. Sönümleyicinin tasarım kriterini karşılayacak yay için bir tasarım prosedür geliştirilmiş ve bir örnek üzerinden gösterilmiştir. Yay elemanın ömrünü tahmin etmeye yönelik bir prosedür verilmiştir ve bir örnek üzerinden gösterimiştir. Sönümleyicinin yapısal tasarımı, sönümleyicinin doğal frekansının, ayarlanmış frekansına kıyasla daha büyük olacak şekilde yapılmıştır. Son olarak, tasarımı doğrulamak için modal analiz yapılmış ve nihai tasarımı doğrulayan sönümleyici parametereleri elde edilmiştir.

Anahtar Kelimeler: Ayarlı kütle sönümleyici, girdap akım sönümü, titreşim kontrol, ömür için tasarım

To my family

ACKNOWLEDGEMENTS

TABLE OF CONTENTS

LIST OF TABLES

LIST OF FIGURES

FIGURES

xvi

xvii

LIST OF ABBREVIATIONS

ABBREVIATIONS

DOF	: Degree of freedom
FEA	: Finite element analysis
FRF	: Frequency response function
PSD	: Power spectral density
RMS	: Root mean square
SDOF	: Single degree of freedom
SMD	: Single mass damper
TVA	: Tuned vibration absorber
VEM	: Viscoelastic material

LIST OF SYMBOLS

SYMBOLS

α	: Helix angle of spring
α	: Buckling constant of spring
σ	: Conductivity
τ	: Shear stress
ξ	: Damping ratio
ω	: Frequency
μ	: Mass ratio
ρ	: Resistivity
δ_{max}	: Maximum compression length of spring
ω_n	: Natural frequency
ω_d	: Damped natural frequency
A(ω)	: Accelerance
B	: Magnetic flux density
c	: Damping coefficient
C	: Spring index
C_c	: Clash clearance
d	: Wire diameter of spring
D	Nominal diameter of spring
D_f	: Maximum outer diameter of spring
D_i	: Inner diameter of spring
D_o	: Outer dimeter of spring
$D_{O\,solid}$	: Maximum outer diameter of spring
E	: Young modulus
E[D]	: Expected damage
f_n	: Natural frequency

g	: Acceleration of gravity
G	: Shear modulus
$G(f)_{PSD}^{Input}$	: Input psd
$G(f)_{PSD}^{Response}$	: Stress output psd
H(ω)	: Transfer function
J	: Current density
k	: Stiffness
k	: Correction Coefficient
K_S	: Stress factor
K_w	: Stress concentration factor
L_b	: Buckling length of spring
L_f	: Free length of spring
L_s	: Solid length of spring
m	: Mass
m_n	: m th spectral moment
N_a	: Number of active coils
N_T	: Number of total coils
p	: Pitch of spring
$p(S)$	: Probability density function
Y (ω)	: Mobility
v	: Velocity

CHAPTER 1

INTRODUCTION

Tuned vibration absorber (TVA) is a device that can used to reduce vibrations of the main structure to which it is attached. TVA is a single degree of freedom system and consists of mass, damping element and stiffness element.

Design of a TVA consists of several steps: definition of problem, specifying working conditions and environmental conditions, conceptual design, detailed design and validation. The first step is to define the vibration problem of main structure (i.e. forced vibration problem, resonant vibration problem, excitation, structure of interest). After vibration problem is defined, the expected TVA performance should be specified. In the other words, main goal of TVA should be specified, i.e., 80% reduction in response amplitude of main structure at a particular frequency (resonance or forcing frequency). This expected vibration reduction performance affects tuning parameters of TVA, which are basically tuning frequency, TVA mass and damping. TVA parameters must be determined carefully and it depends on modal parameters of main structure, attachment point of TVA, desired performance of the TVA, forcing acting on the structure, etc.

The next step is definition of working conditions of the TVA. For example, if the main structure is a tank barrel, TVA is exposed sun, dust, pyro shocks, etc. If the main structure is a building, probably TVA is indoor and working conditions is different from previous example. These conditions affect to selection and design of TVA structural elements.

The other step is selection of element types. A TVA consists of mass, spring element and damping element. These elements should be selected so that vibration reduction performance requirements are satisfied under the specified working conditions. Working conditions may change the design and selection TVA main elements. If TVA should work properly between -40°C and +70°C, damping element can also work this temperature range.

After element types are selected, overall conceptual design alternatives should be developed, which can potentially satisfy both determined tuning parameters of the TVA and environmental requirements. Among these design alternatives, the best alternative design should be selected to satisfy the TVA design requirements.

After best conceptual design is selected, detailed design should be completed. All dimension, shapes, type of parts etc. should be decided at the end detailed design process. Usually a prototype TVA is also fabricated at the end of this step.

The last step is to validate TVA performance and requirements. Tuning frequency of TVA is directly related to its performance which means it should be checked experimentally. Another important point is TVA damping level because vibration energy is consumed by damping element. Both vibration displacement and shock displacement depend on damping level. Equivalent stress or strain, fatigue life etc. should ideally be also checked after design to ensure TVA works properly.

A design process for a TVA is described above briefly but this thesis does not consist of all stages of such a design process. This thesis focuses on detailed mechanical design of a TVA with already determined values of tuning frequency. Fatigue life estimation of TVA spring element and simulation-based design and estimation of

magnetic damping of an eddy current based damping system are main contributions of this thesis work along with original structural design of a passive TVA. The tuning parameters and the vibration problem definition of the TVA design task are taken from a previous master's thesis work by Büyükcivelek [1]. Büyükcivelek dealt with a vibration control problem battle tank gun barrel. The vibration problem was identified through actual operational vibration measurements and the thesis work presents work which includes simulation-based determination of optimum TVA parameter to address the vibration reduction problem. Büyükcivelek's study consists of calculation of effective mass, and stiffness and damping of TVA. A detailed design, a physical prototype of the TVA that provides the determined effective TVA parameters, fatigue life-based analysis and design of the TVA are topics that were not covered in Büyükcivelek's work. This thesis work actually addresses those issues so it can be considered as the continuation of Büyükcivelek's work. While doing this, approaches for detailed design of a TVA and eddy current damping mechanism are also developed and presented in this thesis.

The main aim of this thesis is to design a passive TVA with adjustable eddy current damping considering fatigue life and shock loading capability. A design procedure of helical compression spring used in the proposed TVA is developed both taking into stiffness value and maximum displacement of effective mass of the TVA. Actual TVA effective parameters are also experimentally identified using a physical prototype and vibration measurements which validates the design thus the developed analysis-based design procedures for the spring element and the eddy current based damping mechanism of the TVA.

Chapter 2 of the thesis is the literature survey and it starts first about information about TVAs. This is followed by design alternatives according to spring element and damping elements used in TVAs are also given. Previous works that deal with eddy

current damping with their magnet and conductor size and achieved damping levels are also given in this chapter.

Chapter 3 of the thesis presents the mechanical design work conducted for the TVA of interest. Target stiffness value and vibration and shock are considered for design of helical spring. After that natural frequency and life of the spring is studied. Damping of the TVA comes from an eddy current based mechanism which consists of magnets and copper plates. Design and selection of them is done using magnetic analysis-based estimation of damping level of the eddy current damping system. Finally, design of TVA mass, its linear motion parts and TVA body are detailed.

Chapter 4 of the thesis presents experimental characterization of the physical prototype of the TVA. Tuning frequency and damping level of the TVA is estimated using measured frequency response functions of the TVA as a standalone single degree of freedom system. Natural frequency, which corresponds to the tuning frequency of the TVA, is extracted for various magnet and conductor placement configurations. Estimated and experimental eddy current damping level is compared. Specification of realized TVA is also given here.

In Chapter 5 the conclusions of the thesis work is summarized. Potential working opportunity is given in the last part.

CHAPTER 2

LITERATURE SURVEY

2.1. Tuned Vibration Absorbers

Tuned vibration absorber (TVA) is a device which is used for reducing the vibrations of the structure to which it is attached. It is used for reducing the vibration level at or around a specific resonant frequency or specific forcing frequency. TVAs can be categorized three main groups according to energy consumption: passive TVA, active TVA and semi-active TVA. There are also hybrid TVAs and multiple TVAs.

For passive TVA, its properties, mass, stiffness and damping ratio, are constant so its tuning frequency and damping level are stationary. TVA is added to main structure to reduce its vibration at only one resonant frequency or specific forcing frequency (which corresponds to the tuning frequency of the TVA). If main structure properties and environmental conditions do not change them, TVA performance will be constant. It works effectively only in a narrow frequency bandwidth. When TVA is not tuned correctly, it may increase main structure vibration.

To reduce more than one frequency, adaptive TVA has been developed. Main idea of adaptive TVA is to change to TVA parameters via changing generally its stiffness or/and damping ratio and rarely its mass to adopt to tune the TVA.

In active TVAs, active forces are applied to the main structure to reduce vibration, so external energy consumption is required. In this system, sensors, actuator, electronic

system, control algorithm are other requirements. Multiple TVA is a combination of two and more passive TVAs. Each passive TVA is added to main structure for different resonant frequency or a forcing frequency, so vibration reduction is achieved for more than one frequency or broader frequency range. When modes of structure are well separated, more than one passive TVA can be used to reduce main structure vibration at different resonance frequencies. For instance, five cantilever beams with different cross section area and length have five different natural frequencies so they can be used as multiple TVA. Hybrid TVA is a combination of an active and passive TVA. The scope of this thesis is related only passive TVA so detail information about others is not given.

Some commercial passive TVAs and their properties are given in Table 2.1. Frahm's patent[2], "Device for Damping Vibrations of Bodies" is the first known TVA. Den Hartog [3] developed a method that calculate tuning parameters of TVA for harmonic excitation. There are also a lot of studies deal with TVA parameters in the literature. These studies generally focus on finding tuning parameters or how to change them for discrete systems ([4–6]).

In the literature TVA has been described using various terms which are given as follows:

- Tuned Vibration Absorber [7]
- Mass Spring Damper [8]
- Dynamic Vibration Absorber [9]
- Tuned Mass Damper [10]
- Smart Vibration Absorber [11]

Table 2.1. Some commercial TVAs and their properties

Company	Type	Damping Mech.	Tuning Freq. [Hz]	TVA Mass	Orientation**	Main Structure
Moog–CSA ([12, 13])	SMD	Eddy Current	9-200	0.23-0.95 kg	V / H	General purpose
Deicon [14]	VEM	VEM	7	45 kg	V	Floor
Deicon [15]	SMD	Viscous	6-9	-	V	Balcony
Flow Eng. [16]	SMD	-		3000 kg	H	Windseeker
Fujita [17]	SMD	-	2.7	280 kg	V	Floor
Gerb [18]	SMD	-	0.8-2.2	58X 1000-2500	V / H	Millennium Bridge
Gerb [18]	Pendulum	-	0.8-2.0	11X5000	H	Burj Al Arab Hotel
Maurer Söhne ([19, 20])	SMD	MR Damper	2.7	1660	V	Bridge
Maurer Söhne ([19, 20])	SMD	-	1.159	1900	H	Bridge
Maurer Söhne ([19, 20])	Pendulum	Friction & viscous	0.45	2100	H	Power Plant Chimney
Vibratec [21]	SMD	Viscous damper	1.85	340	V	Bridge

* SMD : Single mass damper **V: Vertical, H: Horizontal

In this study, it is used as defined as Tuned Vibration Absorber or in abbreviated form TVA. TVA is a discrete device which is added the main structure to reduce its vibration level at or around a specific frequency. Figure 2.1 shows FRF of a 3 degree of freedom (DOF) system with and without a TVA. As it can be seen, total number of DOFs is increased when TVA is added. Target frequency in this example is about 78 Hz. and there is a peak at that frequency. When a properly tuned TVA is added, this peak disappears and emerges two new peaks. One of them is right side of disappeared one and the other is left side of it so vibration at 78 Hz. is reduced.
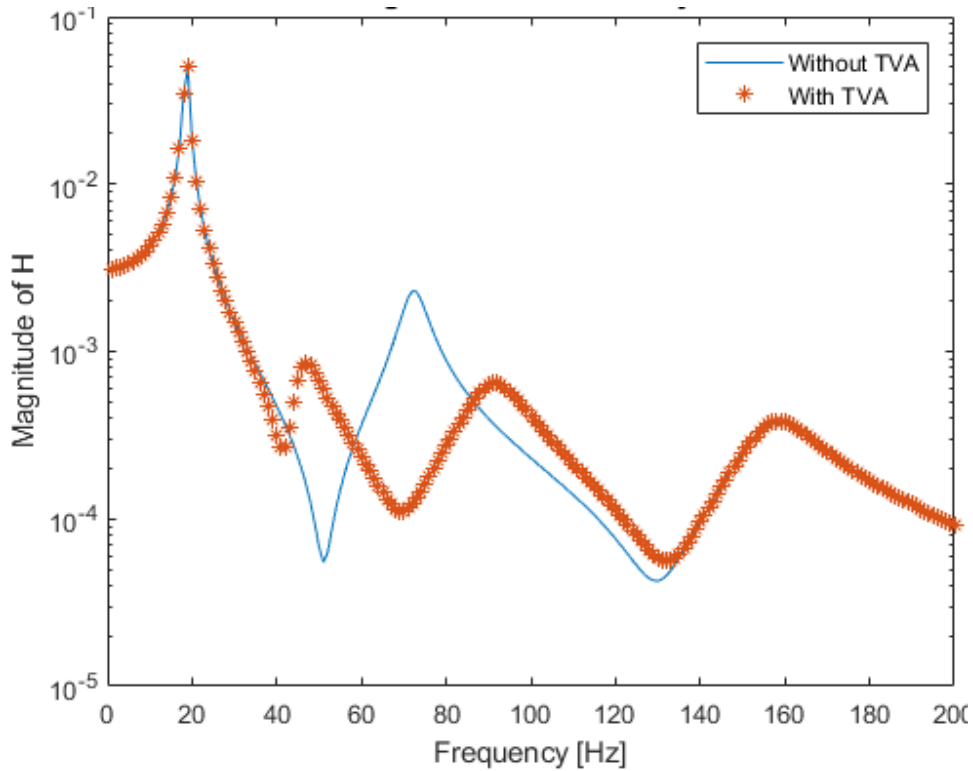
Figure 2.1. Driving point FRF of the main structure with and without TVA

Tuning of a TVA depends on main structure troublesome mode parameters and type of excitation. The scope of this thesis does not consist of specifying TVA parameters. When a TVA is not correctly tuned, performance of TVA decreases. This device works effectively when resonance frequency is constant and TVA is tuned correctly.

In Figure 2.2, both TVA and main structure are shown as single dof system, where m_2, k_2, c_2 refers mass, stiffness and damping of TVA and m_1, k_1, c_1 refers mass, stiffness and damping of main structure. TVA should not change main structure natural frequency, so mass of TVA is crucial, mass ratio of TVA is defined as given in Equation 2.1.

8
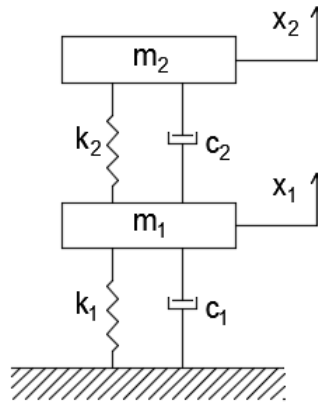
Figure 2.2. A two dof system

$$\mu = \frac{m_2}{m_1}$$
Equation 2.1

Specifying TVA mass is a trial-error process, any formulation could not be found in literature for continuous system, but generally μ is taken about 0.05 for discrete system.

Den Hartog[3] proposed a tuning criteria for harmonic excitation. His criteria gives optimum tuning frequency and optimum damping ratio of TVA under harmonic excitation. Sadek [4] proposed a tuning method for discrete system under seismic loading. His method calculates optimum tuning frequency and damping ratio for known mass ratio. This study shown that the tuning criteria suppress main structure acceleration and displacement for different earthquake excitation. Leung & Zhang [22] developed an algorithm to reach optimum TVA parameters for viscously damped single DOF system. Tigli [23] prosed a closed form formulation to obtain optimum TVA parameter under random vibration for linear damped discrete system. TVA parameters were proposed to minimizing variance of the displacement, velocity and

acceleration of the main structure which main mass subjected white-noise excitation. There are also more studies [9, 24–28], deal with determining TVA parameters for discrete systems but they are not given here for simplicity.

An example of determination of optimum TVA parameters for continuous system is given in Büyükcivelek's study [1]. His objective is to reduce amplitude of tank barrel under random base excitation at fixed end of barrel and TVA is added to the free end of the barrel. Büyükcivelek found tip displacement and dominant frequency of barrel under random vibration and specified that troublesome frequency is the first resonance frequency of the barrel. Firstly, TVA mass was tried to determine for undamped case. To determine optimum mass, harmonic analysis and spectrum analysis were done for reducing tip displacement of the barrel. For different TVA masses ranging between 1kg and 30 kg, RMS displacement amplitude of barrel was found and given in Figure 2.3.
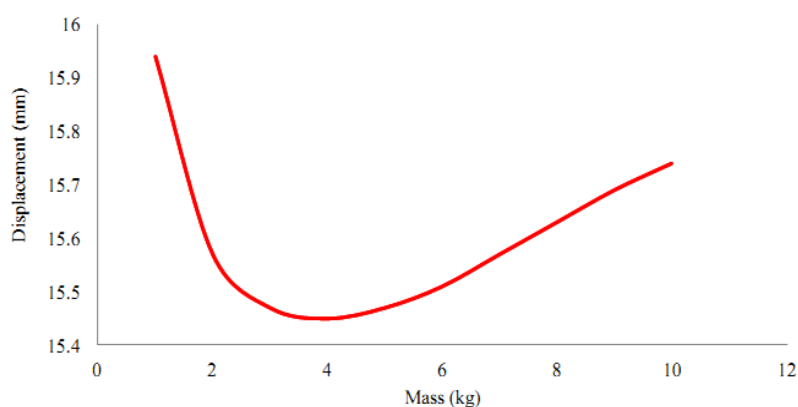
Figure 2.3. RMS displacement amplitude of barrel and TVA mass [1]

In Büyükcivelek's study [1], it was concluded that optimum TVA mass is 4kg. After finding the optimum value of the TVA mass, TVA displacement and response of the barrel was found for various damping ratios. Searching for the best tuning frequency

10

finally, optimum TVA parameters obtained in Büyükcivelek's study is given in Table 2.2. As mentioned in Chapter 1, his TVA parameters are used as target optimum TVA parameters in this thesis.

Table 2.2. Summary of optimum TVA parameters [1]

TVA Mass	4 kg
Tuning frequency	5.67 Hz
Spring stiffness	5070 N/m
Damping coefficient	284 Ns/m ($\xi = 1.0$)

2.2. Passive TVAs

This thesis study deals with detailed mechanical design of a passive TVA under operational conditions so information relevant to this type of TVA is presented in this section. According to how target stiffness, damping values of a TVA are realized, passive TVAs can be divided into four main groups as given in Figure 2.4 and Figure 2.5.

Helical spring TVA consists of a discrete mass, helical spring(s) and a damper. Many commercial products are in this category ([1], [2], [5], [8], and [29]). Both compression or extension spring can be used as a spring element. This type of TVA is a very simple device, TVA is a single DOF system, so its mass is supposed to move only one direction. A rod and a linear bearing are generally used for constraining motion of the TVA mass. Linear bearings are fixed on TVA mass and rods are passed through these linear ball bearing. Any damping element can be used such as dashpot, eddy current damper, wire rope, etc. This type of TVA is commonly used in buildings, bridges, towers, etc. ([20, 30]).

```
                        ┌─────────────┐
                        │ Passive TVA │
                        └──────┬──────┘
          ┌────────────┬───────┴───────┬────────────┐
    ┌───────────┐ ┌───────────┐ ┌───────────┐ ┌───────────┐
    │  Helical  │ │ Beam like │ │ Pendulum  │ │VEM-Rubber │
    │Spring TVA │ │   TVA     │ │   TVA     │ │ like TVA  │
    └───────────┘ └───────────┘ └───────────┘ └───────────┘
```
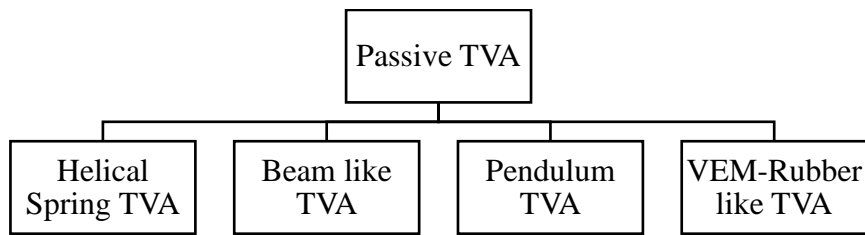
Figure 2.4. Type of passive TVA according to stiffness element used.

```
                        ┌─────────────┐
                        │ Passive TVA │
                        └──────┬──────┘
       ┌────────────┬──────────┴────────┬─────────────┐
┌────────────┐ ┌────────────┐ ┌────────────┐ ┌────────────┐
│Viscoelastic│ │            │ │            │ │            │
│  Material  │ │Eddy Current│ │            │ │            │
│(VEM)-Rubber│ │  Damping   │ │  Viscous   │ │Friction-base│
│    like    │ │            │ │            │ │            │
└────────────┘ └────────────┘ └────────────┘ └────────────┘
```
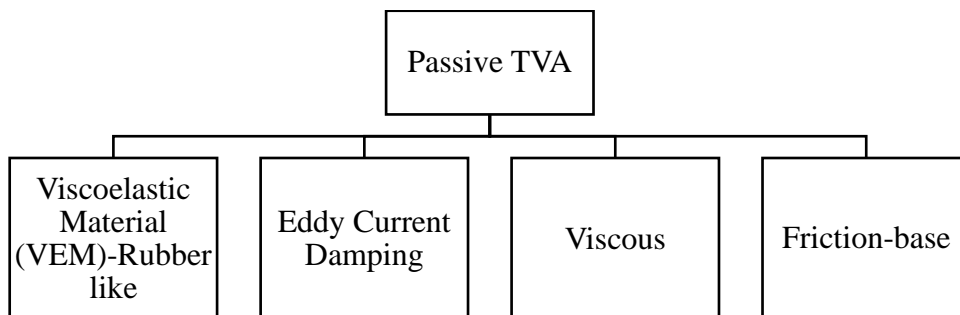
Figure 2.5. Type of passive TVA according to damping element used.

Beam-like TVA consists of a beam and rigid mass. Beam could be in vertical or horizontal direction ([17, 31–38]). Beam stiffness and damping depends on mass and location of it and boundary conditions, material and cross section of the beam. A fixed-fixed beam with attached mass can be given as an example. Natural frequency of this TVA can be altered by changing location of mass.

A pendulum can also be used as a TVA ([20, 39]). A pendulum TVA consists of a rod, string or rope, a mass, and a spherical hinge. Length of rod of the TVA changes natural frequency of the TVA. Mass is fixed at the end of the rod and it can move one or two directions. Due to direction of acceleration of gravity, this type of TVA can only be used for horizontal direction vibration.

12

In viscoelastic material (VEM) rubber-like TVA, viscoelastic material is used as both spring element and damping element. Advantages of this material is that its loss factor is higher than these of other materials, such as steel, aluminum. Main disadvantage of the viscoelastic material is that its modulus and loss factor are very sensitive to change of temperature, strain and frequency. Therefore, vibration level, working temperature and frequency range of this type TVA is narrow and dramatic change of one of them may lead to mistuning. As it can be seen in Figure 2.6, VEM material could be in tension or shear stress. Both stiffness and damping of the TVA rely on viscoelastic material.
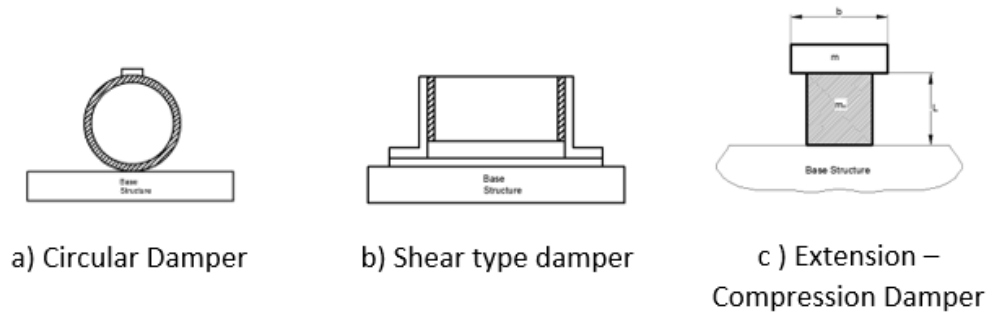
Figure 2.6. Different types of VEM type TVA adapted from [37]

Eddy current damping TVA obtains damping by eddy current effect (currents generated by permanent magnets moving relative to a conductor element). Interaction between a magnet and its conductive material provides damping force. Relative velocity between them is proportional to damping force. In this type of damping mechanism, there is no contact between them. Damping force changes linearly with velocity like viscous damping ([40–44]). Damping force depends also on magnet class, size, conductive material type and size and distance between them. Copper is usually used as the conductive material due to its low electrical resistivity. Further information, about eddy current damping is given next section.

In viscous based TVA, a commercial dashpot might be used as damping element [19]. Vibration energy is converted into heat which leads temperature of the dashpot increases as long as dashpot works.

Wire-rope and stock- bridge damper can be used as damping element in a TVA. A wire-rope consists of several twisted ropes. Damping force occurs due to friction between strands of these ropes. A wire rope has different stiffness in all direction so it can be used for in 3 directions but tuning frequency of the TVA will be different in each direction.

2.3. Damping Elements of TVA

This thesis deals with passive TVA so in this section only passive damping alternatives are considered. Structural damping in metals cannot be used as damping element in a TVA because it is lower than other options as seen in Figure 2.7.

First option is viscoelastic material, this type of material has more damping than other materials. As it can be seen in Figure 2.7, viscoelastic materials has more damping than structural alloys at the same strain levels. Main disadvantage of that material is that loss factor and modulus depends on both temperature and frequency. Its shape could be elastomeric mounts. But its main disadvantage is maximum displacement which is very limited. Elastomeric mounts properties, loss factor and stiffness, depends on temperature, static and dynamics strain so its properties are not stable.

A dashpot is other option and it can work push and/or pull way. Damping coefficient is adjustable and can be set before installation. Damping coefficient, stroke and maximum damping force are not constant and different configuration options of a

commercial product are available as given in Table 2.3. Damper force depends on fluid velocity. Damping force F could be from $F = CV^{0.4}$ to $F = CV^{1.8}$ where C is the viscous damping coefficient and V is relative piston velocity of the damper [45].
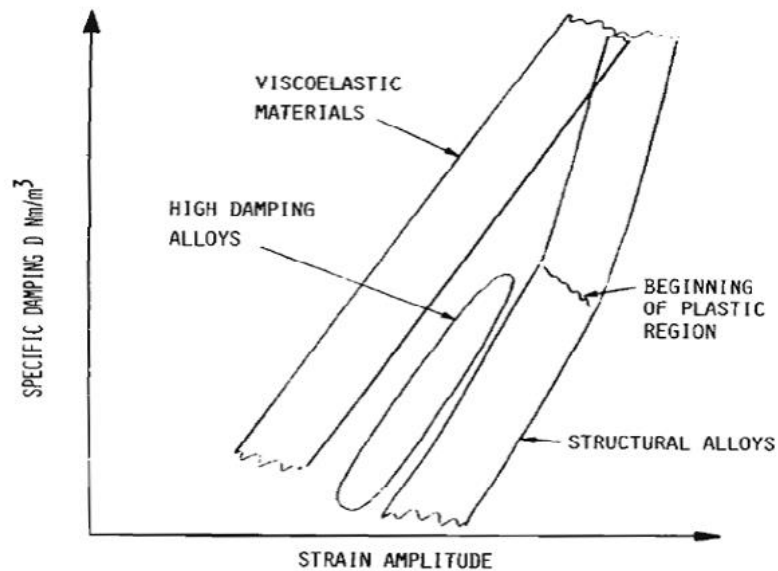
Figure 2.7. Damping versus strain for various materials [37]

Table 2.3. Some commercial hydraulic damper properties [45]

Model	Stroke [mm]	Extended Length [mm]	Max Compression Force [N]
Model I	25	90	800
Model II	50	140	800
Model III	75	190	800
Model VI	109	240	350
Model V	150	340	350

Another option is eddy current damper. Eddy current force occurs in opposite direction of motion when a conductive material moves in a magnetic field. There are several studies using eddy currents to control vibration. Schieber [46] offered a formulation to calculate breaking force of rectangular cross section magnet and conductor. Eddy

current force change linearly with change of velocity between magnet and copper plate. Eddy current damping coefficient is found by dividing eddy current force to velocity between magnet and conductor material. One of the earliest studies using eddy currents for vibration control by Cunningham [47] uses eddy current for reducing vibration of the cryogenic turbomachinery. Damping coefficient can be calculated with Equation 2.2 [47].

$$c = k \frac{B^2 v}{\rho}$$
<div align="right">Equation 2.2</div>

where B is magnetic flux density [Tesla, $\frac{N}{mA}$], v is volume of fields/conductor intersection, ρ is resistivity of conductor and k is dimensionless correction constant. v is volume of the conductor material immersed in the magnetic field and it is assumed that it is constant. Resistivity ρ is material properties of the conductor material and it is also assumed that it is constant. Correction coefficient k is unknown and it can be found experimental study. For this stage, it is assumed that it equals to one. Damping coefficient of TVA is directly related with magnetic flux density B. There are a lot of parameters effects magnetic flux density B. Some of them is given below.

- Magnet
  - Size
    - Cross Section
    - Thickness
  - Shape
  - Class
- Conductor Material
  - Size

- Cross Section
- Thickness
  - o Shape
  - o Resistivity
- Orientation of magnet and conductor material
- Distance between magnet and conductor material

Distribution of magnetic flux density is different for each problem and obtaining magnetic flux density of conductor material is a difficult problem. In the literature, researcher uses different methods to obtain it. Cunningham [47] measured magnetic flux density of C shape Alcino 5 with gaussmeter and calculated magnetic flux density with empirical formulation. There are some studies offered eddy current damping to vibration control that calculate damping level of the offered TVA analytically. Beek [48], Huang [49] and Tian [50] also tried to estimated damping level analytically. Sodano [43] used eddy current damping to reduce vibration of cantilever beam, where magnetic flux density was formulated and calculated numerically. Kienholz [51] used two dimensional boundary element method to obtain magnetic flux density. There are also several studies ([41, 42, 52–58]) that deal with eddy current damping without damping estimation even if damping coefficient is formulated in terms of magnetic flux density. They only measured damping level experimentally. Details of these studies, magnet size, conductor size and damping level of studies in literature are given in Table 2.4.

As it can be seen in Equation 2.2, when conductor resistivity decreases, damping coefficient increases. Resistivity of common metals are given in Table 2.5. Resistivity of copper and silver are lower than others. One of them can be used as a conductor.

Table 2.4. Summaries of studies dealing with eddy current damping

	Magnet Size	Conductive Material Size	Damping (Experimental)	Damping (Estimated)
Beek [48]	50x20x10	67.5x28x10	54.7 Ns/m	50.5 Ns/m
Sodano [59]	Ø12.7x12.7	Ø12.65x0.62	34* %	42* %
Bae [60]	Ø20x10	Ø27x500	11.021 kg/s	10.290 kg/s
He [50]	52x34x44	46x38x2	2228 Ns/m	2810 Ns/m
Huang [49]	40x40x20	260x120x5	20.8 Ns/m	21.4 Ns/m
Cheah [44]	Ø38.1x9.52	Ø23.1x12.7	5.5 Ns/m	7.9 Ns/m
Zhihao [61]	100×100×50	5x240x100	14.5 %	30.8 %
Pan [52]	Ø52x34	Ø52x5	86.3 Ns/m	-
Lian [53]	100X50X10	200x200x2	35.6 %	-
Shi [54]	40x20x5	180x110x2	7.46 %	-
Chen [56]	2.5x10x50	5x70x50	5.81 %	-
Guo [57]	Ø15x8.4	Ø18.5x60	2.5181 Ns/m	-
Ruber [58]	Ø12.7x12.7	Ø17x25	5.21 Ns/m	-
Ebrahimi [42]	Ø25x5	Ø25x12	28 %	-

* These values were read approximately from the graphic.

Table 2.5. Resistivity for common metals at room temperature [62]

Element	Resistivity [Ω.m]
Aluminum	2.82×10^{-8}
Copper	1.7×10^{-8}
Gold	2.44×10^{-8}
Iron	1.0×10^{-7}
Lead	2.2×10^{-7}
Mercury	9.8×10^{-7}
Platinum	1.1×10^{-7}
Silver	1.59×10^{-8}
Tungsten	5.6×10^{-8}

Eddy current damping has several advantages which are as follows:

- There is no contact surface for damping.
- Damping force does not depend on temperature.
- Damping force does not cause temperature change during operation.

The main disadvantages of eddy current damping are as follows:

- Neodium magnets start to lose its magnetic effects after 80°C.
- Estimation of eddy current damping is not easy.
- If the main structure has electrical equipment, magnetic fields can be harmful. Main structure may be vulnerable to EMI (Electromagnetic Interference) and EMC (electromagnetic Compatibility).
- A magnet can react some metals near around.

When design of TVA is completed, it is compulsory to measure TVA parameters. In order to see the effect of magnets on an accelerometer, a simple test was conducted. The main aim of this test specifies if magnetic fields due to magnets affects measurement capability of the accelerometer. A cantilever beam is excited on free end and experiment was conducted for two cases. PSD acceleration of the free end of the beam was measured without and with magnets. Test set-up can be seen in Figure 2.8. The distance between magnets and beam is 2 mm. Aluminum beam dimension is 38mmx205mmx1.1mm, also there are three different holes on it. The beam is fixed at one end and the other end is free. Neodium magnet class is N42 and its dimensions are 40mm x25mm x10mm.
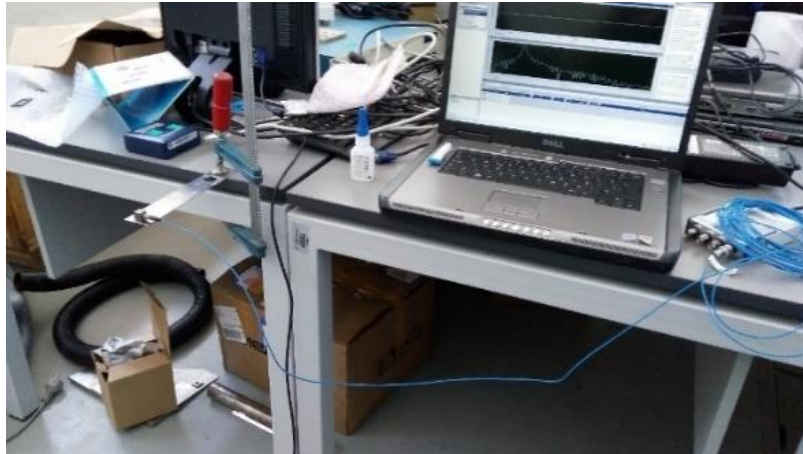
Figure 2.8. Test set-up
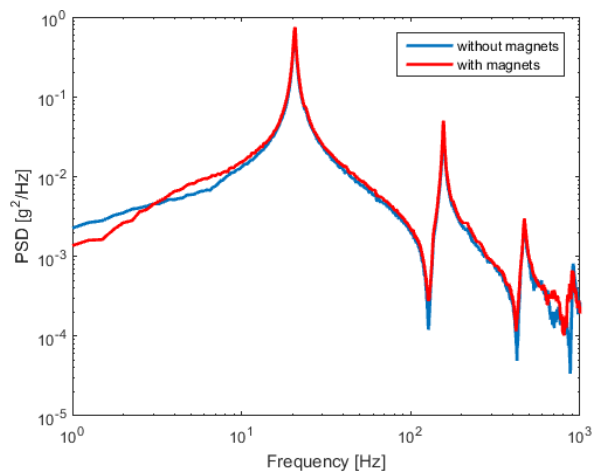
Figure 2.9. PSD acceleration of the beam with and without magnets

As it can be seen in Figure 2.9, PSD acceleration of beam is almost equal to each other. There is a little difference between them below 10 Hz. With these two results, it can be said that magnets do not affect measurement capability of accelerometer.

Torsional damper is another alternative. But rotational motion should be converted to linear motion. There is a commercial eddy current torsional damper [63].

2.4. Elements Used in TVA

A TVA works near at resonance frequency, so its parts and their connections are crucial. TVA mass moves only one direction which means all other degree of freedom is supposed to be constrained. Information about elements can be used in the TVA are given in the following sections.

Basically, a TVA consists of a TVA mass, a stiffness element and a damping element. Stiffness element could be a helical spring, a viscoelastic material, a beam or an air spring etc. Generally, commercial TVA products consist of a helical spring ([12, 16, 17, 19, 29, 64]). When a helical spring is used in a TVA, spring is supposed to connect with TVA mass and TVA body. Connections of helical springs to TVA mass or TVA body is a problem. Although it looks like very easy, it is actually very difficult how to mount a spring to another body. There are few alternatives accessories for mounting spring where it works.

2.4.1. Spring Mounting Methods

A helical compression spring should be mounted with a spring mounting element. Spring mounting can be divided into six groups as given in Figure 2.10.
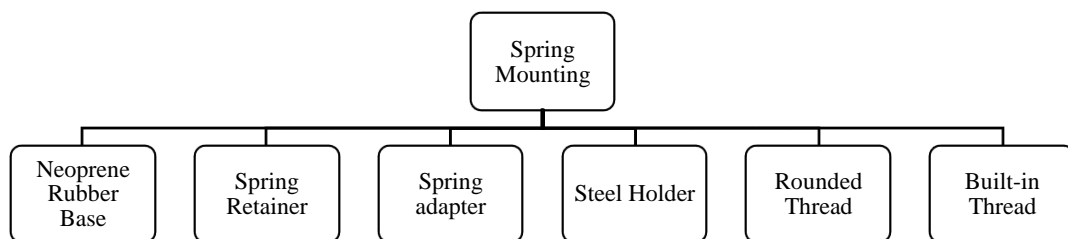
Figure 2.10. Types of mounting for compression spring

Neoprene rubber base is used generally in heating ventilation and air conditioning systems, centrifugal axial fans, air handling units, and small compressors. It is used for mounting spring to ground for vibration isolation from seismic excitation. It can be used for both ends or one end of spring. Spring sits on the inner surface of neoprene base. Outer diameter of the spring is smaller than neoprene rubber inner diameter. There are some holes for bolt on the neoprene rubber which is used for mounting another body.

The other alternative is steel holder which is consist of two parts (Figure 2.11). Spring is sat one of them. Part of it is guided by other part, so spring can move only one direction.
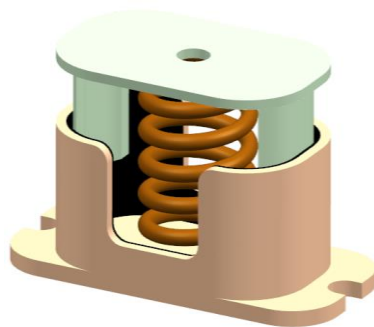
Figure 2.11. Steel holder adapted from [65]

Another alternative is spring retainer which is shown in Figure 2.12. Spring sits on a metal part housing. Inner diameter of the retainer is bigger than outer diameter of the spring. To constrain moving direction other than axial direction there is a rod which is center of the retainer and spring can move only axial direction.
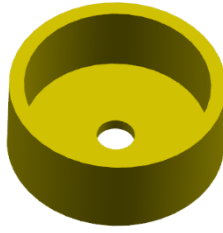
Figure 2.12. A spring retainer adapted from [66]

Another alternative is spring adapter, also called internal plug (Figure 2.13). It looks like a spring retainer but, in this case, outer diameters of adapter is smaller than spring diameter so spring sits on the adapter. Spring is guided with inner surface spring.
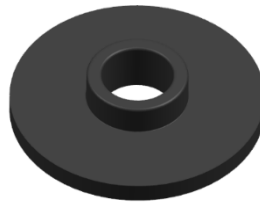
Figure 2.13. Spring adapter adapted from [67]

A spring can be mounted to the other body with a bolt (Figure 2.14). Mounted body should have threaded hole; bolt length is bigger than length of thread hole. Bolt pitch and spring pitch are also equal so bolt can be installed both body and spring at the same time.
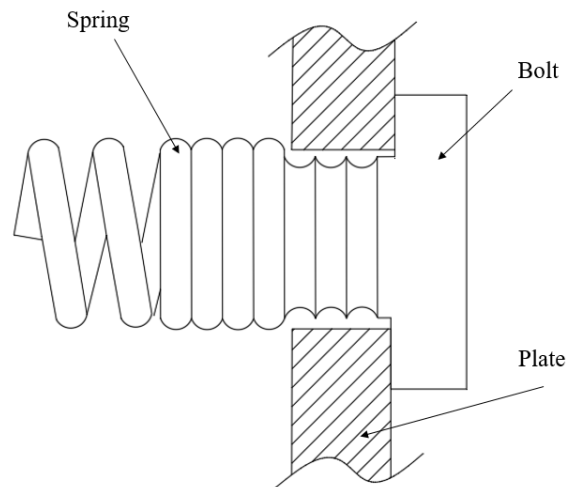
Figure 2.14. A bolt and mounted helical spring adapted from [68]

Figure 2.15. Machined compression helical spring

Machined spring is another good alternative to mounting a spring. In Figure 2.15, there is a thread on the one end of the spring. It can be mounted to TVA mass with a bolt. This type of spring is manufactured with machining operation and its price is much

higher than wire spring price. Another disadvantage is that its compression length is lower than these of wire spring.

Welding of the spring is an alternative but it is not a good solution because welding causes a permanent deformation on the spring. When compressed or extend a helical spring, inner and outer surface move inner or outer so designer should take account inner and outer diameter of the retainer and adapter.

2.4.2. Linear Motion Elements

Passive TVA is designed and used for only one mode of main structure so it is a single DOF system so effective mass of TVA should move only one direction. Following alternatives can be used for this purpose.

- Bushing & Rods (Figure 2.16)
- Linear Bearing (Figure 2.17)
- Linear Motion Platform (Figure 2.18)
- Square Bearing (Figure 2.19)

Using of bushing and rod is a very simple alternative; TVA mass can be constrained in one-dimension motion with bronze bushing and a steel rod. Bushing is mounted to TVA mass and rod passes through bushing so it can move along rod axis. To reduce friction between rod and bushing, surface quality of both bushing inner face and rod should be minimum. Generally bushing is self- lubricating part and oil comes out when it works [69]. Coefficient of friction between bronze bushing and steel rod is between 0.08-0.14. It is between 0.12-0.18 if there is no lubricant[70].
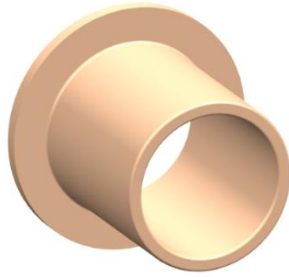
Figure 2.16. A bushing

Bronze bushing can be affected dust and dirty environmental conditions. Linear bearing (plain or ball bearing) and a rod is another alternative. Coefficient of friction is about 0.05 and it does not change over the life but it needs lubricant except self-lubricated ones. It has high working temperature range, -200 °C /200°C [71].

Figure 2.17. Linear ball bearing [71]

Another alternative is rail and carriage platform. A carriage can moves on the rail. In this case, it is capable of resisting moments all rotations. Between carriage surface and rail surface there is no metal contact there is a plain bearing and a gliding surface. Coefficient of friction is about 0.1-0.15. Working temperature range is between 0-80°C [72].

Figure 2.18. Rail and carriage platform [72]

The last alternative is square bearing. This alternative has one major advantage. One bearing is enough to constrain linear motion of TVA mass. Degree of freedom of this alternative is less than round bearing so rotation around moving direction is constrained.

Figure 2.19. A square bearing [73]

Table 2.6. Linear motion alternatives

	Friction Coefficient	Working Temperature Range	Lubricant Requirement
Bushing & Rods	0.08-0.14	-	Yes
Linear Bearing	0.05	-200°C /200°C	Yes
Linear Motion platform	0.1-0.15	0-80°C	Yes
Square Bearing	Unknown	-240°C /204°C	Yes

CHAPTER 3

DETAILED DESIGN OF THE TVA

Design of a TVA consists several steps. A flow chart which shows design steps of TVA is given in Figure 3.1. The scope of this thesis does not consist of the definition of the problem and the determination of effective TVA parameters. They are taken from Büyükcivelek's[1] study. Nevertheless, first two steps are briefly mentioned in this section.

At the beginning, vibration problem should be decided whether TVA can be used for defined problem. As mentioned before passive TVA works properly if it is tuned correctly which means its parameters are set to minimize vibration of the main structure. To define vibration problem and if it can be used for this problem, frequency response function of the main structure should be obtained. Natural frequency, amplitude of displacement or acceleration, modal damping ratio, etc. should be extracted from it. Excitation type may also help to the design procedure. There are some studies on TVA parameter extraction according to excitation type. Tuning frequency is constant which means a passive TVA works properly only when the target troublesome frequency is constant. In Büyükcivelek's work, it was decided that one TVA can solve defined problem. After deciding to use TVA, next step is that determining number of TVA and location of attachment point(s). Because TVA parameters and its performance are affected from them. Therefore, number of TVAs and their locations should be defined to achieve to reduced vibration level. For determining optimum TVA parameters for a discrete system, the common method is given by Den Hartog [3] and there are also several offered method in the literature.

For continuous systems, this process is more demanding, and details can be found Büyükcivelek's study for the TVA that will be designed in this thesis.

After determining TVA parameters, working and environmental conditions should be considered because working conditions affect the detailed design process of the TVA. If TVA has to work at elevated temperatures all TVA elements should work properly at these temperatures. A magnet can be used for eddy current damping, if maximum working temperature is limited to 80 °C because neodium magnet losses its magnetic capability after this temperature [74]. Furthermore, properties of TVA should be known in the operation the temperature range. For instance, temperature difference may cause to change properties of damping or spring element. Possible working environmental conditions that should be considered when designing a TVA are as follows

- Shock
- Static acceleration
- Environment and working temperature range
- Humidity
- Dustiness
- Working space (indoor or outdoor)
- Orientation

After specified TVA parameters and working conditions, TVA requirements are supposed to be defined by considering TVA parameters and working conditions, because type of elements used in TVA depends on requirements. These possible TVA requirements are as follows

- Response of TVA mass

- Life & reliability expectations

- Maximum mass & volume of the TVA

- Maintenance requirement

The main requirement of the TVA is its performance which is strongly related with TVA parameters (i.e. achieving the target effective TVA mass, tuning frequency and damping level). In addition, maximum displacement and velocity of TVA mass should be considered because stiffness and damping element should work under these conditions. Maximum displacement capacity of spring should be higher than TVA mass displacement. Maximum displacement of TVA mass under vibration and shock should be considered, because compression or extension length of the spring and stroke of the damping element should be greater than displacement of effective mass of TVA. Velocity of the TVA mass is also considered because damping element should work at that speed.

Life and reliability of the TVA should be considered because TVA should work properly during its life. If one or more TVA structural element life is shorter than target TVA life, maintenance or replacement may be required.

TVA effective parameters, working & environmental conditions and TVA requirements are given in Table 2.2 and Table 3.1, respectively.

Table 3.1. Working conditions and requirements of the TVA

Maximum displacement of TVA mass	17 mm [1]
Shock (in all directions)	1000 g, 0.5ms duration [1]
Total Mass	Minimum
Orientation	Horizontal / Vertical / Inclined

Vibration Problem
- Troublesome
- Frequency
- Amplitude
- Displacement, velocity, amplitude
- Excitation type

Specifying TVA Parameters
- Attachment point & number
- Performance
- Mass
- Stiffness
- Damping
- Degree of freedom

Working & Environmental Conditons
- Temperature
- Humidity
- Dustness
- Shock
- Acceleration
- Orientation

TVA Requirements
- Stroke & velocity of TVA mass
- Maximum mass and volume
- Life & reliability

Conceptual Design
- Alternative desings
- Comparing concepts
- Selection of best concept

Detailed Design
- Spring element
- Damping element
- Total Mass
- Mass constrain
- Body
- Connection elements
- Connection to main structure

Validation
- Performance
- Fatigue Life
- Maintaince
- Certification Tests

Tuned Vibration Absober

Figure 3.1. Flow chart of how to design TVA

32

TVA is single dof system so TVA mass moves only one direction. Stiffness element and damping element should allow to move TVA mass. Displacement of TVA mass due to vibration is 17mm[1]. TVA is also subjected shock in all directions. Shock profile is not given by in Büyükcivelek's study and it is assumed that its profile is half-sine in this study. Displacement of TVA mass under shock is calculated in the next section.

Total mass of TVA comprises TVA mass and mass of non-moving parts, such as structure, bolts, bearings, plates, etc. When TVA is installed on main structure and total mass of main structure increase. Total mass of TVA should be minimum to not change dynamics of main structure.

Some commercial TVA's are given in Table 2.1, only few of them can work both vertical and horizontal. In this study, a versatile TVA is developed so it can work any orientation.

The next step is conceptual design. A conceptual design should satisfy both TVA requirements and target values of TVA effective parameters. Best conceptual design is selected some criteria. Main criteria that could be considered when choosing a conceptual design alternative for the TVA are as follows

- Size & Mass (Low redundant mass and compact design)
- Low maintenance requirement
- Versatility in orientation (could be used in Vertical & Horizontal & Inclined orientation)
- Manufacturability

- No or less sensitivity to temperature, dust etc.
- Fabrication cost
- Ease of assemble and unassembled

Size & Mass criteria refers both redundant mass and dimensions of TVA. Redundant mass is defined as difference between total mass of TVA and TVA mass (the effective mass of the TVA). TVA mass is already defined according to tuning criteria. Redundant mass is not considered during tuning of TVA so it should be zero in the ideal case but it is not possible. Redundant mass of the TVA may change dynamic characteristics of main structure, so it should be kept as minimum as possible.

In this study, the best conceptual design is selected taking into account the above criteria and it is given in Figure 3.2. This alternative consists of a TVA mass, two preloaded helical compression springs, two magnet sub-assemblies, TVA body and some connection parts. It can be used in either vertical or horizontal orientations. Rods and bushings constrain TVA mass motion in one direction. Spring force and damping force depends on relative displacement and speed of TVA mass, respectively and they change continuously. Difference between them makes bending moment. Number of them and their location should be defined so that bending moment is minimum. Spring element, damping element, TVA mass are symmetric along centerline so they do not produce bending moment. As a result, friction force between rod and bushing remains constant.

Helical compression springs is preloaded for four reasons. Firstly, preloaded springs has more spring life than unpreloaded spring. Secondly, relation between displacement and force is more proportional. Thirdly, contact between TVA mass and spring end should not be left, so it should be pre-loaded more than maximum displacement of TVA mass therefore contact between them is ensured. Lastly, TVA

can be used vertically so there is need more preloaded due to weight of TVA mass. Stiffness of the spring change linearly with displacement and connection between TVA mass and spring is ensured. Also preloading also enables the use of TVA in any orientation, helical springs will be in compression at all times even when the weight of the mass causes tensile loads on the springs.
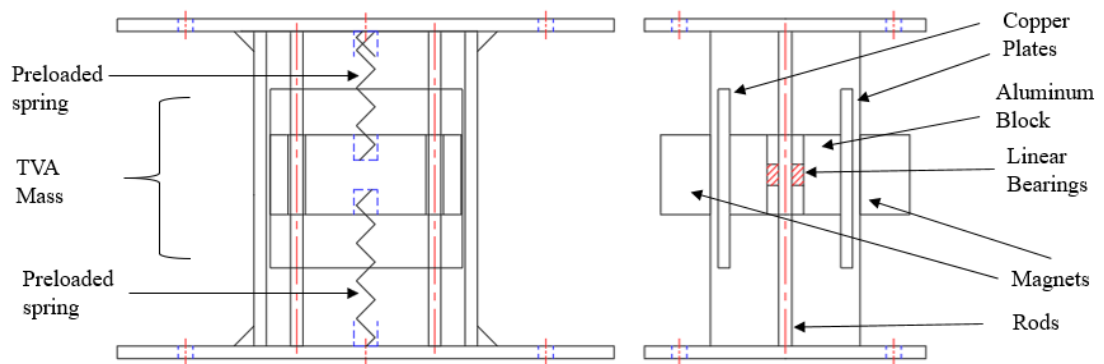
Figure 3.2. Selected conceptual design of the TVA

Eddy current damping is the chosen alternative in this design work because of its advantages, which are given in previous chapter. Damping element is also symmetric with respect to direction of motion. There are two copper plates on the TVA mass. Damping force is occurred on the copper plates. Damping force on them is equal to each other. Most parts of this TVA are off-the-shelf parts and assembly of the TVA is expected to be relatively easy.

TVA is a single DOF system and it is assumed that TVA mass and other parts of TVA are rigid. So, TVA mass (effective mass) should move in one direction. To do this, mass is constrained with two linear bearings and two rods.

After selected best conceptual design, detailed design of the TVA should be conducted. Detailed design work of the TVA is given in the next section.

3.1. Detailed Design of the TVA

Detailed design work for all of the TVA parts is presented in this section. Selected conceptual design, optimum parameters and requirements of the TVA is given in Figure 3.2, Table 2.2 and Table 3.1, respectively.

Spring element is the most important part of the TVA because tuning frequency of the TVA is critical for its ultimate vibration reduction performance, and it is function of its stiffness and TVA mass. Damping element of the TVA is also critical because vibration energy is consumed on this element and TVA performance is directly related with amount of damping and there is a target damping value for the TVA to achieve for desired vibration reduction performance. Compression length of spring and stroke of damping element are another important point because they limit TVA performance even if TVA is tuned correctly. Firstly, design process of spring and damping element are given in the next two sections of this chapter. Then, design work of other parts of the TVA are presented in the following sections.

3.1.1. Design of Spring Element of TVA

In the selected conceptual design, TVA mass is suspended with two helical springs. There are two alternatives for helical spring, compression and tension spring. Helical compression springs are used in this study because its strength is more than tension spring for similar size. TVA spring element life should be as much as possible for minimum maintenance requirement. Additionally, spring should not be buckled under working condition.

Maximum displacement of TVA mass during the operation is given in Table 3.1 but maximum displacement due to shock is missing so shock response of the TVA mass is analyzed in the next section. After that, spring design for strength, natural frequency and life are studied in following sections.

3.1.1.1. Maximum Displacement of TVA Mass

Displacement of TVA mass under vibration and shock should be known for spring design. In this study it is assumed vibration and shock is exposed separately. Displacement of TVA in moving direction is calculated for different damping ratios. Maximum displacement of TVA mass due to vibration is given 17 mm. Maximum displacement of TVA mass due to shock is not given but in Büyükcivelek's study which it is specified that TVA is expected to be subject to a shock load of 1000g in all directions. A TVA is shown in Figure 3.3 and it is subjected base excitation of main structure.
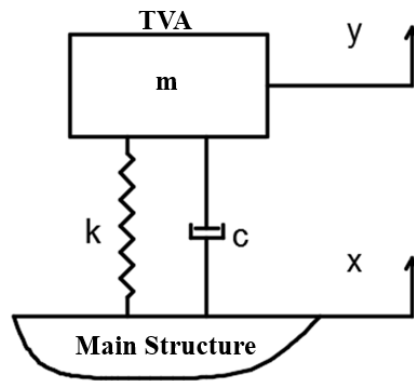
Figure 3.3. TVA mass, spring and damping system subjected by base acceleration

TVA is subjected by base acceleration and its equation of motion is given in Equation 3.1.

$$m\frac{d^2y}{dt^2} = -k(y-x) - c\left(\frac{dy}{dt} - \frac{dx}{dt}\right)$$
Equation 3.1

where m is TVA mass. k is stiffness of spring element. c is damping coefficient of damping element. x(t) is absolute displacement of main structure where TVA is installed. y(t) is absolute displacement of TVA mass. $z(t)$ is the relative displacement of TVA mass. Equation of motion in relative coordinate is given in Equation 3.2.

$$\frac{d^2z}{dt^2} + 2\xi\omega_n\frac{dz}{dt} + \omega_n^2 z = -\frac{d^2x}{dt^2}$$
Equation 3.2

where ω_n is natural frequency of TVA. ξ is damping ratio TVA. They can be calculated with Equation 3.3 and Equation 3.4.

$$\omega_n = \sqrt{\frac{k}{m}}$$
Equation 3.3

$$\xi = \frac{c}{2m\omega_n}$$
Equation 3.4

Equation 3.2 is very similar to the differential equation of motion of a single dof excited by a force. Only difference is the right-hand side of the equation. Relative displacement of the system can be found with convolution integral inserting $-\ddot{x}(t)m$ instead of force. Relative displacement of TVA mass is given in Equation 3.5 [75].

38

$$z(t) = -\frac{1}{\omega_d} \int_0^t \ddot{x}(t) e^{-\xi \omega_n (t-\tau)} \sin \omega_d (t-\tau) d\tau \qquad \text{Equation 3.5}$$

where ω_d is damped natural frequency of TVA. τ is shock duration. $\ddot{x}_m$ is amplitude of the shock. Damped frequency ω_d can be calculated with Equation 3.6 for underdamped system.

$$\omega_d = \omega_n \sqrt{1-\xi^2} \qquad \text{Equation 3.6}$$

Relative displacement of TVA mass under shock for different damping levels are found with convolution integral with "conv" built-in Matlab™ command and given in Figure 3.4.
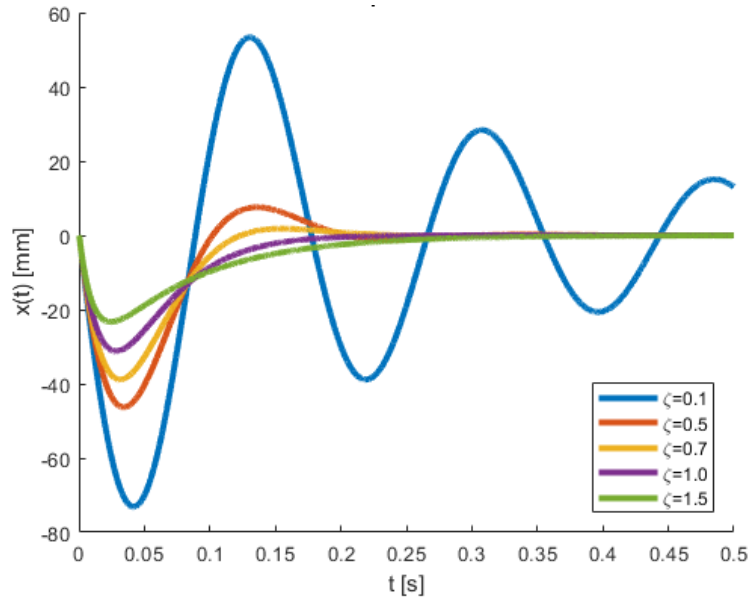
Figure 3.4. Relative displacement of TVA mass due to a shock input for optimized mass and natural frequency for different damping ratios

As it can be seen Figure 3.4, relative displacement decreases while damping increases. It is assumed that maximum relative displacement of TVA mass is as taken as 30 mm.

3.1.1.2. Design of Helical Compression Spring Based on Stiffness and Maximum Displacement

The most important specification of spring used in TVA is stiffness because tuning frequency is dependent on that value. A deviation from the calculated spring stiffness would cause mistuning of TVA which would then decrease TVA's vibration reduction performance. Second important specification is compressible length. TVA mass should move between double amplitude of relative displacement of the TVA mass. Designed spring should allow to move the TVA mass more than amplitude. Therefore, both must be satisfied by spring element. Apart from spring stiffness and maximum displacement, natural frequency is also critical, natural frequency of spring should not be close tuning frequency of the TVA. A commercial spring catalog shows a lot number of springs, but each spring has different wire diameter, spring stiffness, free length, etc. Springs in a catalog may not match required spring parameters so a new spring should be designed from scratch to ensure that TVA works properly. There are too many unknowns in spring design, and these are as follows

- Spring stiffness
- Spring index
- Free length
- Solid length
- Wire Diameter
- Spring material
- Spring ends
- Boundary conditions

- Number of active coils
- Pitch
- Helix angle
- Natural Frequency of spring

In the literature ([76–78]), design of a spring starts with specified dimensions such as wire diameter, and nominal diameter, etc. Spring design handbooks focuses on maximum force capacity, occurred stress, etc. A design procedure is developed in this thesis to obtain the desired spring stiffness and satisfy the maximum displacement limit simultaneously.

Before derivation, some definitions are given here. Front view and the top view of a helical compression spring is shown in Figure 3.5. Free length L_f is length of the spring when there is no force on it. Pitch p is distance between two sequential coils. Nominal diameter D is the diameter of the spring. Inner diameter D_i is diameter of the spring measured from inner surface of the coils. Outer diameter D_O is diameter of the spring measured from outer surface of the coils. Inner diameter D_i and outer dimeter D_o of the spring can be calculated with Equation 3.7 and Equation 3.8.
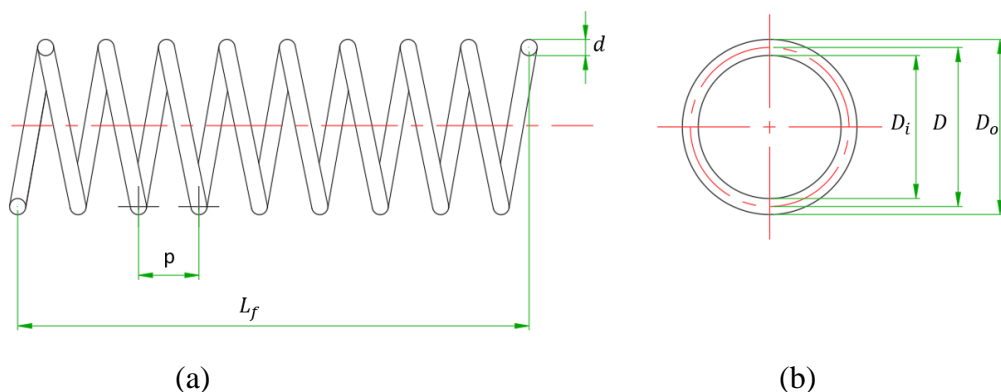
(a)   (b)
Figure 3.5. (a) front view and (b) top view of a helical compression spring

$$D_i = D - d \qquad\qquad \text{Equation 3.7}$$

$$D_O = D + d \qquad\qquad \text{Equation 3.8}$$

A compression helical spring loading conditions is shown in Figure 3.6. When one end of the spring is fixed and a compression force F is applied to the other end of the spring, it is shortened. Maximum compression length δ_{max} is allowable displacement when it is subjected a force. When it is reached maximum compression length, there should be gaps between coils. Total gap between coils is defined as clash clearance C_c.
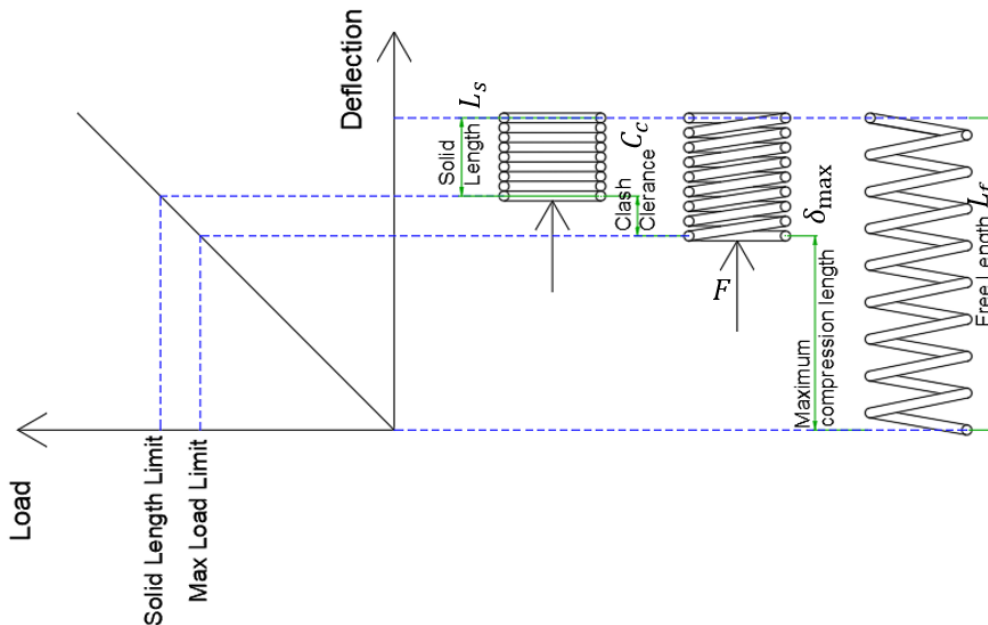
Figure 3.6. Loading conditions of compression helical spring

Compression force F should not be increased after this point for following reasons

- to not approach the yield limit: yield stress limit is generally higher than stress at solid length.
- to avoid clash of the spring [79]

- to avoid impact and surface deterioration [79]

If compression force F is increased after maximum compression length, it is compressed until coils touch each other and height of the spring at this condition is defined as solid length L_s. Clash clearance C_c can be calculated with Equation 3.9.

$$C_c = L_f - L_s - \delta_{max}$$

Equation 3.9

The ratio of nominal diameter D to wire diameter d is defined as spring index C.

$$C = \frac{D}{d}$$

Equation 3.10

Stress concentration factor K_w of the spring due to curvature should be also considered and it can be calculated with Equation 3.11 [80].

$$K_w = \frac{4C-1}{4C-4} + \frac{0.615}{C}$$

Equation 3.11

It depends on only spring index C, change of stress concentration factor versus spring index C is given in Figure 3.7. Stress concentration factor K_w decreases when spring index increases. Manufacturing of spring with low spring index C is difficult and its values of 3.5 to 15 are commercially available [76].
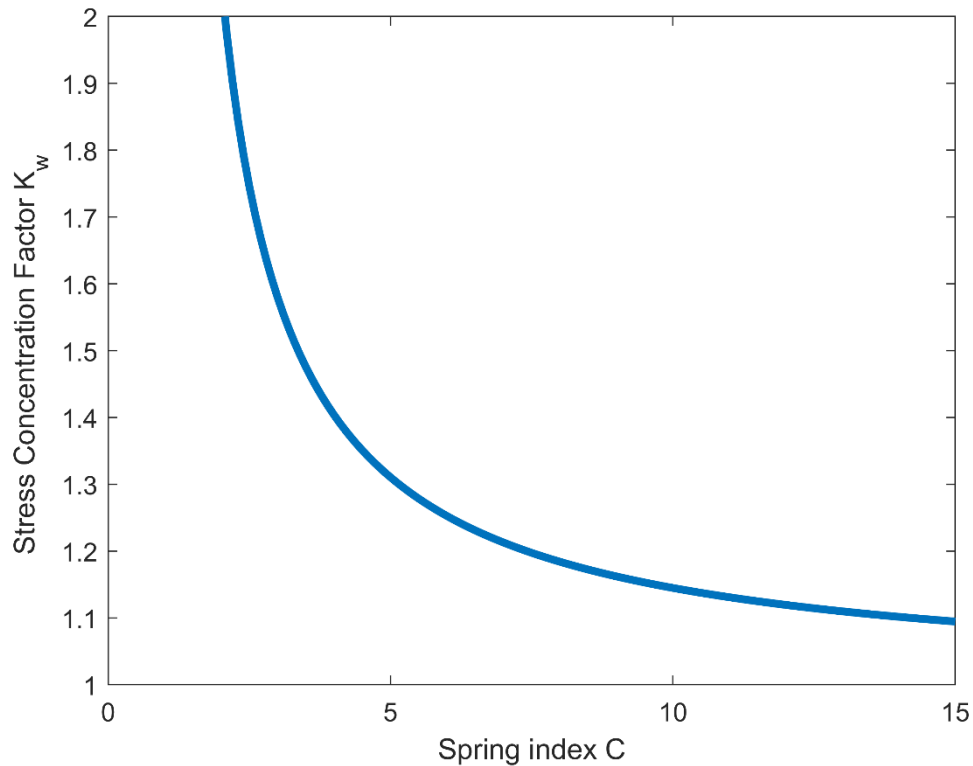
Figure 3.7. Stress concentration factor K_w v.s. Spring index C diagram

Spring stiffness k can be calculated with Equation 3.12 [79].

$$k = \frac{Gd^4}{8D^3 N_a} \qquad \text{Equation 3.12}$$

where G is shear modulus of spring material. d is spring wire diameter. D is nominal diameter of spring. N_a is number of active coils. Spring stiffness k can be calculated with Equation 3.12 but it is not considered to maximum displacement δ_{max} of spring. Nominal diameter D can be eliminated with a mathematical manipulation by using spring index C so this equation can be rewritten as given in Equation 3.13.

$$k = \frac{Gd}{8N_a} \frac{1}{C^3} \qquad\qquad \text{Equation 3.13}$$

Number of active coils N_a of a spring depends on spring ends. There are four spring ends as shown in Figure 3.8. Pitch and coils are not changed in plain ends. Last coil of spring is formed to touch previous coil in closed end. In ground end, coil is cut to obtain a surface which is perpendicular to spring axis. In squared & ground end, last coil of ground end spring is formed to touch previous coil.

	Plain	Closed	Ground	Squared & ground
Active coils, N_a	N_t	$N_t - 2$	$N_t - 1$	$N_t - 2$
Free length, L_f	$N_a p + d$	$N_a p + 3d$	$N_t p$	$N_a p + 2d$
Solid length, L_s	$(N_t p + 1) d$	$(N_t p + 1) d$	$N_t d$	$N_t d$

Figure 3.8. Coil numbers and free length of spring for different spring ends [79]

Active coil number N_a of squared & ground end spring can be calculated with Equation 3.14.

$$N_a = \frac{L_f - 2d}{p} \qquad\qquad \text{Equation 3.14}$$

With help of Equation 3.9 and Equation 3.14, number of active coils N_a can be found in following form.

$$N_a = \frac{C_C + L_s + \delta_{max} - 2d}{p}$$

Equation 3.15

First and last coils of the squared & ground spring is inactive so Equation 3.15 can be rewritten, solid length L_s of squared & ground spring can be calculated with Equation 3.16.

$$L_s = N_a d + 2d$$

Equation 3.16

By using Equation 3.15 and Equation 3.16, number of active coils N_a can be found in Equation 3.17.

$$N_a = \frac{C_C + \delta_{max}}{p - d}$$

Equation 3.17

where p is pitch of spring. Pitch p is defined as distance between two consecutive coils and can be calculated with following equation.

$$\tan \alpha = \frac{p}{\pi D}$$

Equation 3.18

where α is helix angle and it is angle between coils and base of spring.
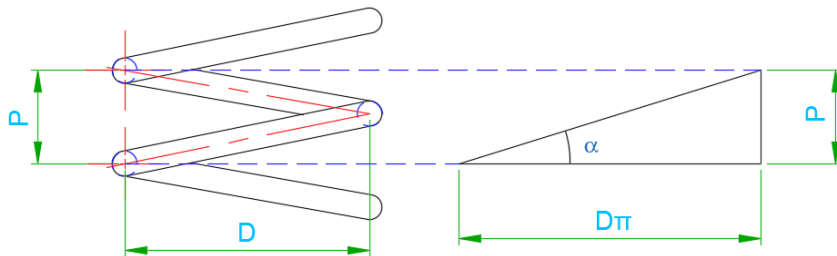
Figure 3.9. Helix angle of a helical compression spring

Pitch p is obtained from Equation 3.18 and nominal diameter D is obtained from Equation 3.10, they are put in Equation 3.19 to obtain active coil number N_a.

$$N_a = \frac{C_c + \delta_{max}}{d(\pi C \tan \alpha - 1)}$$

Equation 3.19

Lastly, active coil numbers N_a is putting in Equation 3.10 and spring diameter d in terms of spring stiffness k and maximum displacement δ_{max} is obtained. The wire diameter of the spring can be found with Equation 3.20.

$$d = \sqrt{\frac{8k(\delta_{max} + C_c)C^3}{(C\pi \tan \alpha - 1)G}}$$

Equation 3.20

After calculated spring diameter d, corrected shear stress S_c and buckling condition of the spring should be checked. Maximum permissible stress should be larger than corrected shear stress S_c of the spring, it can be calculated with Equation 3.21 [76].

$$S_c = \frac{8Dk\delta_{max}}{\pi d^3} K_w$$

Equation 3.21

Spring should not be buckled to work properly. Critical buckling length L_b of a spring can be calculated with Equation 3.22 [79], it should be more than free length L_f of spring.

$$L_b = \frac{\pi D}{\alpha} \left[\frac{2(E-G)}{2G+E} \right]^{1/2}$$

Equation 3.22

where E is young modulus of spring material. α is buckling constant and depends on spring boundary conditions. Buckling constant α for different boundary conditions is given in Table 3.2.

Table 3.2. Buckling constant α of helical spring for different boundary conditions [79]

End Condition	α
Spring supported between flat parallel surfaces (fixed ends)	0.5
One end supported by flat surface perpendicular to spring axis (fixed); other end pivoted (hinged)	0.707
Both ends pivoted (hinged)	1
One end clamped; other end free	2

Free length L_f of the spring can be calculated with Equation 3.23.

$$L_f = N_a p + 2d \qquad \text{Equation 3.23}$$

If corrected shear stress is more than allowable stress or buckling is happened then increase wire diameter and repeat the calculations to find minimum spring wire diameter. After calculated minimum spring wire diameter, select a bigger wire diameter available in the market. All dimensions of the spring can be found after selected wire diameter and assumptions. Active coil numbers N_a is already calculated with Equation 3.19, total coil number can be calculated with Equation 3.24.

$$N_t = N_a + 2 \qquad \text{Equation 3.24}$$

Inner diameter D_i and outer diameter D_o of the spring are calculated with Equation 3.7 and Equation 3.8. Free length L_f of the spring is already calculated and solid length L_s of the spring are can be found with Equation 3.25.

$$L_s = N_t d \qquad\qquad \text{Equation 3.25}$$

A flow chart showing design procedure is constructed and given in Figure 3.10. In the next section, helical compression spring for the TVA is designed with this process.
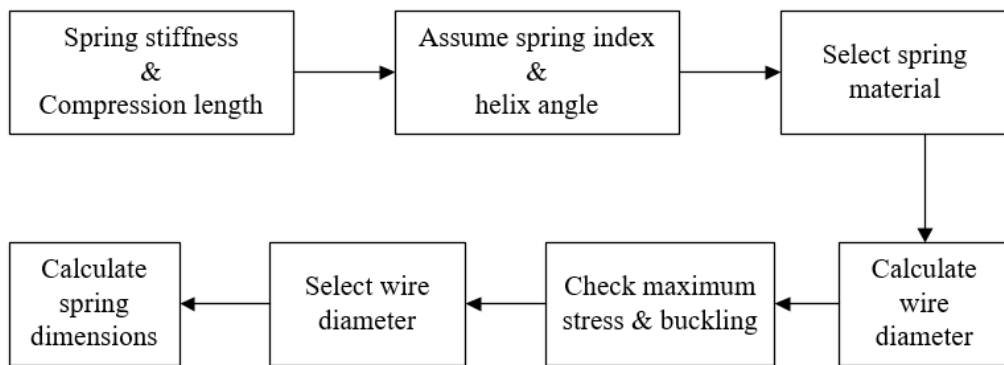
Figure 3.10. Flow chart for design of a compressive helical spring for TVA

3.1.1.3. Study Case: Design of TVA Spring

The best alternative has two preloaded helical compression springs. The optimum spring stiffness is 5 $\frac{\text{N}}{\text{mm}}$ so stiffness of each spring is 2.5 $\frac{\text{N}}{\text{mm}}$. Maximum displacement of TVA mass is assumed 30 mm. The preload of spring should be more than TVA displacement so preload is selected as 40 mm so maximum displacement δ_{max} of spring is 70 mm.

The second step of design of helical spring is assuming spring index C and helix angle α. As it can be seen in Figure 3.7, stress factor K_w decreases when spring index C increases. K_w contains stress concentration factor and shear factor. Low spring index C is difficult to manufacture, and 3.5-15 spring indexes are commercially available[76]. It is assumed that spring index is 12.5-to achieve low stress factor which is 1.11. The helix angle α is assumed to 9.6^o. ASTM313 302 Class II stainless steel is used as spring material because of slight magnetic property [81] and high ultimate strength [82].

Table 3.3. Summary of the parameters of the designed spring

Wire diameter	d	3.2 mm
Nominal diameter	D	40 mm
Outside diameter	D_0	43.2 mm
Inside diameter	D_i	36.8 mm
Spring index	C	12.5
Active coil number	N_a	5.65
Total coil number	N_t	7.65
Solid length	L_s	24 mm
Free length	L_f	132 mm
Spring stiffness	k	2.5 N/mm
Pitch	p	22.2 mm

Clash allowance C_c is recommended to set 10 % of the maximum displacement [79]. Minimum spring wire diameter is found 2.8 mm with Equation 3.20. Corrected shear stress S_c is found 803 MPa by using Equation 3.21. Minimum tensile strength of the material is 2000 MPa[82]. Allowable shear stress of the material is between 45-55 % of the tensile strength of the material[79]. In this study, allowable shear stress of material is assumed 1000 MPa so corrected shear stress S_c is lower than allowable shear stress of the material. Free length L_f of the spring is found 100 mm via Equation 3.23. With Equation 3.24 critical length L_b for buckling is calculated 189 mm and it is higher than free length L_f of the spring. 2.8 mm diameter satisfy spring requirements

but 3.2 mm wire diameter d is selected to obtain more spring life. All dimensions of the spring are found for new selected spring wire diameter d. Properties of the spring is given in Table 3.3.

3.1.1.4. Natural Frequency of TVA Spring

After completed spring design, natural frequency of the spring is considered. Natural frequency of spring should not be close to tuning frequency of the TVA which is specified as 5.67 Hz. Finite element analysis is conducted to calculate spring natural frequencies. During operation, spring is preloaded. One end of the spring touch the TVA body, other of the spring touches the TVA mass. Relative displacement of the TVA mass is used for spring compression length so it is assumed that one end of the spring is fixed as shown as A in Figure 3.11 and other end of the spring is constrained in x and z directions as shown as B in Figure 3.11. Preload is given in the latter end in y direction. The 40 mm preloaded spring is compressed due to vibration and shock load which is assumed 30 mm. For different compression length, modal analysis are conducted, both pre-load and compression is applied to same end of the spring which is shown as B in the Figure 3.11.
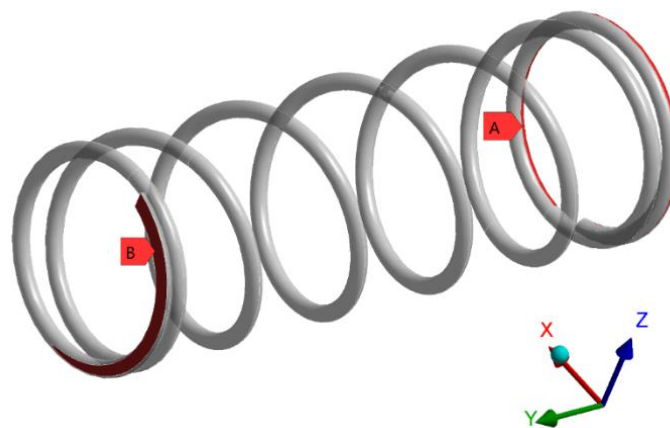
Figure 3.11. Boundary conditions of the spring

Figure 3.12 shows change of first ten natural frequencies of helical spring with respect to compression displacement.
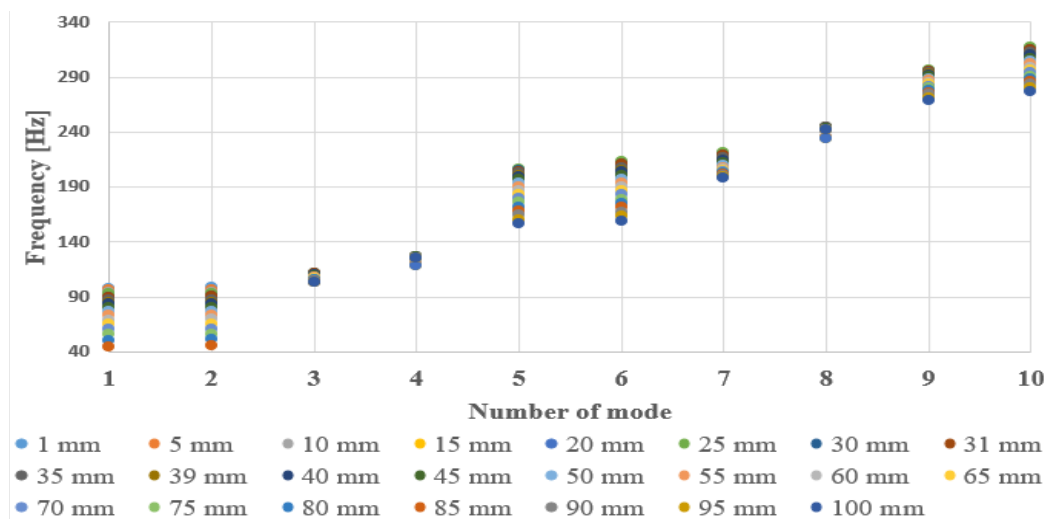
Figure 3.12. Change of first ten natural frequencies of the spring for different compression lengths

Table 3.4. Natural frequencies of the spring for 30mm and 70mm compression

Mode	Natural Frequencies at 40 mm displacement	Natural Frequencies at 70 mm displacement
1	84	60
2	84	61
3	110	106
4	127	125
5	199	179
6	204	183
7	214	204
8	244	242
9	292	282
10	310	294

Table 3.4 shows first ten natural frequencies of the TVA spring for 40 mm and 70 mm compression. When compression increases, natural frequency of the spring decreases.

The spring is loaded between 40mm and 70 mm, lowest natural frequency of the spring is about 60 Hz when compression is 70 mm which is about 10 times greater than target tuning frequency of the TVA.

3.1.1.5. Transient Analysis of TVA Spring

TVA is subjected the shock. In this section, response of spring is given under this shock. Transient structural finite element analysis is conducted to obtained stress distribution of the spring. The TVA is installed on a tank barrel to reduce vibration as shown in Figure 3.13 (a).

When tank shots, TVA is exposed the shock. TVA mass oscillates until shock is totally absorbed. There are two identical preloaded spring which is used for suspending TVA mass. Relative displacement of TVA mass is assumed to equal to spring displacement so a single spring is issued as analysis model as shown in Figure 3.13 (b). Inactive coils of the spring are removed both ends of the spring. One end of the spring is fixed as shown D. Displacement in x and z direction of the other end, shown as E, of the spring is set to zero which means it can move only y direction. A point mass is also defined to this end which refers TVA mass. It is also defined a spring element between point mass and ground and damping coefficient of spring element is $284 \frac{Ns}{m}$ refers to optimum TVA damping.

To find optimum mesh size, static finite element analyzes are conducted for different element size. Boundary conditions is the same as given before but displacement is 40 mm. Maximum shear stress is examined inner surface of the spring.

(a)   (b)
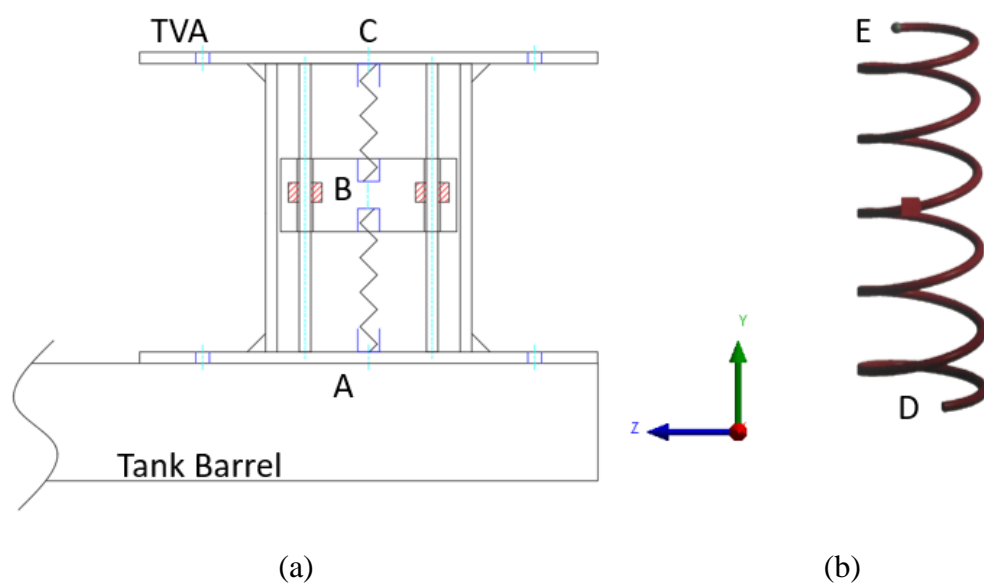
Figure 3.13. (a) Schematic view of installed TVA model, (b) analysis model

Table 3.5. Maximum shear stress of the spring

Element Size [mm]	Maximum Shear Stress [MPa]
5	380.53
4	378.16
3	377.06
2	367.36
1	347.75
0.8	345.68
0.7	344.30
0.6	343.07
0.5	341.72

Maximum shear stress of given point for different element size are given in Table 3.5. Finer mesh takes more times to complete analysis. Transient analysis generally takes more times, difference maximum shear stress between mesh size 1 mm and 0.5 mm is very close. Therefore, mesh size is selected 1 mm for transient analysis. Damping ratio of the spring material is set to 0.005 percent. The shock is applied in y direction to analysis model. Total solution time is 0.2 s. Total analysis time is divided into 8000 substeps.
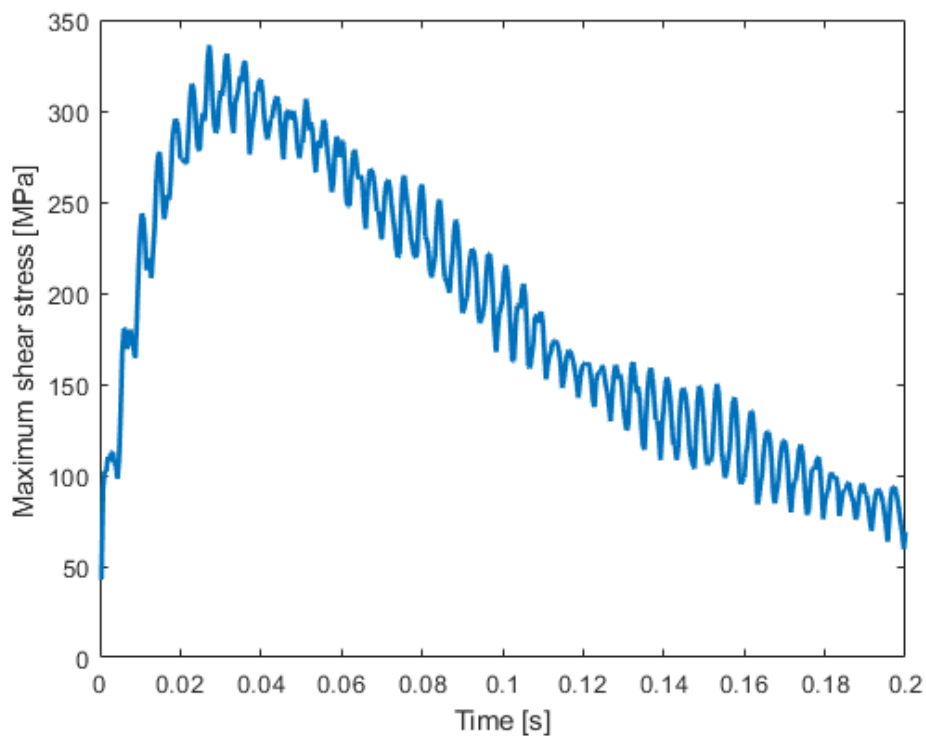
Figure 3.14. Maximum shear stress of the spring under the shock

Maximum shear stress of the spring under defined shock is given in Figure 3.14 and maximum shear stress distribution of the spring is given in Figure 3.15. Maximum shear stress is 336 MPa and its location is inner surface of the coil. The spring is preloaded 40 mm and maximum shear stress due to preload is 348 MPa so total shear

stress due both of them is 684 MPa which is lower than allowable shear stress of the material. It is also possible to use fatigue strength diagram to estimate spring life. Intersection of initial stress factor and maximum shear stress factor gives spring life [76].
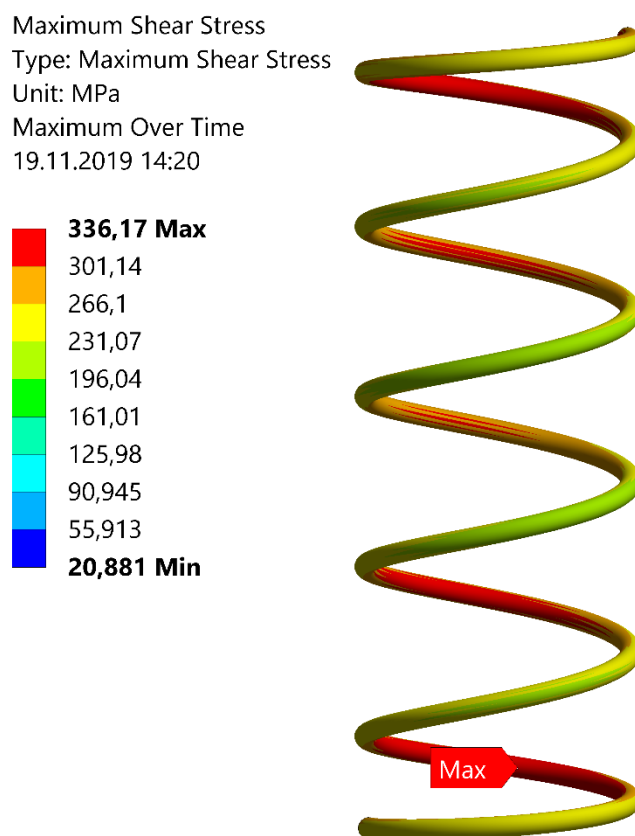
Figure 3.15. Maximum shear stress distribution of the spring under the shock

3.1.2. Design of Damping System of TVA

Eddy current damping mechanism is selected as damping element so magnet and its conductor material are designed in this section. Amount of damping is directly related to TVA performance. The more damping means the more vibration reduction so in this study maximum damping level is tired to achieve. Calculation of eddy current

damping is not straightforward and there is no closed form formula to obtain it. By using Equation 2.2, it is possible to estimate damping coefficient but there is "k" term in this equation called correction coefficient. In the literature, estimated and experimental damping level is different in different conditions. For example, k varies at different distance between magnets and conductor material or different magnet size. Difference between estimated damping and experimental damping level are different in each study as shown in Table 2.4. At the beginning, target damping ratio is 1.0 (284 $\frac{Ns}{s}$), there is no a method determine how much magnet and copper plate is required to achieve target damping level. But as expected the more conductor material and magnet the more damping therefore to achieve maximum damping level, maximum size magnet and copper plate are selected.

3.1.2.1. Modelling of Eddy Current Damping

Eddy current force is emerged when a conductive material moves in magnetic field. One of the magnets or its conductor should be installed on the TVA mass and the other should be installed to the TVA body. Damping of the TVA is estimated with Equation 2.2 in this study. k is dimensionless correction coefficient and unknown. v is volume of the copper plate, ρ is resistivity of copper plate and they are known. To calculate damping coefficient of the TVA, magnetic field flux density B of copper plate must be calculated.

To design an eddy current damping, following should be determined.

- Size of magnet and conductor material
- Shape of magnet and conductor material
- Distance between magnet and conductor material

There two type of magnet shapes in market, rectangular and disk type of magnet. If disk type of magnet is used, its conductor should be circular tube. Due to uncertainty of damping estimation, experimental damping level may not be high enough to achieve expected performance. To increase damping level after experiments, magnet and/or conductive material should be changed. Another option is rectangular magnets and conductor material. If damping level is wanted to be increased after experiments, apart from changing magnet and conductor material, distance between them can be changed in rectangular form. In this study rectangular shape magnet and conductor material are selected because of this advantage.

A schematic view of damping element is given in Figure 3.16, copper plate is installed on TVA mass and it can move in x direction so magnetic density flux of copper plate may change when it moves and it is defined as displacement as shown in Figure 3.16.
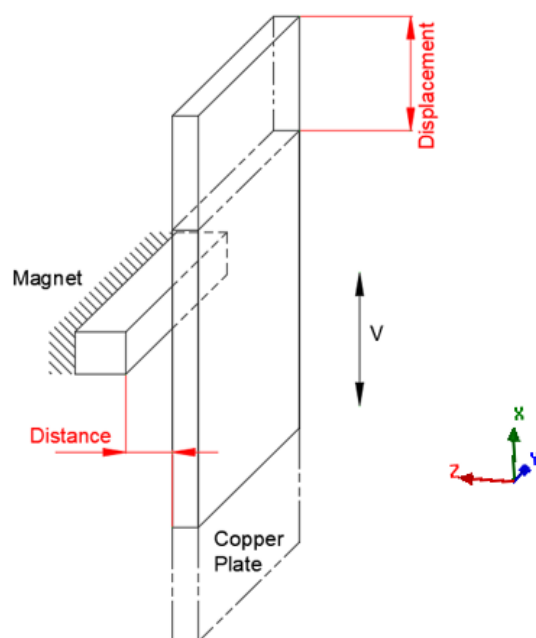
Figure 3.16. Schematic of the damping element

In this thesis, conductive material is copper plate and magnet is static so relative velocity between magnet and copper plate is equal to velocity of copper plate. Current density in conductive material can be calculated with Equation 3.26.

$$J = \sigma \left(v \, x \, B \right)$$

<div align="right">Equation 3.26</div>

where J is eddy current density. σ is conductivity of conductor material. B is magnetic field density and υ is relative velocity between magnet and its conductor. TVA is single dof system and it is assumed motion of the TVA mass is only x direction so Equation 3.26 reduces to Equation 3.27.

$$J = \sigma v \left(B_y k - B_z j \right)$$

<div align="right">Equation 3.27</div>

Magnetic force can be calculated with Equation 3.28.

$$F = \int JxB \, dV$$

<div align="right">Equation 3.28</div>

By using Equation 3.27 and Equation 3.28, force in x direction due to eddy current can be calculated with Equation 3.29. This equation shows that force in x direction is a function of magnetic flux density in y and z direction of conductor material and it is opposite to motion.

$$F_x = -\sigma v \int \left(B_y^2 + B_z^2 \right) dV$$

<div align="right">Equation 3.29</div>

Conductivity is inverse of resistivity. Ratio of damping force to velocity is defined as damping coefficient so damping coefficient of eddy current damping of the TVA can be calculated with Equation 3.30.

$$c = \frac{1}{\rho} k \int \left(B_y{}^2 + B_z{}^2 \right) dV \qquad \text{Equation 3.30}$$

Resistivity of copper is $1.7 \times 10^{-8} \Omega m$. Equation 3.30 shows that damping coefficient of the TVA depends on type of conductor material and square of magnetic flux density of conductor in other two directions. To estimate damping level of the TVA, total square magnetic flux density in y and z direction over the volume of conductor, $\int (B_y^2 + B_z^2) dV$, should be calculated. A commercial software is used to obtain magnetic flux density B. There is a calculator to evaluate magnetic flux density in the software. This calculator is used for this purpose and, damping coefficient is estimated by using Equation 3.30. But B_y is much smaller than B_z so it is assumed that B_y is negligible. Before estimation of the damping coefficient of the TVA, magnet and conductor material should be defined so magnet and conductor material are defined next two sections.

3.1.2.2. Selection of Magnet

To occur force between magnet and its conductor material there should be relative velocity between them. Copper plates are installed on the TVA mass because magnet is more brittle, so it is more fragile than copper plate.

Maximum size magnet available on the market is 50 mm x 50 mm x 25 mm and its class is N35. Two conductor materials are used for more damping so there are two magnet assembly in the TVA. Each assembly consists of three connected magnets side

by side and it is called one magnet block in this study. A magnet block's dimensions 150 mm x 50 mm x 25 mm. Properties of the magnets are given in Table 3.6.

Figure 3.17. Front view of a magnet block

Table 3.6. Properties of the magnets [74, 83, 84]

Density	7400 kg/m^3
Compression strength	950 MPa
Tension strength	80 MPa
Young Modulus	160 GPa
Poisson ratio	0.24
Relative Permeability	1.05
Bulk Conductivity	667000 siemens/m
Magnetic Coercivity	935 kA/m

3.1.2.3. Design of Conductor Material

As shown in Equation 2.2, resistivity of conductor is inversely proportional to damping coefficient so to get more damping, a material which has low resistivity should be selected. Table 2.5 shows possible conductor material and silver resistivity is very low but its price is $14.40[85] in May 2019. Copper is another alternative to be used as conductor material and its price is $2.73[86]. Copper is 5 times cheaper

than silver and their resistivity ratio is 1.5 which means more damping coefficient is obtained if silver is used as conductor material. But using silver as structural material is not common and thick silver plate is not found easily in the market. Therefore, copper plate is used as conductor material in this study. Size of coppers plates depend on following

- Amplitude of relative displacement of TVA mass
- Width of magnet block
- Optimum value of TVA mass

Damping level of the TVA is also depends on thickness of the copper plates so to achieve maximum damping level the thickness of copper plate should be maximum. Figure 3.18 shows front view and side of copper plate and magnets. Dimension of copper plate should be determined according to dimensions of the magnet block. Damping of the TVA should be stable so magnetic density of the copper plate should be stable as much as possible. Therefore, height of copper plate should be more than sum of height of magnet and amplitude of TVA mass. Likewise, width of copper plate should be more than width of the magnet blocks. Copper plates are installed on the TVA mass which is 4 kg. There are two copper plates, an aluminum block, linear bearings and connection parts on the TVA mass. Copper density, 8960 $\frac{kg}{m^3}$, is higher than density of steel and aluminum. Any analysis is not conducted for height of copper plate. Height of the magnet is 50 mm and it is assumed TVA mass can move 30 mm. It is assumed that height of the copper plate is 100mm.

Target optimum mass is 4 kg and two copper plates are used for symmetry so each copper plate mass should be less than 2 kg. Due to this mass limitation, 10 mm thickness is selected. Selected copper plate dimension is 100mm x 160mm x 10mm

and its mass is about 1.4kg. To calculate eddy current level several magnetic analyses are conducted, and they are given in next section.
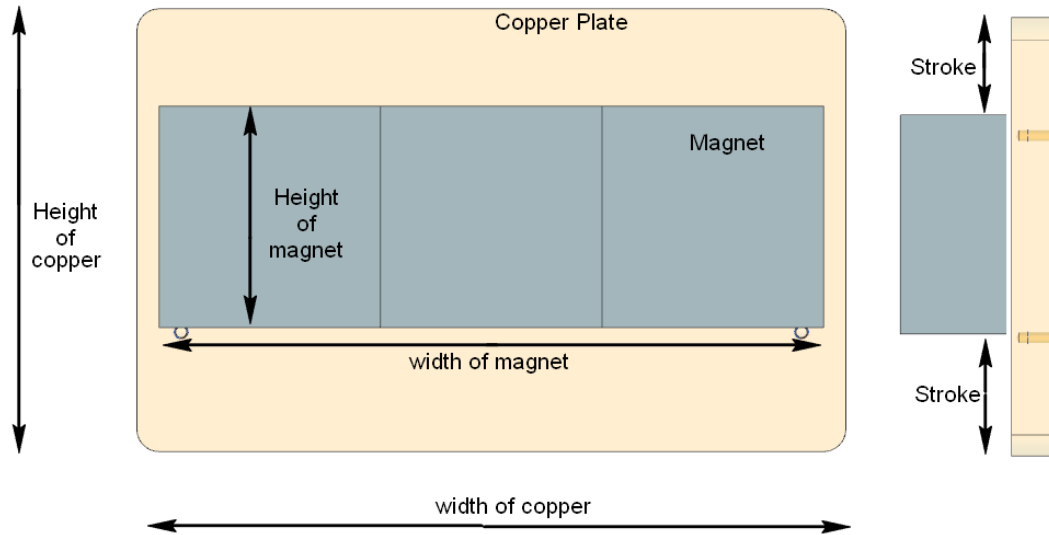
Figure 3.18. Front and side view of copper plate and magnets

3.1.2.4. Estimation of Eddy Current Damping Coefficient

To estimate damping coefficient of the TVA several static magnetic analyses are conducted with a commercial software. There are eleven different TVA configurations in terms of distance between magnets and copper plate and number of magnet blocks. They are given in Table 3.7. Distance and displacement are shown in Figure 3.16.

Magnetic analysis model is shown in Figure 3.19. It contains two copper plates, two magnet housings, two linear bearings, aluminum block between copper plates. One magnet block is used for configurations II-VI. Two magnet blocks are used for configurations VII-XI. Solution domain is a vacuum and its dimension is 300mm x 318 mm x 284 mm. Material properties of these elements are given in Table 3.8.

To estimate damping level of TVA, several magnetic analyses are conducted for different copper plate thickness and for different distance and displacement. Magnetic analysis for Configuration I is not conducted because there is no magnet. Distance changes between 1 mm to 5 mm. To see maximum damping capacity of the TVA, analyzes are also conducted when distance is 0mm.

Analysis are performed static case so they are repeated for different TVA mass location (displacement). Displacement varies between 0 mm to 30 mm. Each analysis is repeated for different displacements, 0mm, 5mm, 10mm, 15mm, 20mm, 25mm, 30mm. Total number of the analysis is 84. Solution domain of the analysis is big enough to analysis and it is vacuum. Magnetic properties of the materials used in the analysis model is given in Table 3.9.

Table 3.7. TVA configurations

Configuration	Distance	Magnet
I	No magnet	-
II	5 mm	One Magnet Block
III	4 mm	
IV	3 mm	
V	2 mm	
VI	1 mm	
VII	5 mm	Two Magnet Blocks
VIII	4 mm	
IX	3 mm	
X	2 mm	
XI	1 mm	

As mentioned before, damping coefficient the TVA depends on magnetic flux density, resistivity and volume of the conductor material. By assuming correction coefficient is equal to 1, damping coefficient of the TVA is estimated with Equation 3.30.

Magnetic flux density is obtained with software calculator. Estimated damping coefficients for one magnet case and two magnet case are given in Figure 3.20 and Figure 3.21, respectively.
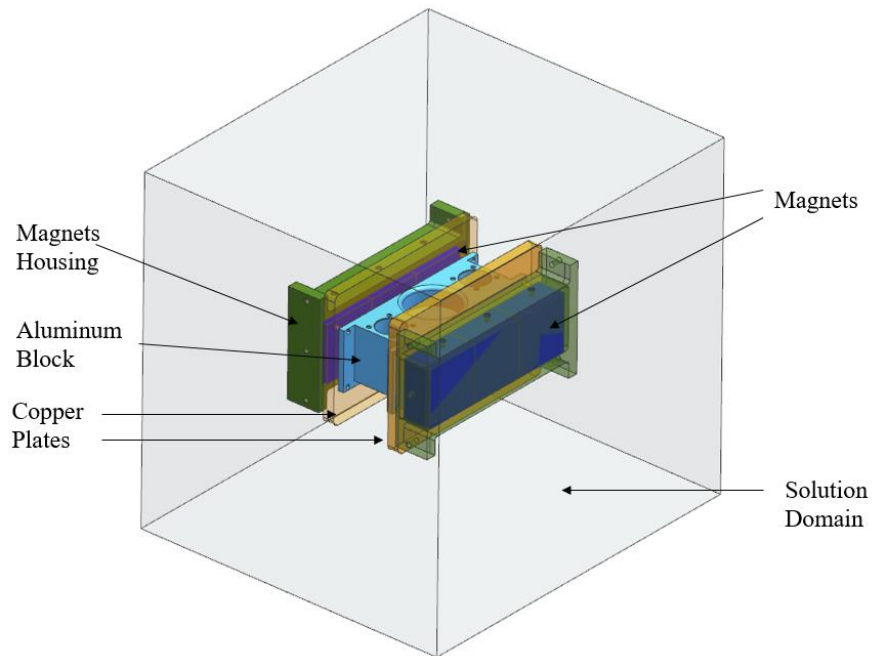
Figure 3.19. Magnetic analysis model

Table 3.8. Properties of material used in magnetic analysis

	Magnet	Copper	Aluminum	Vacuum
Relative Permeability	1.05	0.999	1	1
Bulk Conductivity [simens/m]	667000	58000000	38000000	0
Magnetic Coercivity [kA/m]	935	0	0	0

For one magnet case, the maximum damping coefficient is achieved when displacement is 25 mm when distance are 0,1 and 2mm. After that point it decreases. This increment is seen clearly for 0 mm distance and it disappears while distance increases. The maximum damping coefficient is about $86 \frac{N.s}{m}$ when distance is 0 mm and displacement is 25 mm.

For two magnet case, the maximum damping coefficient is achieved at different displacement. When distance is 0 mm, the maximum damping is achieved at 25mm. When distance is 2mm, the maximum damping level occur at 15 mm. While distance increases, maximum damping point approaches the equilibrium point. The maximum damping coefficient is about 233 $\frac{\text{N.s}}{\text{m}}$ when distance is 0 mm and displacement is 25 mm.
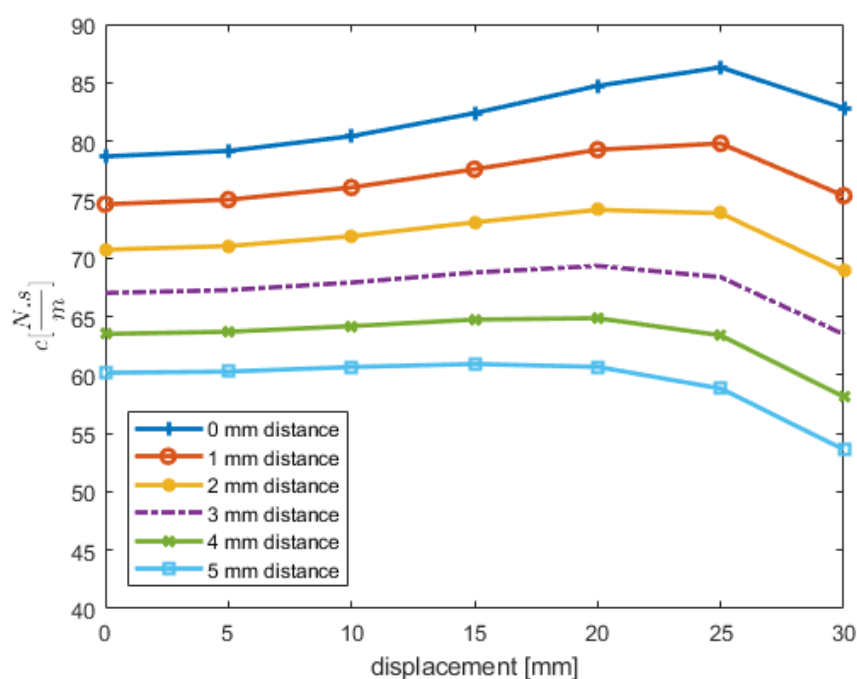
Figure 3.20. Damping coefficients of the TVA with one magnet block

Estimated damping ratio of the TVA for different distance and displacement are given above. Assumed amplitude of TVA mass is 30 mm so damping coefficients are averaged for each different distance.

Sum of damping coefficient is divided by number of summations to obtain average damping coefficient of TVA for different distance. Estimated average damping coefficients are given in Table 3.9.
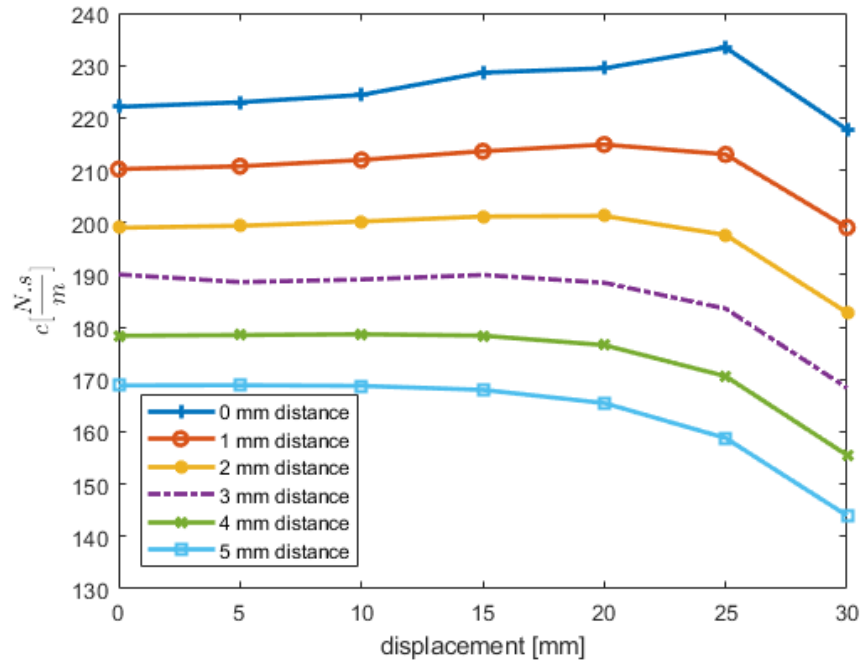
Figure 3.21. Damping coefficients of the TVA with two magnet blocks

Table 3.9. Estimated average damping coefficient of the TVA for different distances

	Distance [mm]	$c[\frac{N.s}{m}]$
One Magnet Block	0	82
	1	77
	2	72
	3	67
	4	63
	5	59
Two Magnet Blocks	0	226
	1	210
	2	197
	3	185
	4	174
	5	163

Maximum estimated damping coefficient of TVA is 210 c$[\frac{N.s}{m}]$ because there must be a gap between magnet and copper plate and it is assumed that its minimum is 1mm. Analysis are conducted for 0 mm distance because its results shows maximum damping capacity of this configuration. Actual damping ratio of the TVA may vary from the estimated ones. To ensure damping ratio of the TVA, it should be measured experimentally, and the results are given in next chapter.

3.1.3. Design of TVA Mass & Location of Spring and Damping Element

TVA mass is subjected to spring force, damping force and inertial force and they continuously change because displacement, velocity and acceleration of TVA mass are not constant. As it can be seen in Figure 3.22, when spring force is maximum, damping force is zero because stroke is maximum, and velocity is zero. When damping force is maximum at the equilibrium point, spring force is minimum because stroke is zero and velocity is maximum. Difference between them may make moment and this moment causes to vary friction force between rod and bearing.
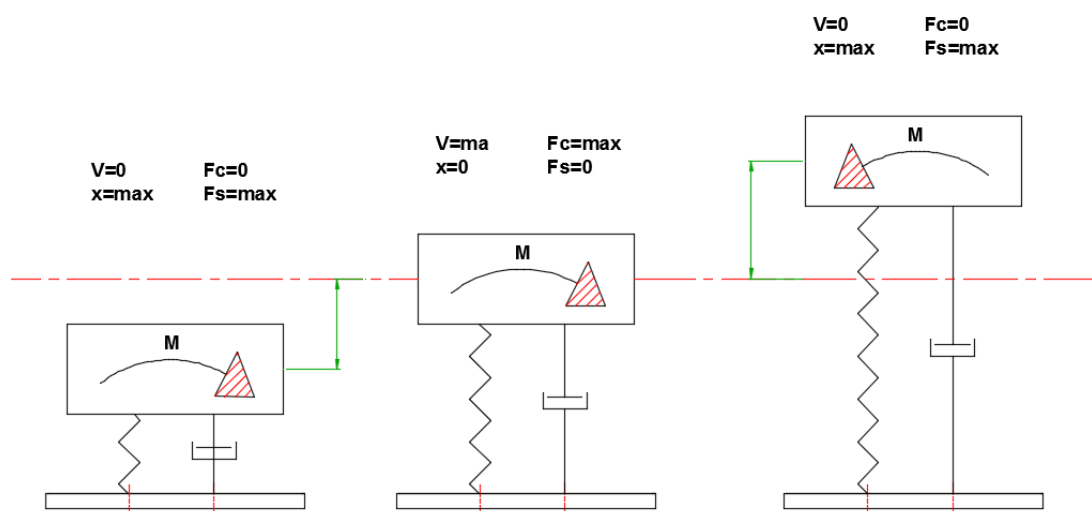
Figure 3.22. Freebody diagram of a single DOF system

To avoid this problem, two spring elements are located in the center of gravity of TVA mass. Distance between linear bearings and center of gravity of TVA mass are equal to each other. Figure 3.23 shows designed TVA mass and its subjected force. Spring forces are acting in the center of the TVA mass and bearing force due to friction are symmetrical to yz plane. All other parts, bolts and copper plates etc, are also symmetrical to yz plane and xy plane. Therefore, it is expected that friction between rods and bearing remain constant.
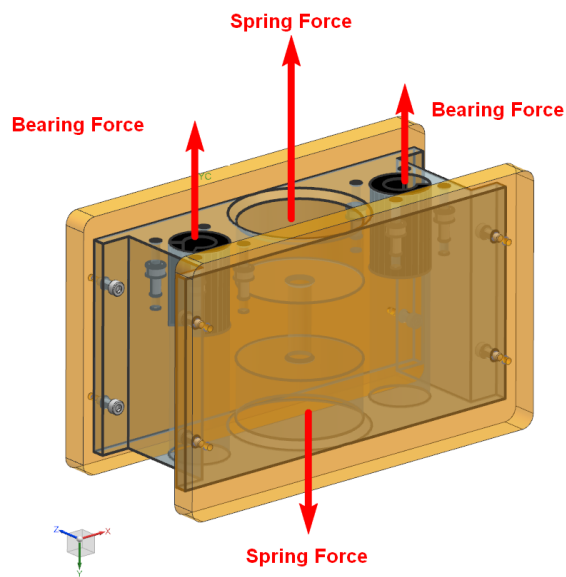
Figure 3.23. Spring and bearing forces subject to the TVA mass

Each spring sits on cylindrical hole on the TVA mass and its diameter should be bigger than maximum outer diameter D_f of the spring. When a helical spring is compressed, diameter of the spring is increased as given in Figure 3.24.
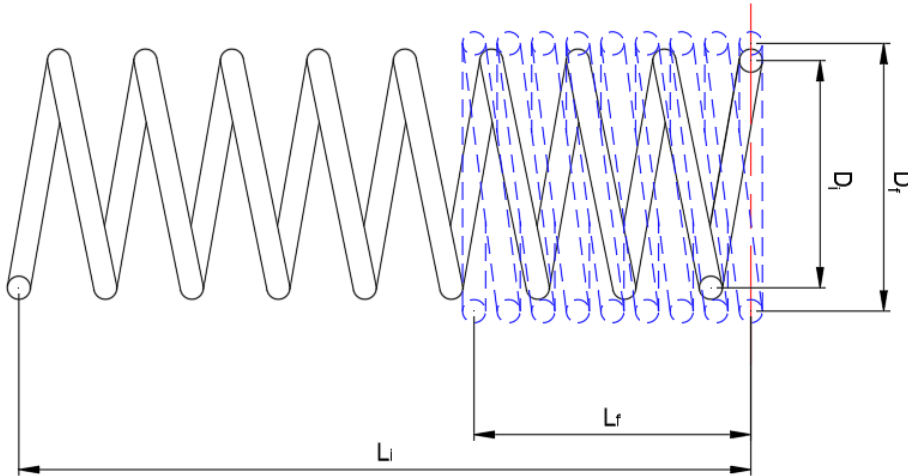
Figure 3.24. Schematic view of free form and compressed helical spring

Maximum change occurs when it is compressed to its solid length. Maximum outer diameter of compression spring can be calculated with Equation 3.31 [87].

$$D_{O \, solid} = \sqrt{D^2 + \frac{p^2 - d^2}{\pi^2}} + d \qquad \text{Equation 3.31}$$

where D is nominal diameter, p is pitch, d is wire diameter. Maximum outer diameter is 43.7 mm and hole diameter should be more than that to ensure spring surface does not touch TVA mass. The diameter of the hole is 46 mm and it is also tapered.

3.1.4. Design Of Magnet Housing And Its Adjustment Mechanism

Magnet should be mounting to the TVA body carefully for two reason. First, mounting may affect TVA performance due to parallelism, distance, etc. Distance between magnets and copper plates can be changed to arrange damping level of the TVA. Second, magnet is dangerous, it may pull some metal part or other magnet near around.

Three different alternatives for mounting and arrangement mechanism is given in this section.

First alternative design for magnet adjustment is given in Figure 3.25. There is a plate behind the magnets to ensure three magnets' flatness. Two rods are mounted this plate via two rod mounts. Linear bearing is installed on the magnet housing so these magnets can move only one direction. To move these magnets there are a bolt and two nuts are installed on the plate. By tighten and loosen these nut magnets can be moved. After magnets are positioned to right location, three bolts are tightened to fix magnets. Magnets materials are too ductile so there is a flexible material between magnets and these bolts. This magnet sub-assembly is installed to the TVA body with four bolts.
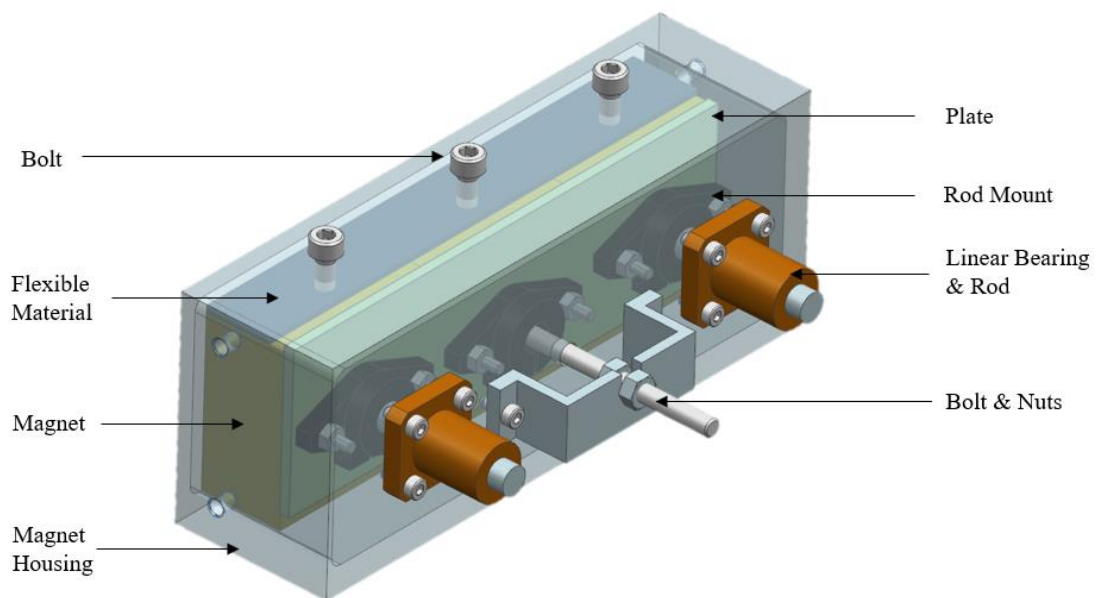
Figure 3.25. First alternative design for magnet adjustment

The second alternative is similar to first one. Magnets are mounted to three bolts to magnet housing and there is also a flexible material between bolts and magnets. But in this alternative, magnet housing should be moved manually to arrange the distance.

71

There are five holes both on the magnet housing and on the TVA body. Distance is arranging manually, and a guide pin attached to both holes to ensure distance is correct. Due to the distance depends on location of holes both on TVA body and on magnet housing, position tolerance of these holes is critical.
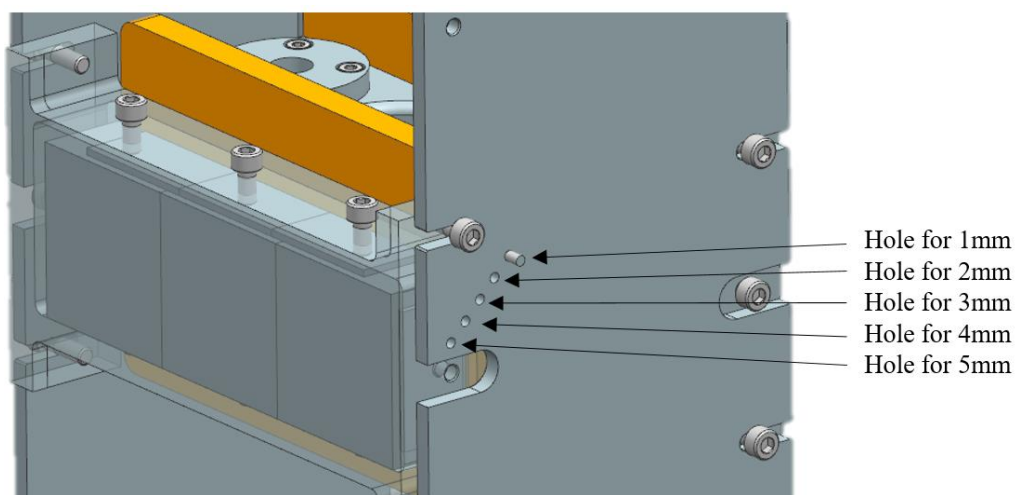
Figure 3.26. Second alternative for magnet adjustment
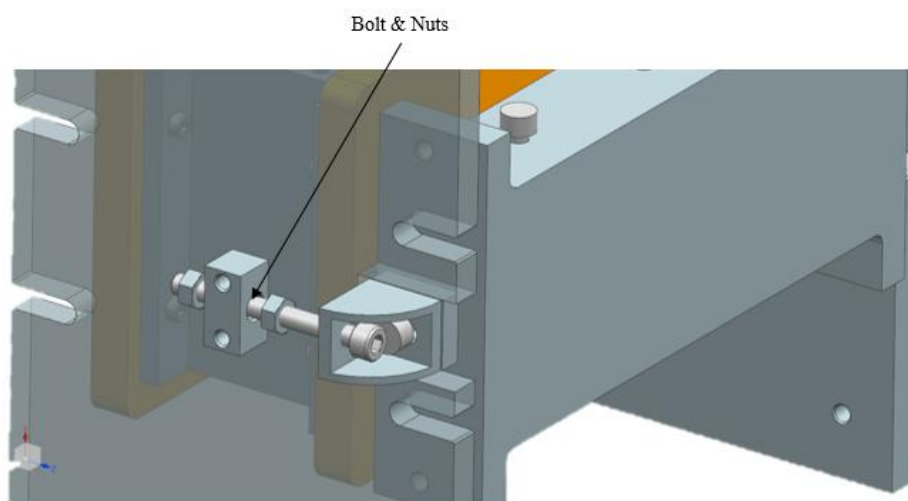
Figure 3.27. Third alternative for magnet adjustment

The third alternative is very similar to first alternative. In this alternative there are two arrangement mechanism for each sub assembly. There are a bolt and two nuts for arrange the distance. But in this alternative whole magnet sub-assembly move instated of only magnets.

The first alternative is selected because it has one arrangement mechanism and it is guided with two rods and bearings so parallelism is ensured.

3.1.5. Design & Selection Of Linear Motion System

Degree of freedom of TVA is one so TVA mass should move only one direction. To constrain other five degree of freedom, two rods and two or four linear bearings are used as given in Figure 3.28. Damping level of the TVA depends on distance between copper plates and magnets so clearance between rods and bearings should be minimized otherwise TVA mass may move other directions which causes to change damping level of the TVA.
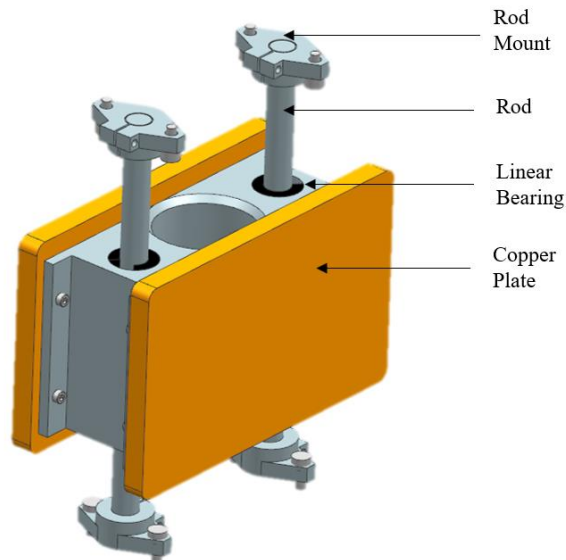
Figure 3.28. TVA mass and its linear motion system

3.1.6. Design Of TVA Body

Design of helical spring, damping element and TVA mass are completed and there is required to a body to connect these parts each other. As shown in Figure 3.29, offered TVA body consists of two side plates, two base plates and eight connection parts. Each plate has simple holes or thread holes for bolt connection.
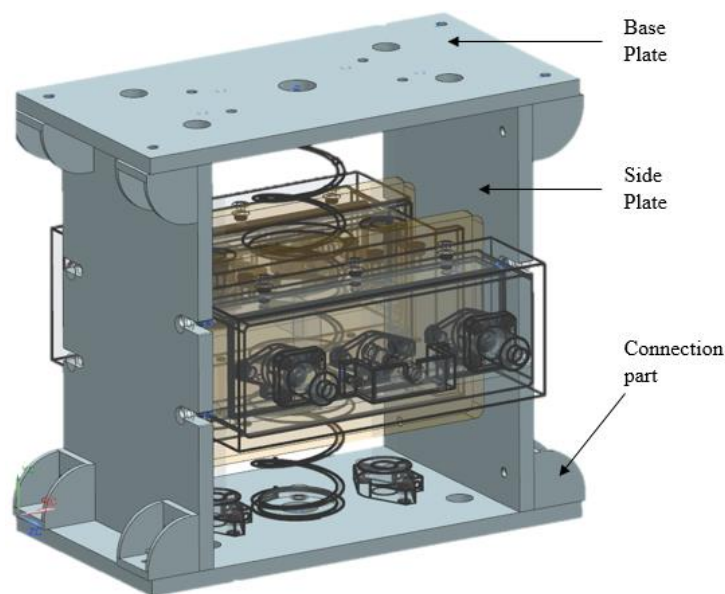
Figure 3.29. TVA body

There are also four connection hole each base plate to connect to the main structure. Its diameter is 13mm so four M12 bolts can be used for mounting the TVA.

3.1.6.1. Modal Analysis Of TVA

Natural frequency of TVA is also important because of resonance. Natural frequencies of the TVA should be as bigger as tuning frequency, such as five times bigger. Modal analysis of TVA is conducted with a commercial software. Analysis model is shown

in Figure 3.30. Solid model of the spring is not used in the analysis model, two preloaded spring elements are added to the analysis model. TVA is fixed with four holes as shown A, B, C and D in Figure 3.30. Frictionless contacts are defined between rods and bearings as shown E and F in Figure 3.30 so TVA mass bearings can move in y direction. Bolts are not added to analysis model and all touched parts are bonded. Material damping and eddy current damping are not defined in the analysis model.
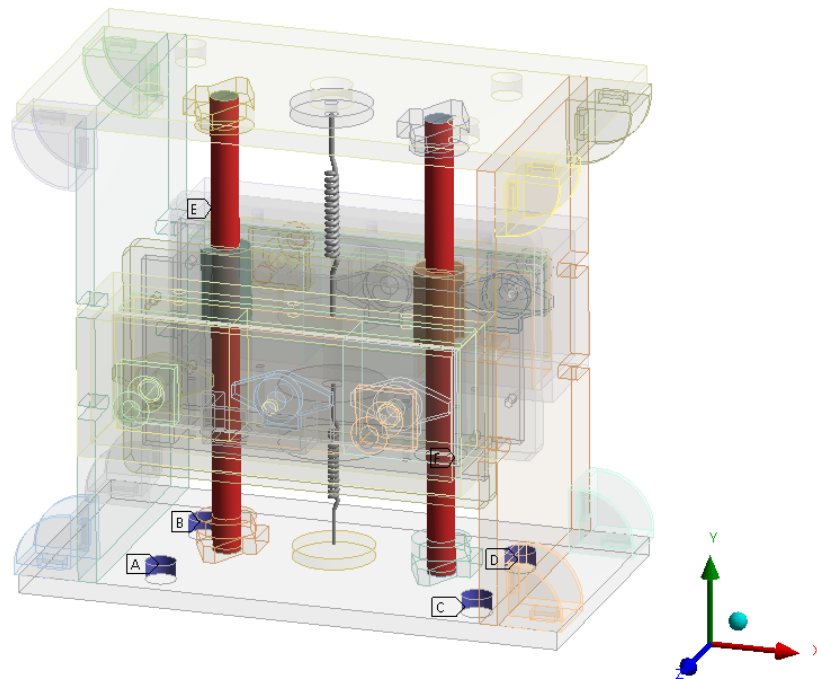
Figure 3.30. Boundary Conditions of TVA

Modal analysis is performed with above given boundary conditions and first ten natural frequencies of TVA are given in Table 3.10. First mode of TVA is tuning frequency and second natural frequency is at 200 Hz and corresponding mode shape of the TVA is given in Figure 3.31. The ratio of the second natural frequency to the first natural frequency is about 35 so it can be said that second natural frequency of the TVA is far enough the tuning frequency.

Table 3.10. First ten structural natural frequencies of TVA

Mode	f_n [Hz]
1	5.67
2	199.64
3	219.64
4	230.53
5	309.62
6	318.27
7	497.42
8	704.74
9	722.18
10	1068.1
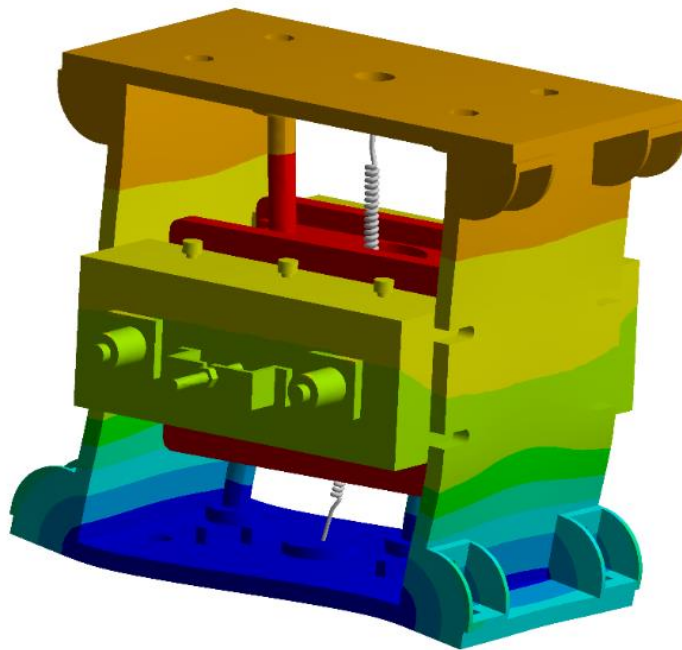
Figure 3.31. Second mode shape of the TVA

Furthermore, TVA natural frequency and main structure natural frequency should not coincidence. Main structure, battle tank in Büyükcivelek's work, natural frequencies

are given in Table 3.11. Second natural frequency of the TVA is higher than first seven natural frequency of the main structure.

Table 3.11. First seven natural frequencies of main structure [1]

Mode Number	Frequency [Hz]
1	6.07
2	19.75
3	45.54
4	93.57
5	145.12
6	178.49
7	191.85

3.1.6.2. Transient Analysis of TVA

It is assumed that TVA is exposed the shock in all directions, separately. Analysis model of the TVA is the same as the analysis model of modal analysis. But in transient analysis model there are two damping sources, eddy current damping and material damping. Eddy current damping is added via spring elements, there are two spring elements so it is defined $142 \frac{Ns}{m}$ damping coefficient for each spring element. It is recommended that 0.05 percent damping for bolted structure under 50 percent yield stress level [88]. It is assumed that damping ratio of TVA is 0.05. Boundary conditions of analysis model is the same as the analysis model of modal analysis Total analysis time is 0.2s and analysis is divided into 8000 substeps. It is assumed that shock load is 1000g half sine in all directions and duration is 0.5ms. Shock is defined in three directions separately.

Maximum von-Mises stress of TVA parts are given in Table 3.12. Yield stress of materials are assumed allowable stress and factor of safety is calculated with Equation 3.33.

$$n = \frac{\sigma}{\sigma_y}$$
Equation 3.32

where n is factor of safety. σ is occurred maximum von-Mises stress. σ_y is yield stress of material.
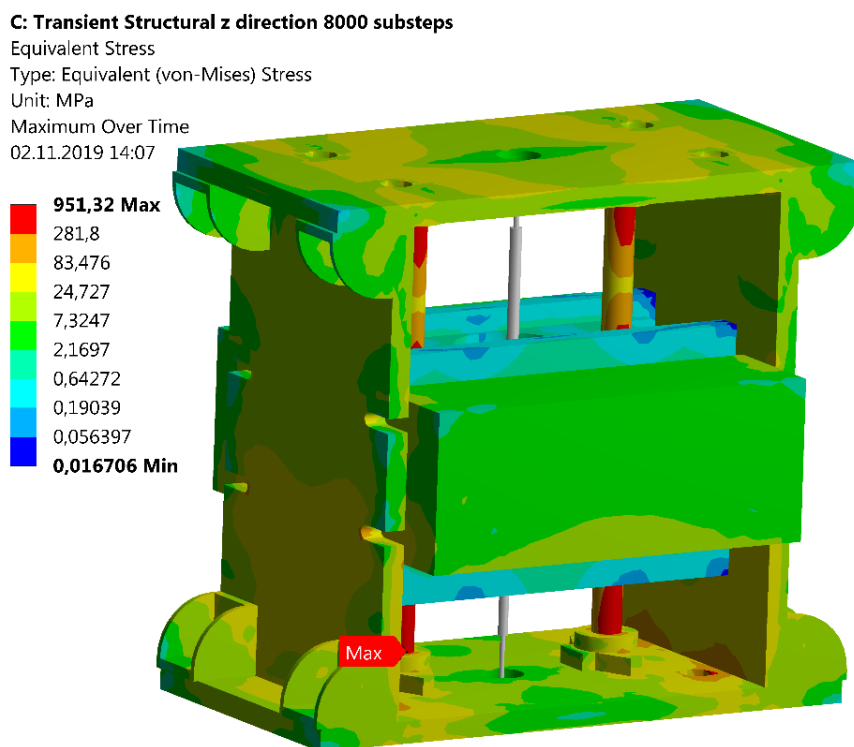
Figure 3.32. Von-Misses stress distribution of the TVA under the shock in z direction

Table 3.12. Maximum von-Mises stress of TVA part and factor of safety

	von-Mises Stress, x direction [MPa]	von-Mises Stress, y direction [MPa]	von-Mises Stress, z direction [MPa]	Max Von-Mises Stress [MPa]	Yield Stress [MPa]	Factor of Safety
Aluminum parts	481	115.2	503.9	450	503 [89]	1.1
Copper parts	3.95	0.33	5.95	5.95	33 [90]	5.5
Magnets	54.8	35.4	69	69	80	1.2
Steel parts (rods)	910.5	73.6	951.3	951.3	1100 [91]	1.2

Maximum von-Mises stress of the copper parts, magnets and steel parts is lower than their yield stress so factor safety of them is higher than 1. Maximum von-Mises stress of the aluminum parts is higher than yield stress. Maximum von-Mises stress, 504 MPa, occurs in one of the connection holes which is used as fixed support. Stress decreases sharply and over the 450 MPa stress is colored black in Figure 3.33 and it is very small area so it is accepted that maximum stress of the aluminum parts is 450 MPa.
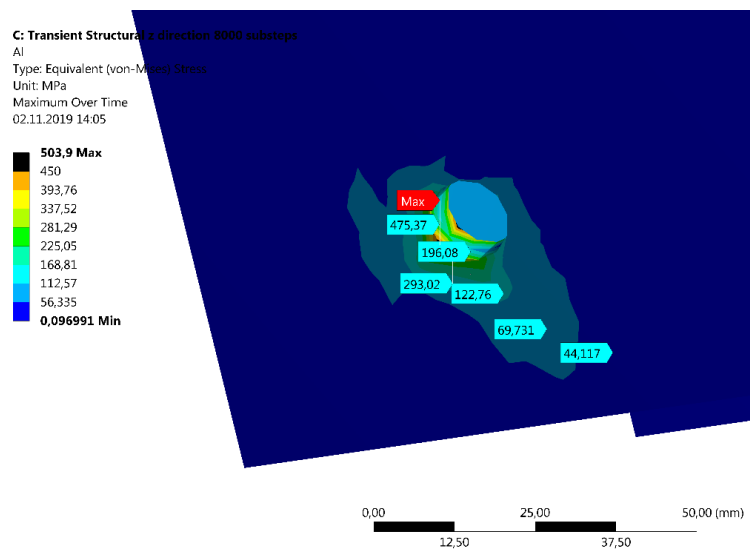
Figure 3.33. Detail view of von-Mises stress distribution of base plate

3.1.7. Fatigue Life Estimation

TVA is expected to be subject to random vibration so life of the TVA is estimated under random vibration. When loading is random or duration of time is long or geometry is complex, estimation of life in time domain is time consuming process and it is not practical. Estimation in frequency domain is a practical approach[92]. Loading and stress are random, so they have multiple amplitude and frequency content. They can be represented using power spectral density PSD and probability density functions PDF.

To estimate fatigue life under random vibration, transfer function $H(\omega)$ between one-unit input and stress output of the system should be obtained. For a linear single degree freedom system, response PSD in terms of stress can be calculated with Equation 3.33.

$$G(f)_{PSD}^{\text{Re}sponse} = \left| H(\omega) \right|^2 . G(f)_{PSD}^{Input}$$

Equation 3.33

where H(ω) is transfer function between input load and output stress of the part. $G(f)_{PSD}^{Input}$ is input psd of the system. $G(f)_{PSD}^{\text{Re}sponse}$ is stress output psd of the system under random vibration. H(ω) is obtained by applied unit input along interested frequency range with a finite element analysis program. After obtained response output psd $G(f)_{PSD}^{\text{Re}sponse}$, probability density function of stress range $p(S)$ is calculated to estimate life of TVA. A typical PDF of stress range is shown in Figure 3.30.
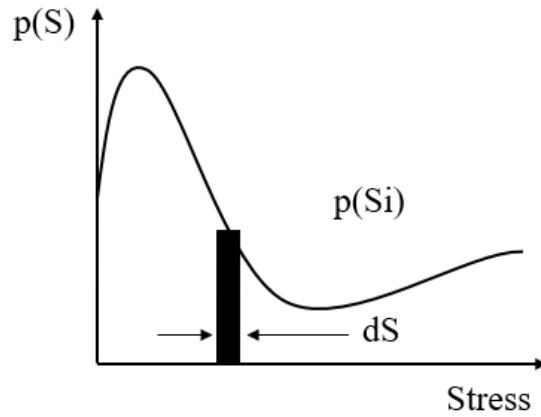
Figure 3.34. A sample of pdf adapted from [93]

In Figure 3.30, dS is bin width S_t is total number of cycles in the histogram. Probability of stress range between $S_i - \dfrac{dS}{2}$ and $S_i + \dfrac{dS}{2}$ can be calculated with p(S).dS. Total number of cycles $n(S)$ for a specific stress level S can be calculated with Equation 3.34.

$$n(S) = p(S).dS.S_t \qquad\qquad \text{Equation 3.34}$$

Stress response of TVA is random so they have different cycles and amplitudes. Let assume n_1 is number of cycles of S_1 stress level. This stress causes damage and total damage for different cycles for specific stress can be calculated with Equation 3.35.

$$D = \sum \frac{n_i}{N_i} \qquad\qquad \text{Equation 3.35}$$

81

A S-N curve shows life a material. Horizontal axis is number of cycle and vertical axis is stress. The curve can be expressed with Equation 3.36.

$$N = C.S^{-b}$$

Equation 3.36

where b is Basquin exponent and C represents interception of vertical axis of S-N curve. Expected damage $E[D]$ can be obtained by using Equation 3.34, Equation 3.35 and Equation 3.36.

$$E[D] = \sum_i \frac{n_i(S)}{N(S_i)} = \frac{S_t}{C} \int_0^\infty S^b . p(S).dS$$

Equation 3.37

To calculate random vibration life, probability density function $p(S)$ in Equation 3.37 should be obtained. There are needed to define statistical terms, spectral moments m_n, upward mean crossing $E[0]$, peaks $E[P]$ and irregularity factor γ to obtain it. A PSD is given in Figure 3.35.
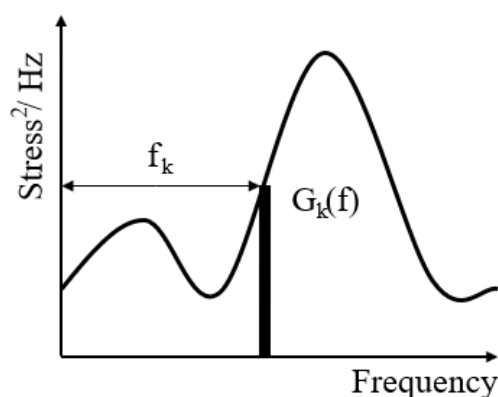
Figure 3.35. Spectral moments of a sample PSD adapted from [93]

Spectral moments m_n of a PSD can be calculated with Equation 3.38 [94].

$$m_n = \int_0^\infty f_n . G(f) df = \sum_{k=1}^m f_k^n \times G_k(f) \times \delta f \qquad \text{Equation 3.38}$$

where δf is frequency increment. Number of upward mean crossing $E[0]$, peaks $E[P]$ can be obtained with Equation 3.39 and Equation 3.40 [94]

$$E[0] = \sqrt{\frac{m_2}{m_0}} \qquad \text{Equation 3.39}$$

$$E[P] = \sqrt{\frac{m_4}{m_2}} \qquad \text{Equation 3.40}$$

Irregularity factor γ of a PSD are defined as following formula.

$$\gamma = \frac{E[0]}{E[P]} = \sqrt{\frac{m_2^2}{m_0 m_4}} \qquad \text{Equation 3.41}$$

Dirlik [95] offered a method for calculating probability density function.

$$p(S) = \frac{\dfrac{D_1}{Q} . e^{\frac{-Z}{Q}} + \dfrac{D_2 . Z}{R^2} . e^{\frac{-Z^2}{2 . R^2}} + D_3 . Z . e^{\frac{-Z^2}{2}}}{2\sqrt{m_0}} \qquad \text{Equation 3.42}$$

where S is stress range and other parameters are given in Equation 3.43 - Equation 3.49.

83

$$D_1 = \frac{2\left(x_m - \gamma^2\right)}{1 + \gamma^2}$$

Equation 3.43

$$D_2 = \frac{1 - \gamma - D_1 + D_1^2}{1 - R}$$

Equation 3.44

$$D_3 = \frac{1 - D_1 + D_1}{1 - R}$$

Equation 3.45

$$Q = \frac{1.25 - \left(\gamma - D_3 - D_2 R\right)}{D_1}$$

Equation 3.46

$$R = \frac{\gamma - x_m - D_1^2}{1 - \gamma - D_1 + D_1^2}$$

Equation 3.47

$$Z_i = \frac{S}{2\sqrt{m_0}}$$

Equation 3.48

$$x_m = \frac{m_1}{m_0} \sqrt{\frac{m_2}{m_0}}$$

Equation 3.49

Life estimation of TVA is conducted with given above method. Life estimation of spring and TVA with spring elements are conducted separately because springs are preloaded. A commercial finite element analysis software and life estimation software are used for life estimation.

A flow chart is shown in Figure 3.36 which is summarized above mentioned life estimation process. Static analysis is conducted for preloaded springs to obtain stress distribution. Output of static analysis is used for both modal analysis and response stress PSD. Modal analysis and harmonic analysis are conducted to obtain transfer function between one unit acceleration input and stress distribution of TVA. All analyzes so far are conducted with FEA software. After this point commercial life estimation software is used to estimate life. It follows given above method.
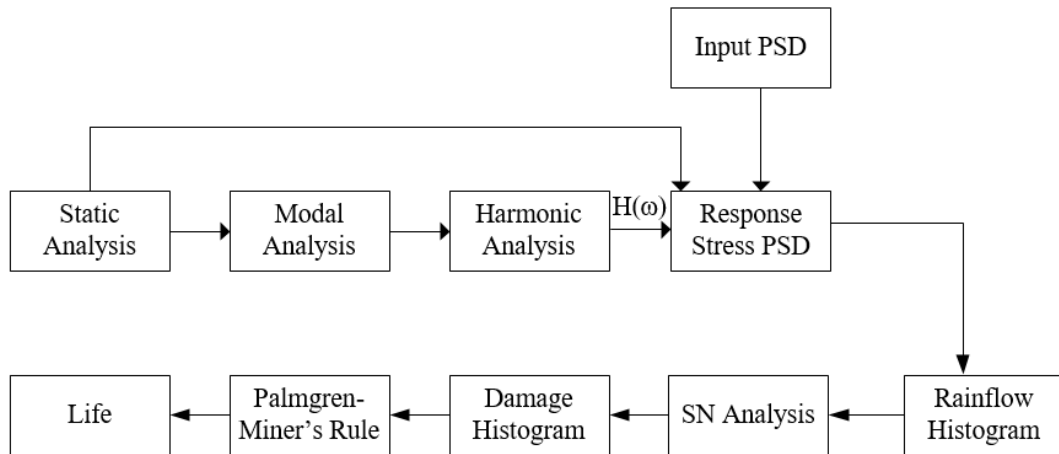
Figure 3.36. Flow chart of life estimation TVA adapted from [92]

3.1.7.1. Fatigue Life Of TVA

Under random vibration, life of the offered TVA is estimated. Life estimation model does not consist of all parts of the TVA. Analysis model contains bearings and magnets but their materials are assigned as aluminum so life estimation does not comprise estimation of them. Bolts are not added analysis model. Springs of the TVA are added as spring elements to analysis model. Boundary condition of the model is same as boundary condition of modal analysis.

Flow chart of estimation of random vibration life for preloaded structure is given in Figure 3.36. Static analysis is not conducted for TVA life estimation. Firstly, modal analysis is performed to obtain estimate random vibration life of the offered TVA body. Then, harmonic analysis is conducted under a unit load to obtain frequency response function. One unit acceleration applied on four connection holes shown as A, B, C and D in Figure 3.30. Maximum frequency range is 500 Hz with 0.05 damping ratio.
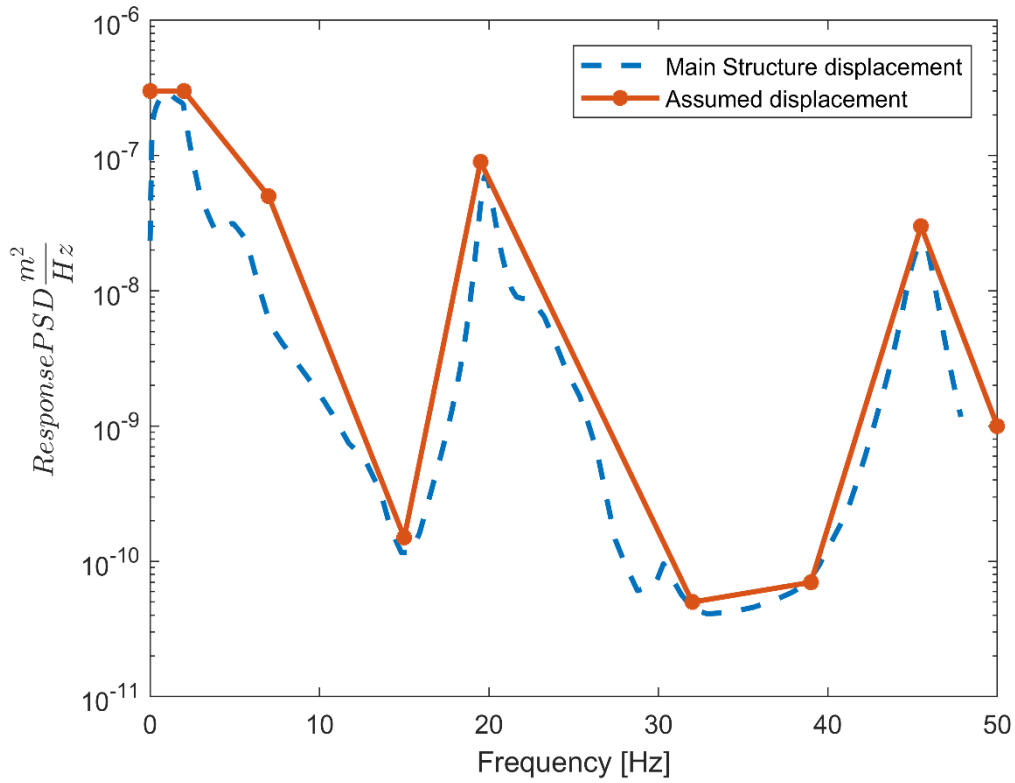
Figure 3.37. Main structure displacement psd and assumed displacement psd

In Büyükcivelek's study, it is given displacement psd of the main structure where the TVA is attached between 0-50 Hz. Main structure displacement psd and assumed displacement psd are given in Figure 3.37. Displacement psd is about $10^{-9}\frac{m^2}{Hz}$ at 50Hz, it is assumed that psd displacement decreases linearly to $10^{-12}\frac{m^2}{Hz}$ at 250 Hz.

After that all information, random input, output of the analysis (transfer function of the system) is entered to the software to obtain fatigue life of the absorber. Dirlik [95]method is used for psd cycling method and absolute maximum principal stress is used for stress combination. Estimated life of the TVA body is given in Figure 3.38 which is infinite.

Table 3.13. Displacement PSD of main structure

Frequency [Hz]	Displacement PSD [$\frac{m^2}{Hz}$]
5.00E-04	3.00E-07
2	3.00E-07
7	5.00E-08
15	1.50E-10
19.5	9.00E-08
32	5.00E-11
39	7.00E-11
45.5	3.00E-8
50	1.00E-09
250	1.00E-012
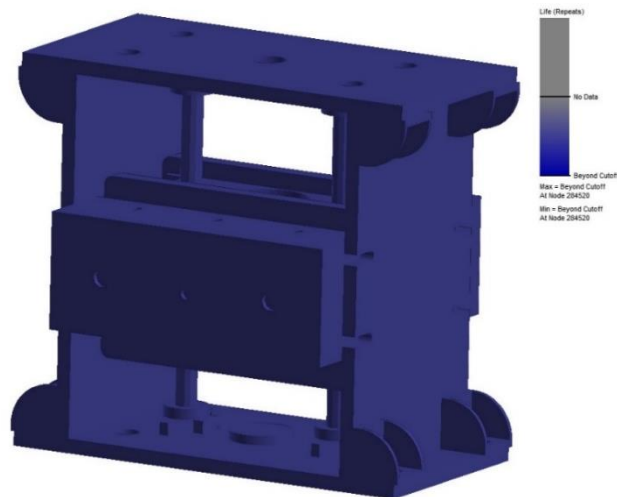
Figure 3.38. Random fatigue life of the TVA body

3.1.7.2. Fatigue Life of TVA Spring

The spring is preloaded so static analysis are conducted to add mean stress due to pre-load. Boundary conditions of static analysis is same as modal analysis boundary

conditions. 40 mm preload is given to one end which is shown as B in Figure 3.11. After that, modal analysis is repeated to obtain natural frequency of the preloaded spring as given previous section.

To obtain transfer function of the spring, a harmonic analysis is conducted until the 260 Hz. The spring is fixed at one end which is shown as A in Figure 3.11 and one unit acceleration in -y direction input is given in other end of the spring as shown as B in Figure 3.11. A constant damping ratio, 0.005 %, is added to analysis model which is represent material damping. Harmonic analysis calculates transfer function for whole domain. As an example, normal stress in y direction of the point is given in Figure 3.39.
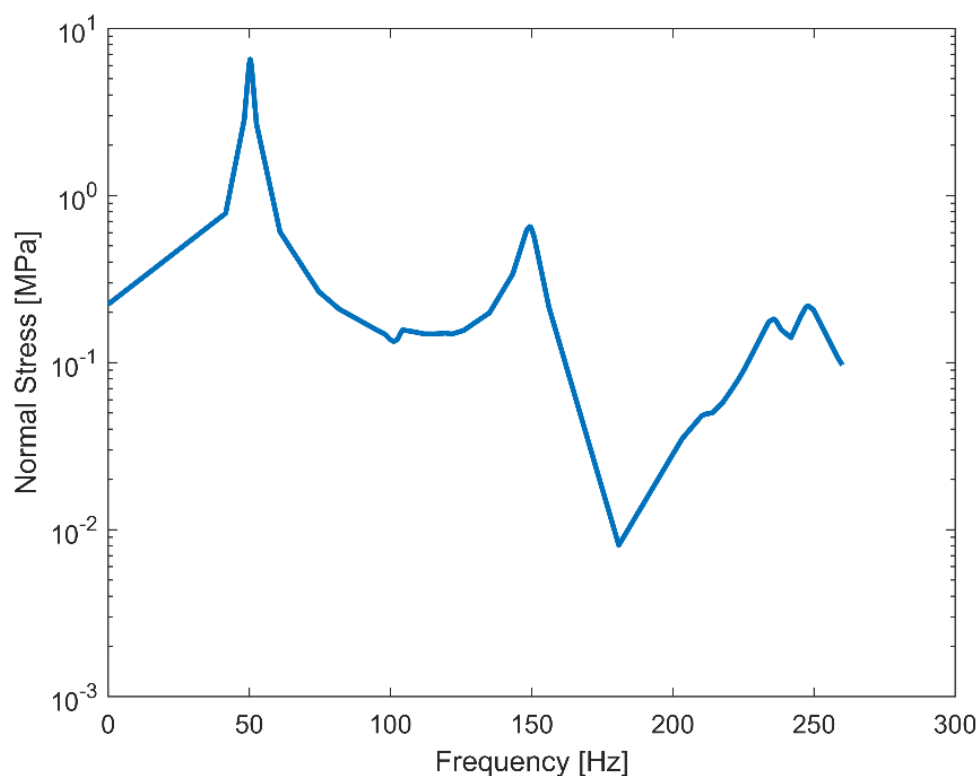
Figure 3.39. Normal stress in y direction Frequency response function of the point in normal

Büyükcivelek calculated relative displacement of TVA mass. Relative displacement of TVA mass and assumed displacement psd of spring end are shown in Figure 3.40. Assumed displacement psd is used as input psd of the spring and they are given in Table 3.14.

Table 3.14. Displacement psd of TVA mass

Frequency [Hz]	PSD [$\frac{m^2}{Hz}$]
0.1	2.50E-02
4	1.00E-07
6	1.00E-07
9	1.00E-10
20	1.00E-13
48	1.00E-16
250	1.00E-17
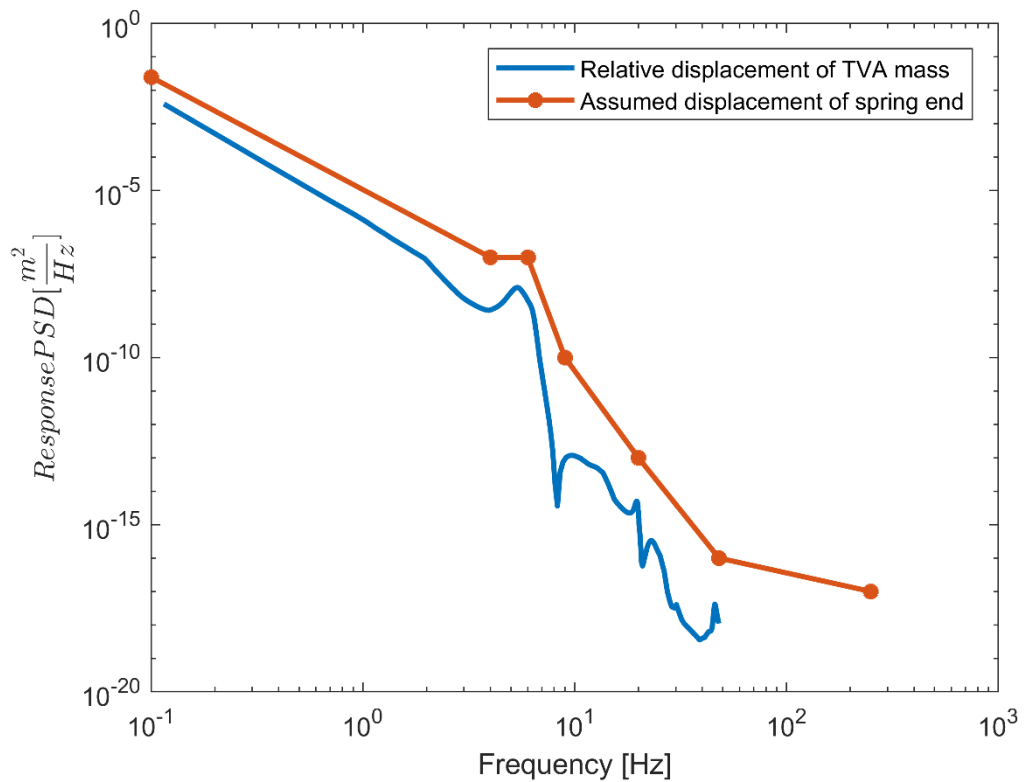
Figure 3.40. Relative and assumed displacement psd of TVA mass

After obtained random input displacement psd and transfer function (output of finite element analysis) between a unit input and stress output, a commercial software is used to estimate spring life. Dirlik method is used for psd cycle counting because it is general purpose technique and applicable to both narrow and broad wideband [92]. Absolute maximum principal stress is used for stress combination. Result of fatigue life estimation by the software is given in Figure 3.41 and life of the spring is infinite.
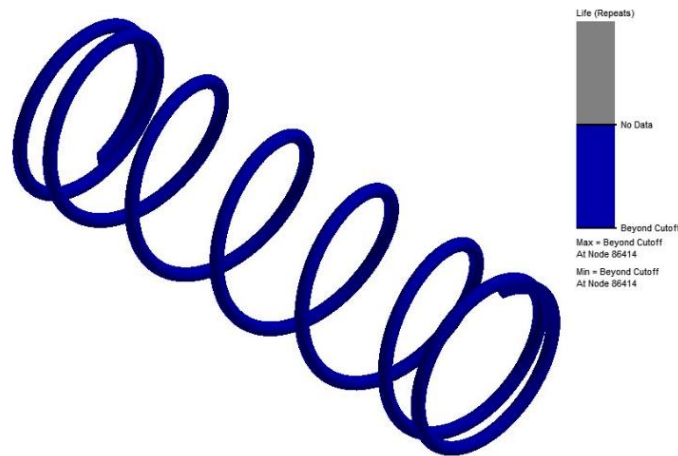
Figure 3.41. Fatigue life of estimation of the spring

After design and prototype fabrication is completed, TVA performance should be validated with experiment. Since tuning frequency and damping level of the TVA is critical in terms of its vibration reduction performance, they must be measured and checked experimentally. Designed TVA is characterized by vibration experiments, for which details are given in Chapter 4.

CHAPTER 4

VALIDATION OF TVA PROTOTYPE

Having designed TVA, it was manufactured as shown in Figure 4.1. It can work between $-40^{o}C$ and $70^{o}C$, there is no limitation for low temperature for damping. Its dimensions are 236mmx123mmx216mm and its total mass 11kg. Its damping level is adjustable via changing distance between magnets and copper plates or number of magnet block. To set distance exactly, a plate which thickness is 1-5 mm is needed.
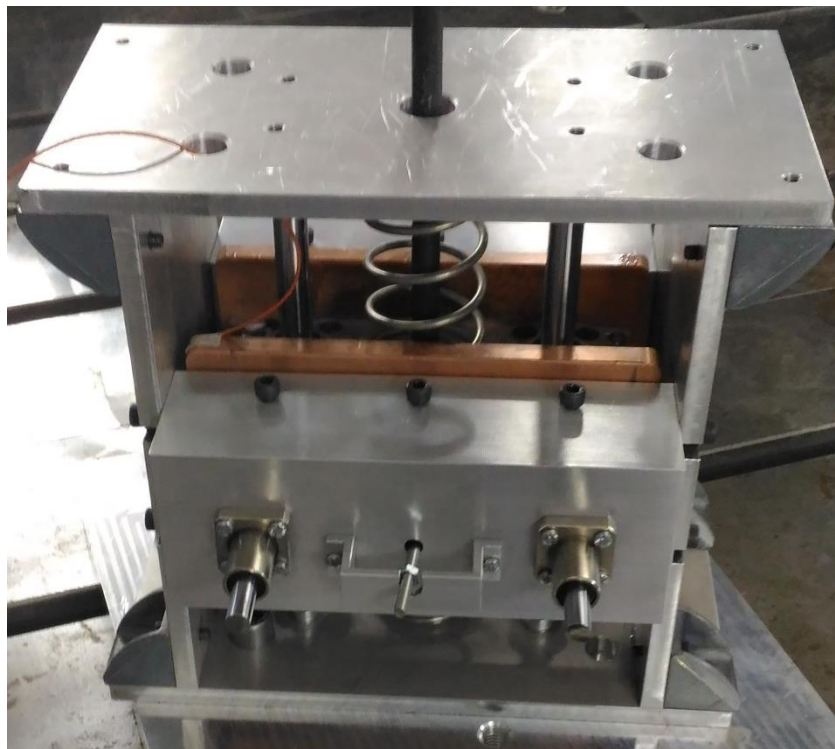
Figure 4.1. Realized TVA

Parameters of TVA are very critical for its performance. If they are not set correctly, it may increase vibration of main structure instead of decreasing it. To ensure TVA parameters are correct, modal test of the TVA is essential.

Spring manufacturers says that stiffness of manufactured spring may change ±10 percent from designed one. This uncertainty may cause approximately ±5 percent tuning natural frequency. Eddy current damping level of TVA may vary likewise tuning frequency. This decrease TVA performance.

To eliminate these uncertainties and specify TVA performance, measurement of natural frequency and damping of TVA is compulsory. Damping of TVA is adjustable via changing distance between magnets and copper plate so experiments are repeated for all configurations.

This chapter deals with measurement of TVA mass, tuning frequency and damping coefficient of TVA. Impact hammer tests are conducted to measure them. Data acquisition system gives directly frequency response function of the TVA. After measurement of frequency response function of TVA, natural frequency and damping are extracted from test data. Test set-up, extraction of TVA parameter process and results are given in the following sections.

4.1. Test Set-Up

Impact hammer test is conducted to determine the TVA parameters. TVA is mounted to a fixture with 4 bolts and it is also mounted to armature of tensile test machine as shown in Figure 4.2. To apply impulse to TVA mass, a M10x200 bolt is installed on TVA mass as shown in the figure.
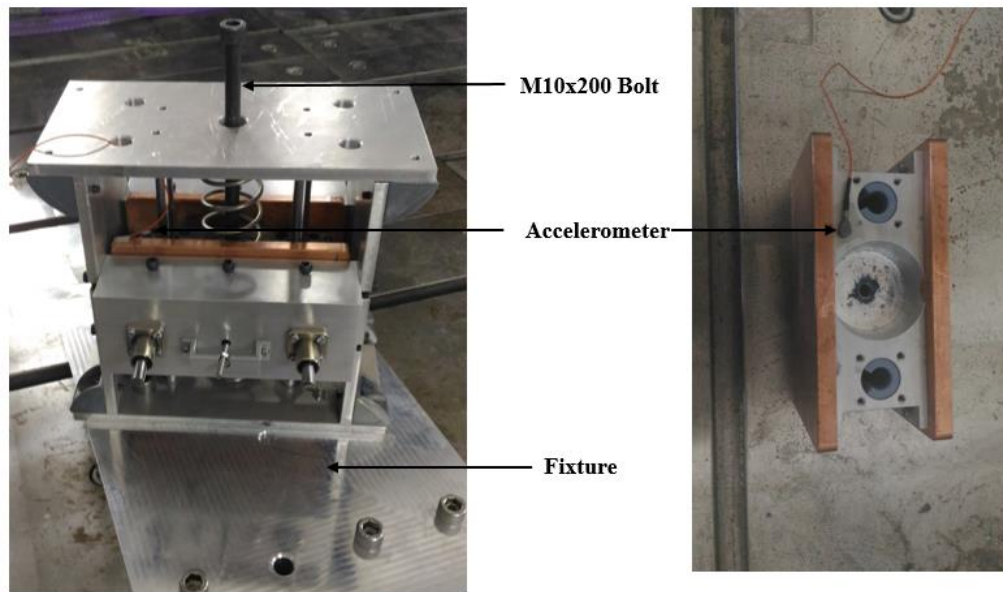
Figure 4.2. Impact hammer test set-up

Test set-up is shown in Figure 4.3. Data is acquired with one accelerometer (Dytran 3225m23) and it is glued on TVA mass as shown Figure 4.2. Mass of the accelerometer is 1g so it is expected that it does not change the dynamics properties of TVA. Its measurement range is 100g.
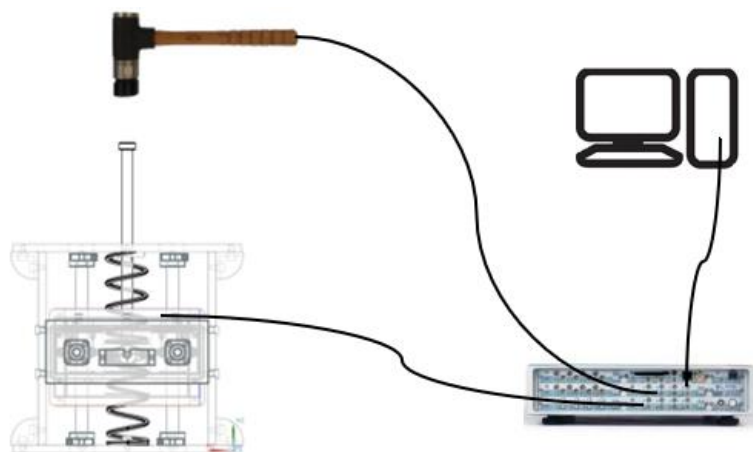
Figure 4.3. Test set-up view

TVA mass is increased because M10x200 is installed. TVA mass is measured without and with M10 bolt. Mass difference between them is 0.1 kg as shown in Figure 4.4. It is assumed that this increment has very limited effect on tuning frequency.

(a)   (b)
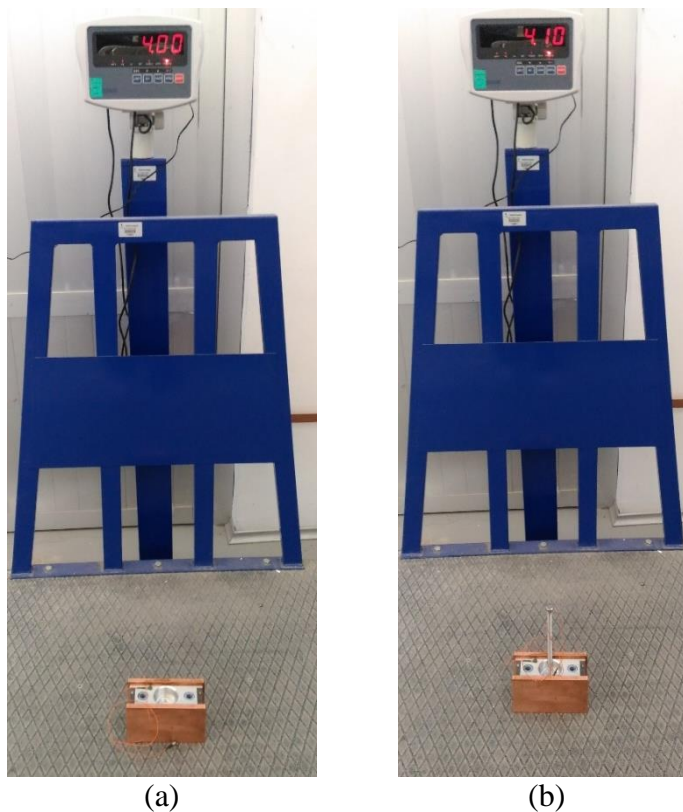
Figure 4.4. Measurement of TVA mass (a) without modification, (b) with M10x200 bolt

To measure frequency response of the TVA, impulse is given with hammer (Brüel & Kjær 8208). Its maximum force 22,2 kN. There is a load cell on the hammer, and it measures input impact force.

Both acceleration and impulse signals are collected with data acquisition system. Its software calculates frequency response function of the TVA as shown in Figure 4.5.

Tuning frequency is 5.67 Hz and second natural frequency of the TVA is 200Hz so only one peak is shown in the figure. To obtain frequency response function, TVA mass is hit ten times and data is collected to 25.6 Hz. Frequency resolution is 0.1 Hz.
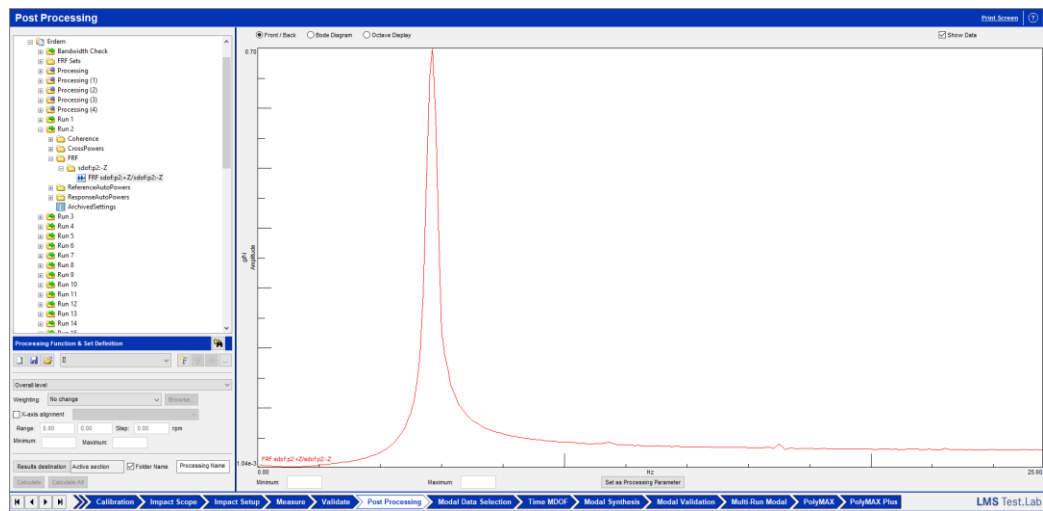
Figure 4.5. Screenshot Measured frequency response function of the TVA by daq system

4.2. TVA Test Configurations

TVA damping level is adjustable via changing distance between magnets and copper plates. Distance range varies between 1mm to 5mm. Cross section view of TVA is shown in Figure 4.6.

There is a plate behind glued to magnets. An arrangement bolt with two nuts connected to the plate. There is also an obstacle plate between nuts so nut cannot move freely. Let assume magnets touch copper plate. Forget Nut #1 and by tightening nut #2, nut try to move -z direction but there is obstacle plate. Therefore, it cannot move and pull bolt, plate and magnets in z direction so distance between copper and magnets increases. To decrease distance, forget nut#2 and loosen nut#1 so nut#1 wants to move

in z direction but there is an obstacle plate and it cannot move in z direction. Therefore, arrangement bolt, plate and magnets move in -z direction so distance between copper and magnets decreases. After distance is arranged upper three bolt tighten to fix magnets.

TVA configurations are given in Table 3.7. The first configuration is without magnet case. It is necessary for measure damping level of the TVA without eddy current damping. Each configuration test is repeated two times and forty-six tests were conducted for all configuration.
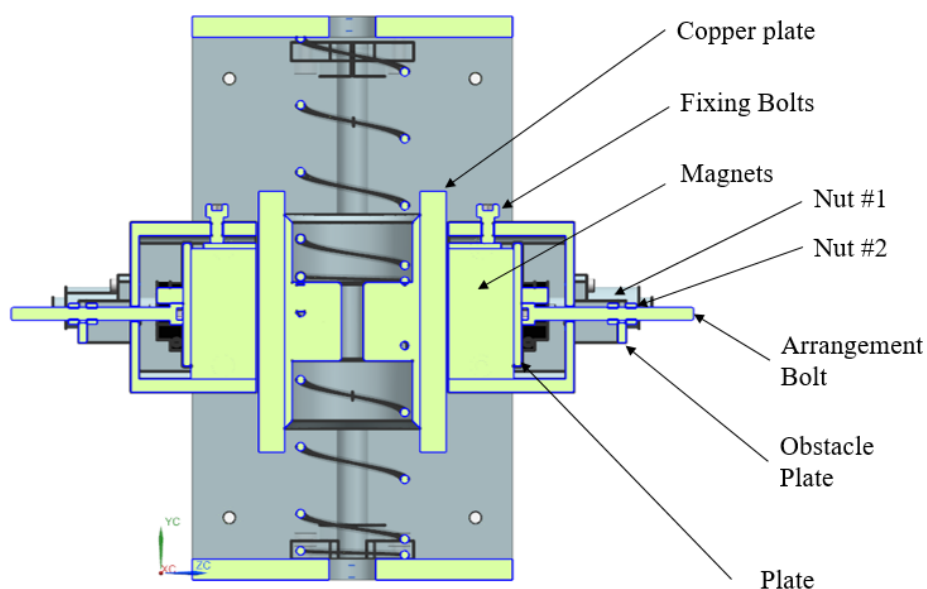
Figure 4.6. Cross section view of TVA

Frequency response function of the TVA for different configurations are measured and magnitude of frequency response functions are given in Figure 4.7.
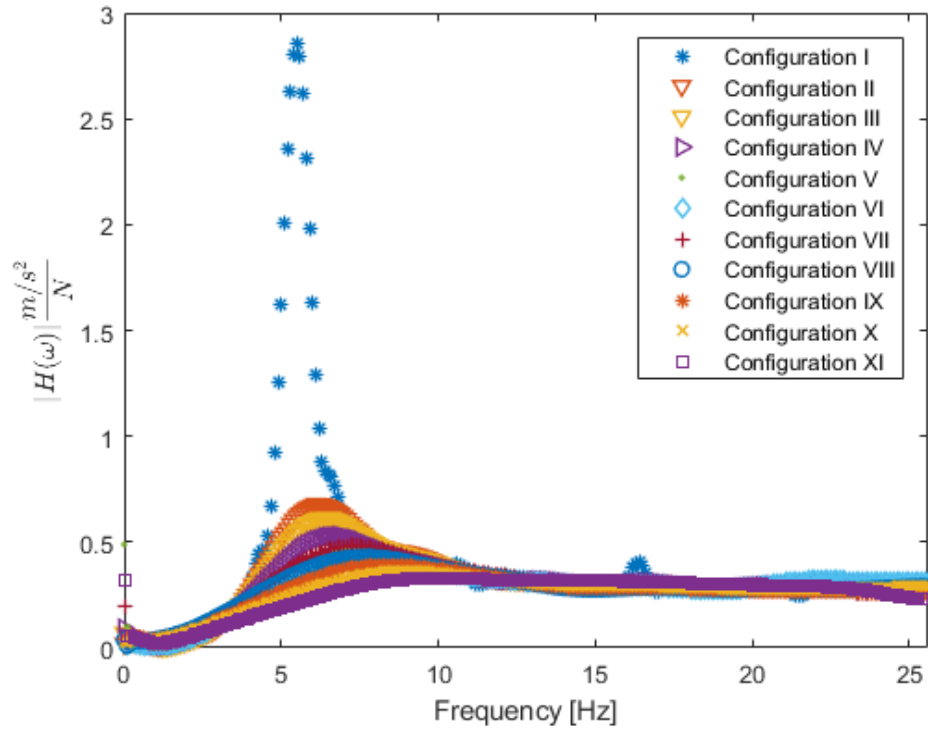
Figure 4.7. Magnitude of frequency response function of TVA for different configurations

Data is collected until 25.6 Hz. There should be one peak on the frequency response function plot for each configuration. Peak for no magnet configuration is the highest, height of peak dramatically decreases when distance between magnets and copper plates decreases or number of magnets increases. This means that damping level of the TVA increases while distance decreases as expected. Level of damping and natural frequency of the TVA for each configuration are estimated in the next two sections.

4.3. Extraction Of TVA Tuning Frequency From Test Data

It is expected that damping level of the TVA is too high. Method for estimation of natural frequency level in the literature is generally for low damping. There are also some methods for higher damping level. But a very simple way is preferred in this

study. Tuning frequency of the TVA is about 5.67 Hz and the second natural frequency of the TVA is about 200 Hz, and data is collected until 25.6 Hz so it can be seen only first degree of freedom of the TVA. Frequency response function of a single degree of freedom system in terms of acceleration and force is called accelerance and can be calculated with Equation 4.1 [96]. There are four variables in this equation.

$$A(\omega) = \frac{-\omega^2}{k - \omega^2 m + i\omega c}$$
Equation 4.1

where ω is frequency. k is stiffness of spring. m is TVA mass. c is damping coefficient of TVA. Frequency response function of the TVA for all configuration is obtained with experiments. If mass, stiffness and damping coefficient of the TVA are known frequency response function can be obtained with the equation. Real part and phase of accelerance of the TVA with optimum mass and stiffness for different damping ratio are given in Figure 4.8 and Figure 4.9.

Natural frequency for all damping level is constant and all curve intersects at tuning frequency, 5.67 Hz. Real part of the accelerance is 0 and phase angle is 90° at the natural frequency. In this study, natural frequency of the TVA is estimated via experimental real part of accelerance and phase angle separately.

To estimate natural frequency of the TVA, two nearest point for each graphics are selected and then they are interpolated to 0 and 90° in real part and phase graphics, respectively. For Configuration I, these interpolated points and estimated natural frequency of the TVA are given in Table 4.1 and Table 4.2

98
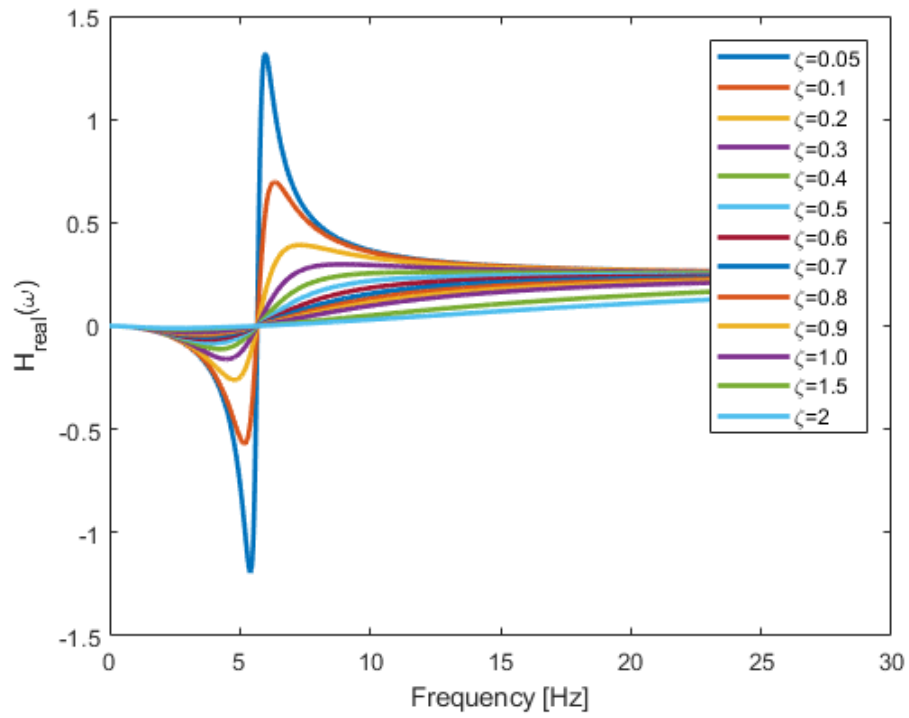
Figure 4.8. Real part of the accelerance of the TVA for different damping ratios
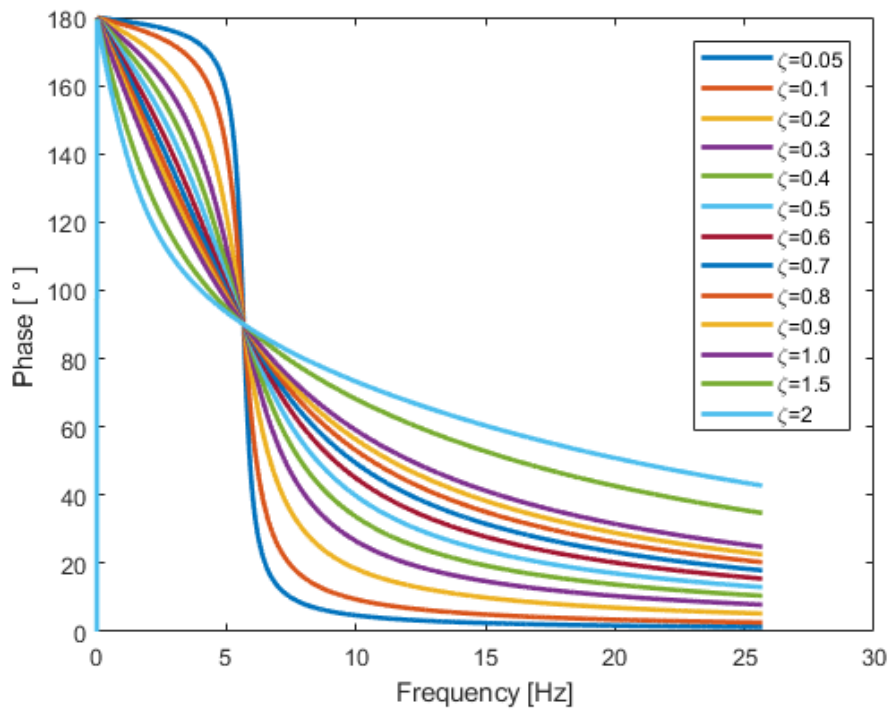
Figure 4.9. Phase angle of accelerance of the TVA for different damping ratios

Table 4.1. Estimated natural frequency of the TVA without magnet via real part of accelerance

	Point I		Point II		
Test No	f	H_{real}	f	H_{real}	f_n^{est} [Hz]
Test #1	5.3	-0.674	5.4	0.04491	5.39
Test #2	5.3	-0.712	5.4	0.02255	5.40

Table 4.2. Estimated natural frequency of the TVA without magnet via phase angle of accelerance

	Point I		Point II		
Test No	f	Phase Angle	f	Phase Angle	f_n^{est} [Hz]
Test #1	5.3	105.423	5.4	89.0554	5.39
Test #2	5.3	105.736	5.4	89.5395	5.40

Estimated natural frequency of the TVA via real part of accelerance is very close that of TVA via phase. It is accepted that natural frequency of the TVA is 5.40 Hz. Natural frequency of the TVA for other configuration are also accepted that it is the same with no magnet configuration's natural frequency because mass and stiffness of the TVA are the same for all configuration.

4.4. Extraction Of TVA Damping Coefficient From Test Data

Having estimated natural frequency of the TVA, damping level of the TVA is estimated via mobility frequency response function of the TVA. Mobility of the a single DOF system can be calculated with Equation 4.2 [96].

$$Y(\omega) = \frac{i\omega}{k - \omega^2 m + i\omega c} \qquad \text{Equation 4.2}$$

It can be written by separating real and imaginary part of mobility as given in Equation 4.3 which is a circle equation whose radius is $\frac{1}{2c}$ and center is at $\left(0, \frac{1}{2c}\right)$ [96].

$$\left(\frac{\omega^2 c}{\left(k - \omega^2 m\right)^2 + \left(\omega c\right)^2} - \frac{1}{2c}\right)^2 + \left(\frac{\omega\left(k - \omega^2 m\right)}{\left(k - \omega^2 m\right)^2 + \left(\omega c\right)^2}\right)^2 = \left(\frac{1}{2c}\right)^2 \qquad \text{Equation 4.3}$$

Nyquist plot of mobility of the TVA with optimum parameters is given in Figure 4.10. As shown in the figure, 1/c is equal to circle diameter. To calculate damping coefficient of the TVA, the largest real part of the mobility is considered and at this point imaginary part of the mobility is very close to zero which are given in Table 4.3. Real part of the mobility is 0.00352. This means that diameter of the Nyquist circle is 0.00352 which is equal to $\frac{1}{c}$ so damping coefficient of the TVA with optimum parameters is $284 \frac{Ns}{m}$.

Table 4.3. Estimated data

	$\text{Re}(Y(\omega))$	$\text{Im}(Y(\omega))$
Estimated point	0.00352	1.94E-06

The data acquisition system gave accelerance of the TVA. Mobility of the TVA is calculated with Equation 4.4.

$$Y(\omega) = \frac{A(\omega)}{i\omega} \qquad \text{Equation 4.4}$$

After converted from accelerance to mobility, damping is estimated for all configuration as mentioned above.

4.4.1. Damping Coefficient Of Configuration I

This configuration is no magnet version of the TVA and damping level of it is minimum as expected. The only damping source is due to structural damping and friction between bearings and rods. Estimated damping coefficient of the TVA is given in Table 4.4 and it is accepted that damping coefficient of the configuration I is 12.27 $\frac{N.s}{m}$.

Table 4.4. Estimated damping coefficient of configuration I

	c $[\frac{N.s}{m}]$
Test #1	12.46
Test #2	12.09

Experimental and estimated nyquist plot and magnitude mobility frequency response function of configuration I are given in Figure 4.10 and Figure 4.11, respectively.

Figure 4.10. Experimental and estimated mobility nyquist plot of the configuration I

Figure 4.11. Experimental and estimated magnitude mobility frequency response function of the TVA for configuration I

4.4.2. Damping Coefficient Of Configuration II

In this configuration, distance between one magnet block and copper plate is 5mm. Estimated damping coefficient of the TVA is given in Table 4.5 and it is accepted that damping coefficient of the configuration II is 56.21 $\frac{N.s}{m}$.

Table 4.5. Estimated damping coefficient of configuration II

	c $[\frac{N.s}{m}]$
Test #1	55.80
Test #2	56.61

Experimental and estimated nyquist plot and magnitude mobility frequency response function of configuration VI are given in Figure 4.12 and Figure 4.13, respectively.

Figure 4.12. Experimental and estimated mobility nyquist plot of the configuration II

Figure 4.13. Experimental and estimated magnitude mobility frequency response function of the TVA for configuration II

104

4.4.3. Damping Coefficient Of Configuration III

In this configuration, distance between one magnet block and copper plate is 4 mm. Estimated damping coefficient of the TVA is given in Table 4.6 and it is accepted that damping coefficient of the configuration III is 63.19 $\frac{N.s}{m}$.

Table 4.6. Estimated damping coefficient of configuration III

	c $[\frac{N.s}{m}]$
Test #1	62.94
Test #2	63.43

Experimental and estimated nyquist plot and magnitude mobility frequency response function of configuration III are given in Figure 4.14 and Figure 4.15, respectively.
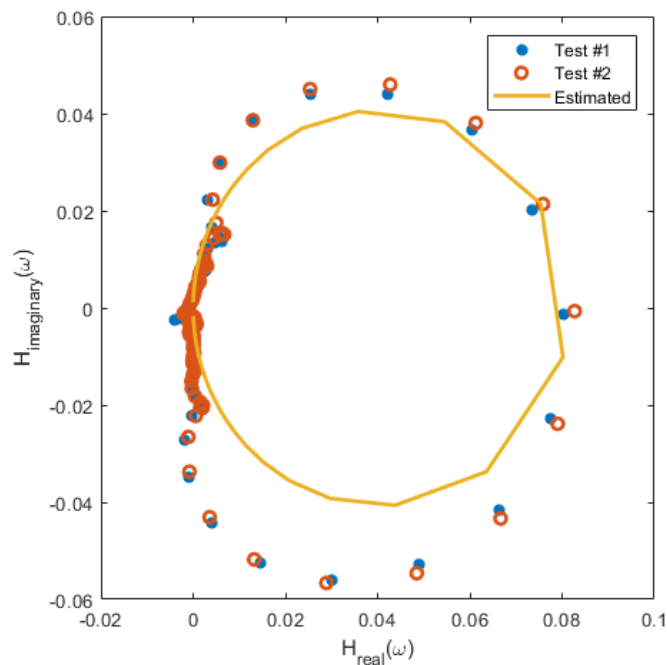

Figure 4.14. Experimental and estimated mobility nyquist plot of the configuration III
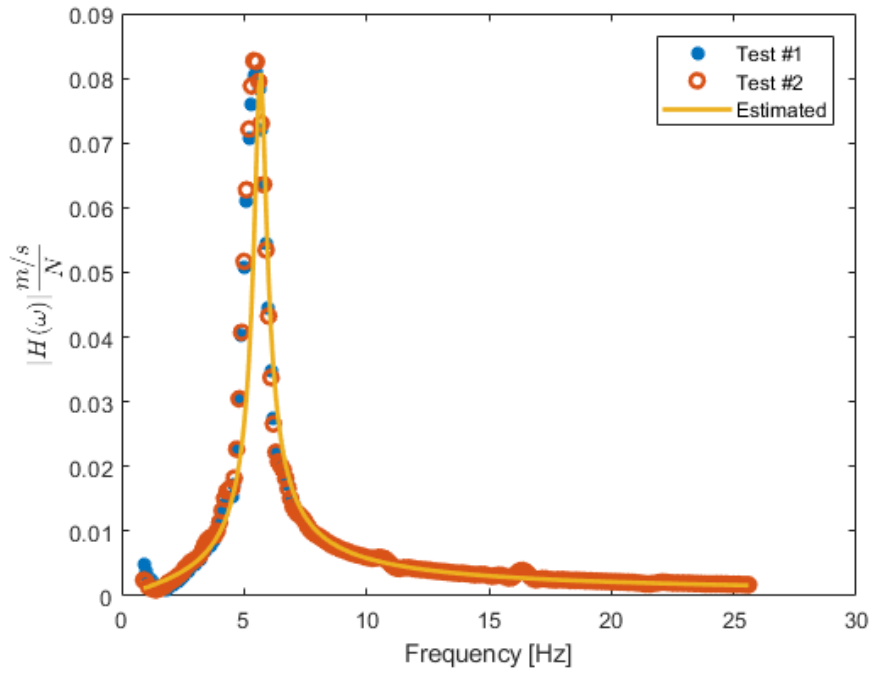
Figure 4.15. Experimental and estimated magnitude mobility frequency response function of the TVA for configuration III

4.4.4. Damping Coefficient Of Configuration IV

In this configuration, distance between one magnet block and copper plate is 3 mm. Estimated damping coefficient of the TVA is given in Table 4.7 and it is accepted that damping coefficient of the configuration IV is 76.59 $\frac{N.s}{m}$.

Table 4.7. Estimated damping coefficient of configuration IV

	c [$\frac{N.s}{m}$]
Test #1	75.17
Test #2	78.00

Experimental and estimated nyquist plot and magnitude mobility frequency response function of configuration IV are given in Figure 4.16 and Figure 4.17, respectively.
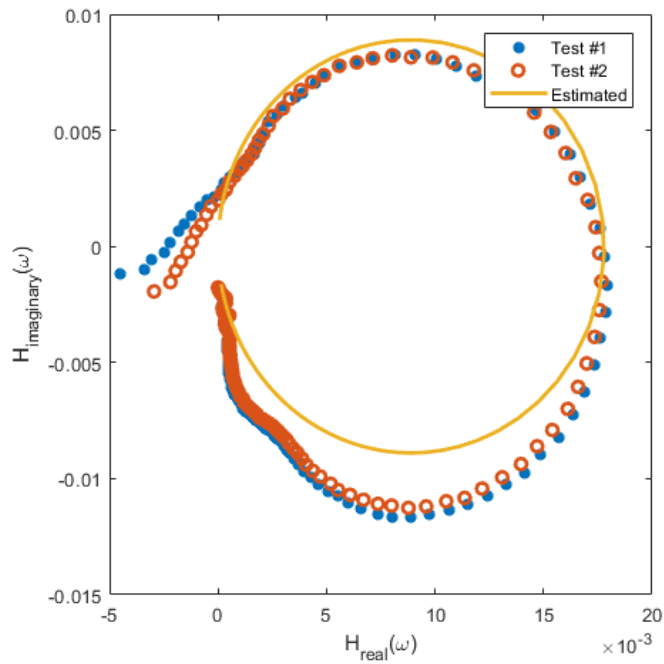
106

Figure 4.16. Experimental and estimated mobility nyquist plot of the configuration IV
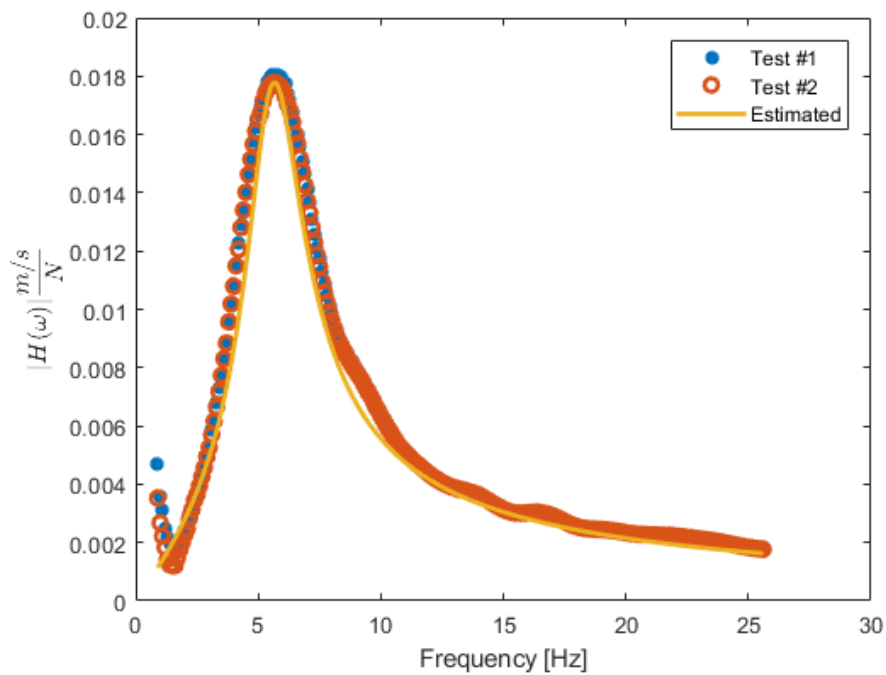

Figure 4.17. Experimental and estimated magnitude mobility frequency response function of the TVA for configuration IV

4.4.5. Damping Coefficient Of Configuration V

In this configuration, distance between one magnet block and copper plate is 2 mm. Estimated damping coefficient of the TVA is given in Table 4.8 and it is accepted that damping coefficient of the configuration V is 89.31 $\frac{N.s}{m}$.

Table 4.8. Estimated damping coefficient of configuration V

	c $[\frac{N.s}{m}]$
Test #1	92.51
Test #2	86.10

Experimental and estimated nyquist plot and magnitude mobility frequency response function of configuration V are given in Figure 4.18 and Figure 4.19, respectively.
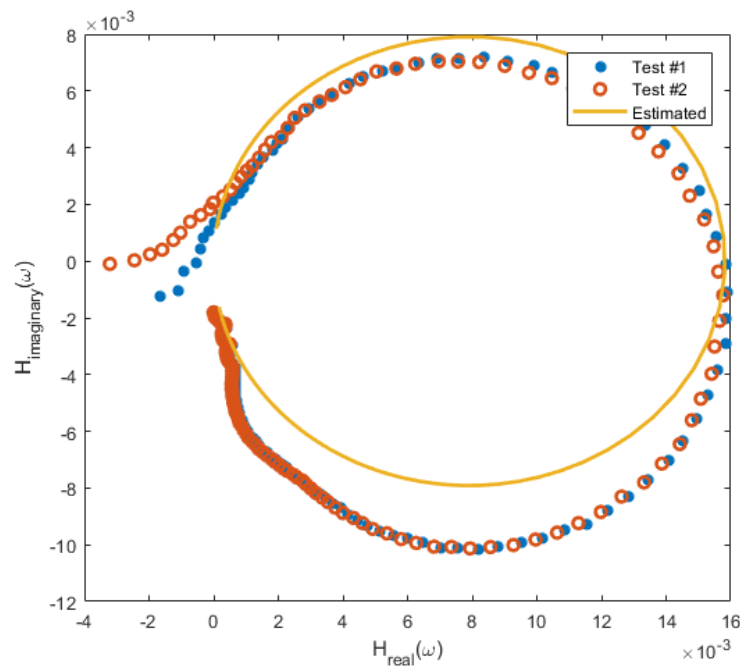

Figure 4.18. Experimental and estimated mobility nyquist plot of the configuration V
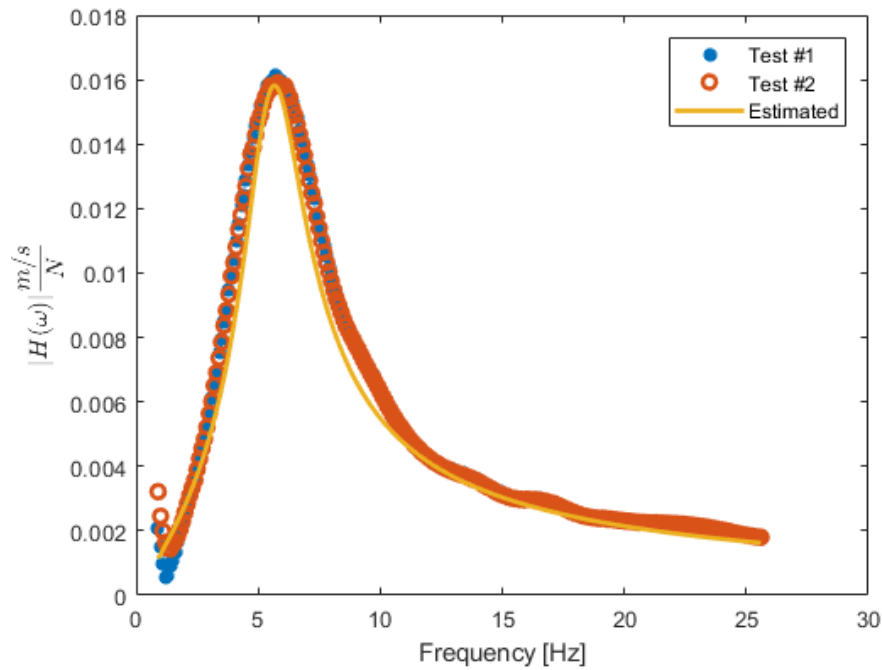
Figure 4.19. Experimental and estimated magnitude mobility frequency response function of the TVA for configuration V

4.4.6. Damping Coefficient Of Configuration VI

In this configuration, distance between each magnet block and copper plate is 1 mm. Estimated damping coefficient of the TVA is given in Table 4.9 and it is accepted that damping coefficient of the configuration VI is 101.59 $\frac{N.s}{m}$. Damping of this configuration is the highest because distance between magnets and copper plate is the closest.

Table 4.9. Estimated damping coefficient of configuration VI

	c $[\frac{N.s}{m}]$
Test #1	103.89
Test #2	99.29

Experimental and estimated nyquist plot and magnitude mobility frequency response function of configuration VI are given in Figure 4.20 and Figure 4.21, respectively.
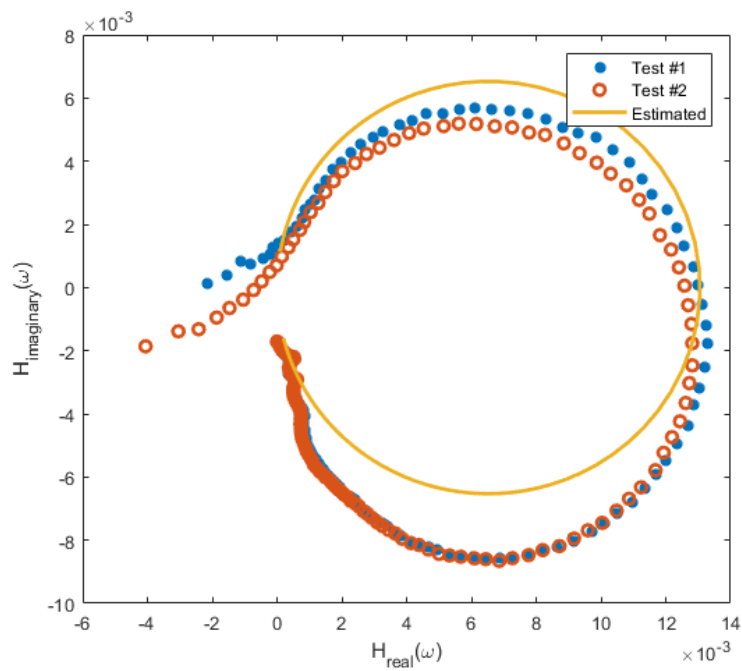
Figure 4.20. Experimental and estimated mobility nyquist plot of the configuration VI
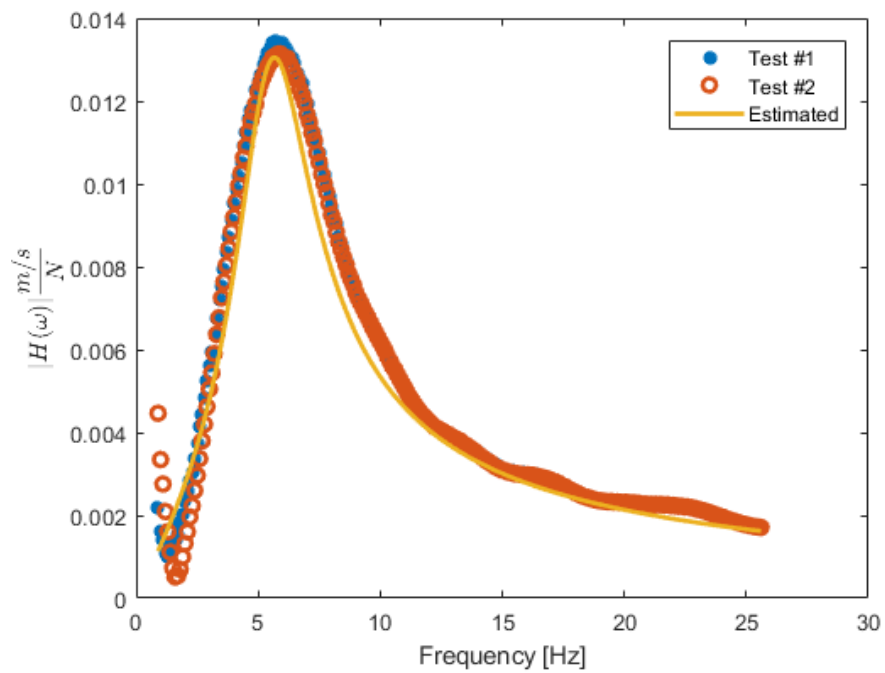

Figure 4.21. Experimental and estimated magnitude mobility frequency response function of the TVA for configuration VI

4.4.7. Damping Coefficient Of Configuration VII

In this configuration, distance between each magnet block and copper plate is 5mm. Estimated damping coefficient of the TVA is given in Table 4.10 and it is accepted that damping coefficient of the configuration VII is 87.03 $\frac{\text{N.s}}{\text{m}}$.

Table 4.10. Estimated damping coefficient of configuration VII

	c $[\frac{\text{N.s}}{\text{m}}]$
Test #1	86.90
Test #2	87.17

Experimental and estimated nyquist plot and magnitude mobility frequency response function of configuration VII are given in Figure 4.22 and Figure 4.23 respectively.
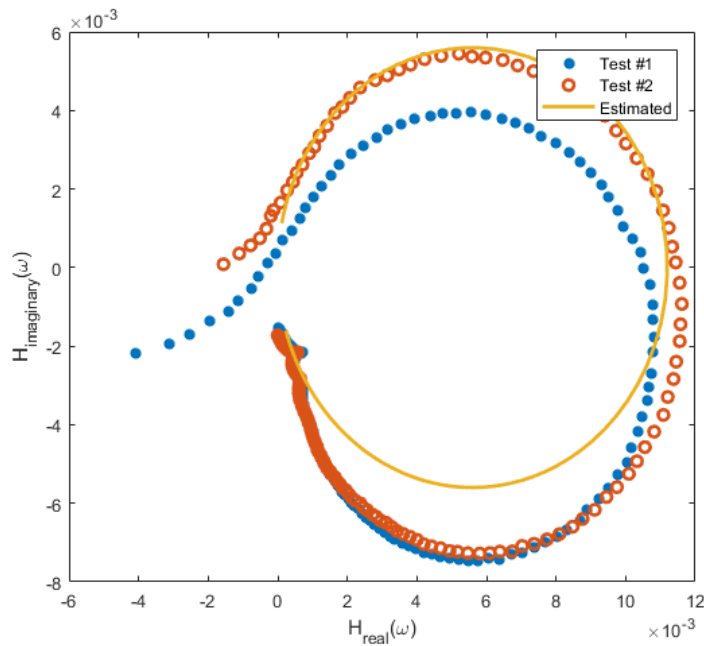

Figure 4.22. Experimental and estimated mobility nyquist plot of the configuration VII

Figure 4.23. Experimental and estimated magnitude mobility frequency response function of the TVA for configuration VII

4.4.8. Damping Coefficient Of Configuration VIII

In this configuration, distance between each magnet block and copper plate is 4 mm. Estimated damping coefficient of the TVA is given in Table 4.11 and it is accepted that damping coefficient of the configuration VIII is $99.36 \frac{N.s}{m}$.

Table 4.11. Estimated damping coefficient of configuration VIII

	c $[\frac{N.s}{m}]$
Test #1	100.24
Test #2	98.48

Experimental and estimated nyquist plot and magnitude mobility frequency response function of configuration VIII are given in Figure 4.24 and Figure 4.25, respectively.

112

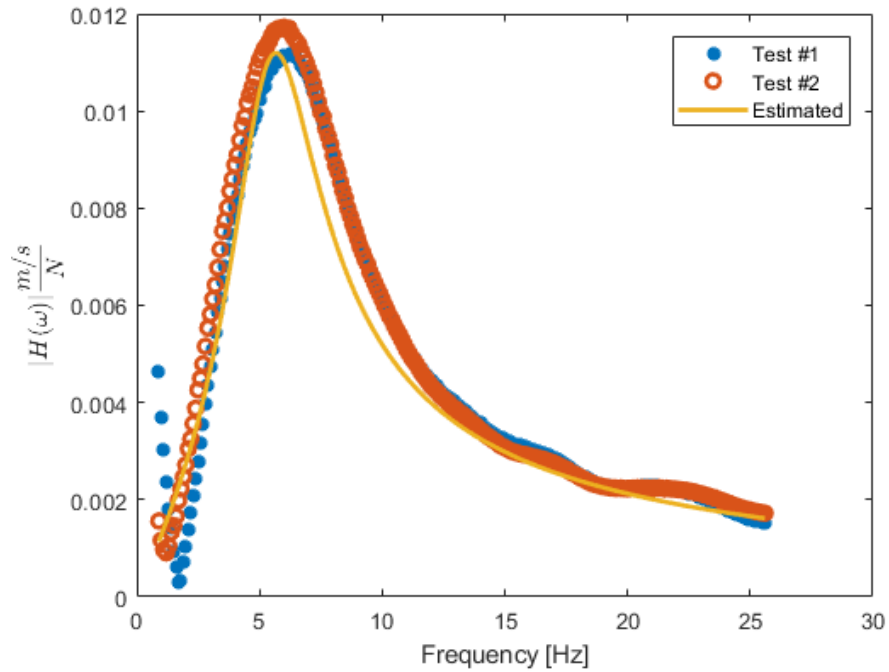Figure 4.24. Experimental and estimated mobility nyquist plot of the configuration VIII

Figure 4.25. Experimental and estimated magnitude mobility frequency response function of the TVA for configuration VIII

4.4.9. Damping Coefficient Of Configuration IX

In this configuration, distance between each magnet block and copper plate is 3mm. Estimated damping coefficient of the TVA is given in Table 4.12 and it is accepted that damping coefficient of the configuration IX is $117.87 \frac{N.s}{m}$.

Table 4.12. Estimated damping coefficient of configuration IX

	$c \ [\frac{N.s}{m}]$
Test #1	119.47
Test #2	116.28

Experimental and estimated nyquist plot and magnitude mobility frequency response function of configuration XI are given in Figure 4.26 and Figure 4.27, respectively.
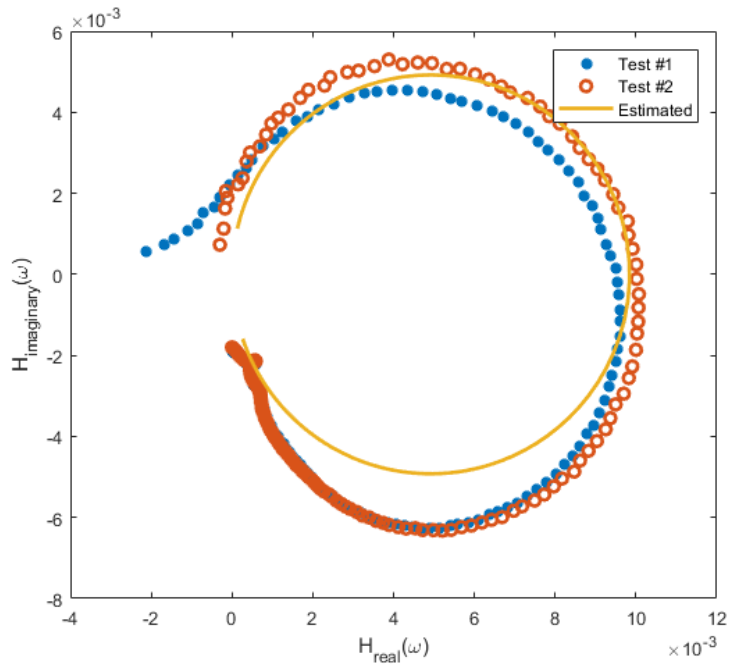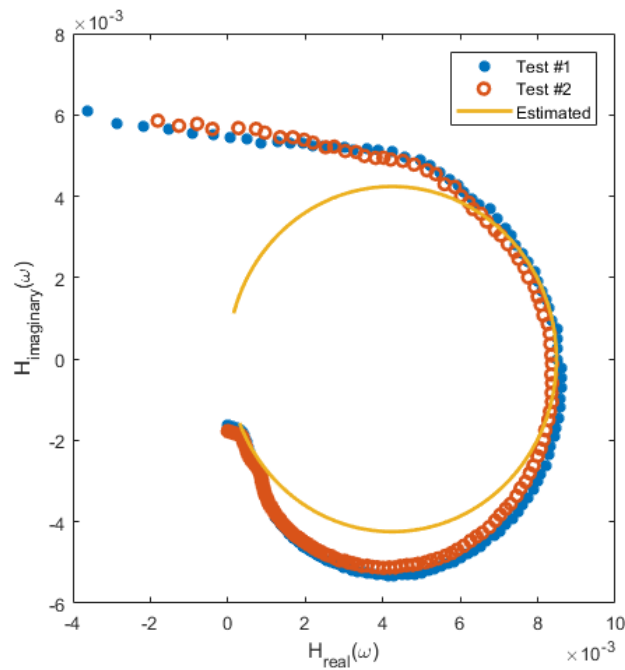

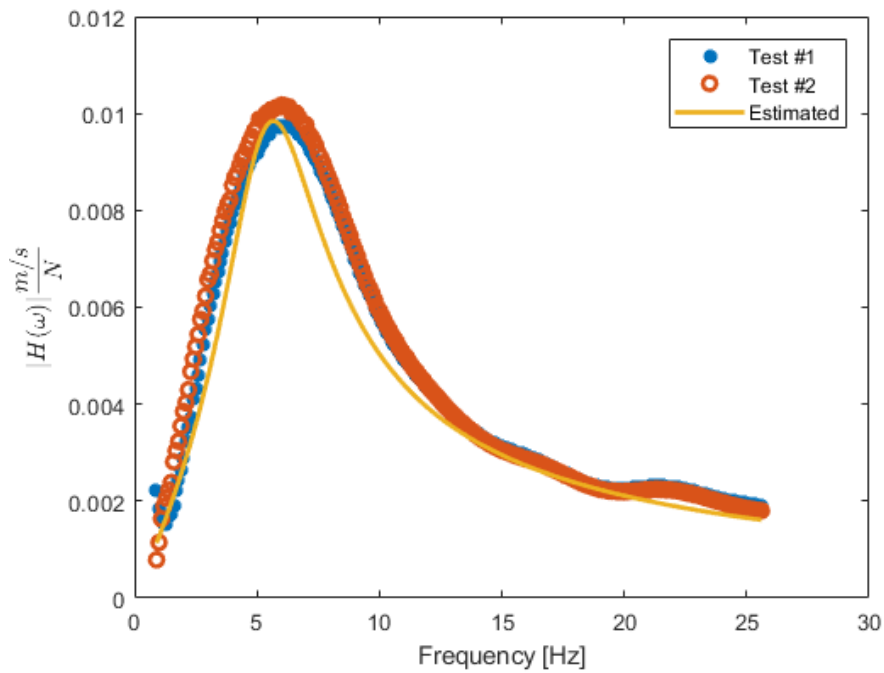Figure 4.26. Experimental and estimated mobility nyquist plot of the configuration IX
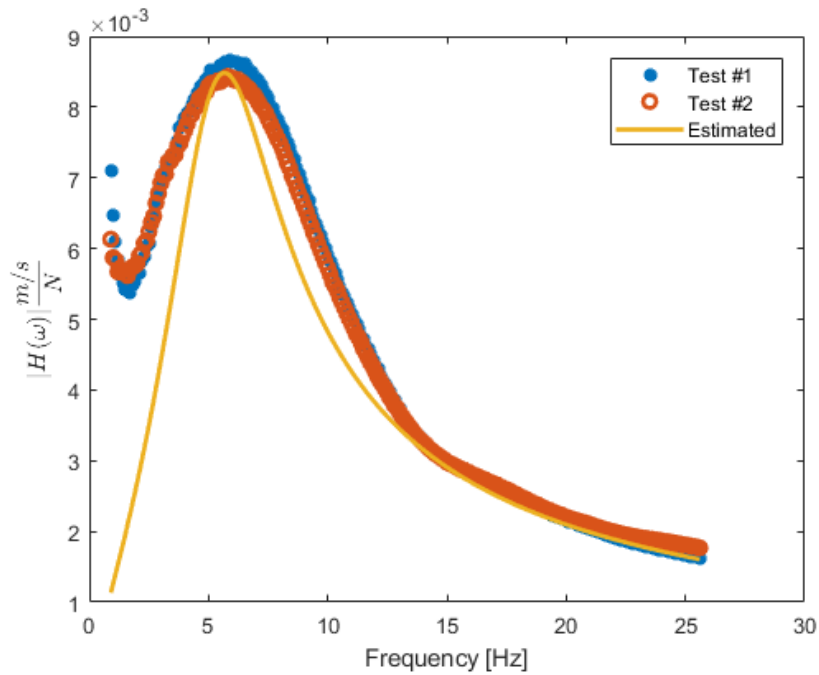
Figure 4.27. Experimental and estimated magnitude mobility frequency response function of the TVA for configuration IX

4.4.10. Damping Coefficient Of Configuration X

In this configuration, distance between each magnet block and copper plates is 2 mm. Estimated damping coefficient of the TVA is given in Table 4.9 and it is accepted that damping coefficient of the configuration X is $136.47\frac{\text{N.s}}{\text{m}}$.

Table 4.13. Estimated damping coefficient of configuration X

	c $[\frac{\text{N.s}}{\text{m}}]$
Test #1	139.45
Test #2	133.48

Experimental and estimated nyquist plot and magnitude mobility frequency response function of configuration X are given in Figure 4.28 and Figure 4.29, respectively.
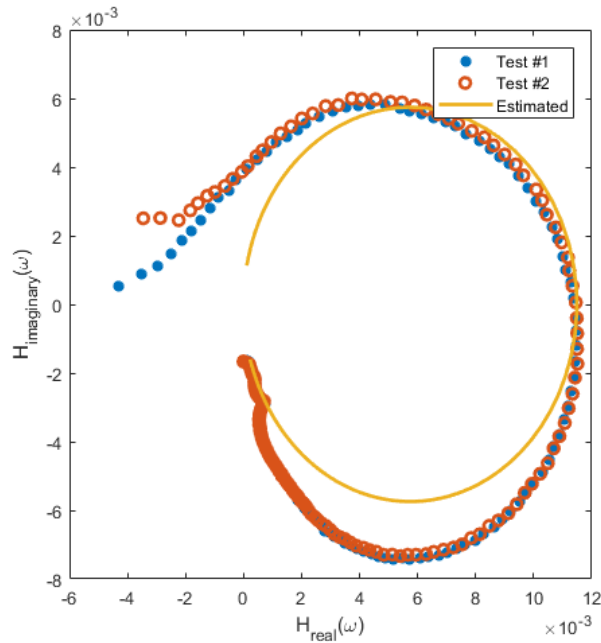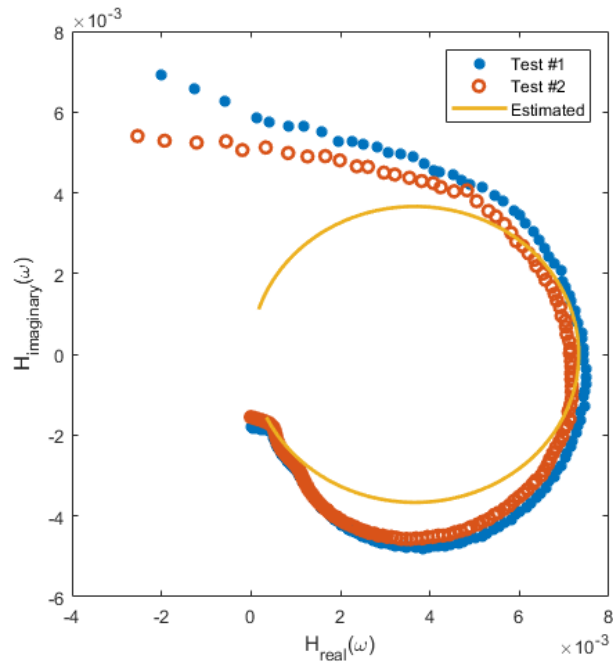
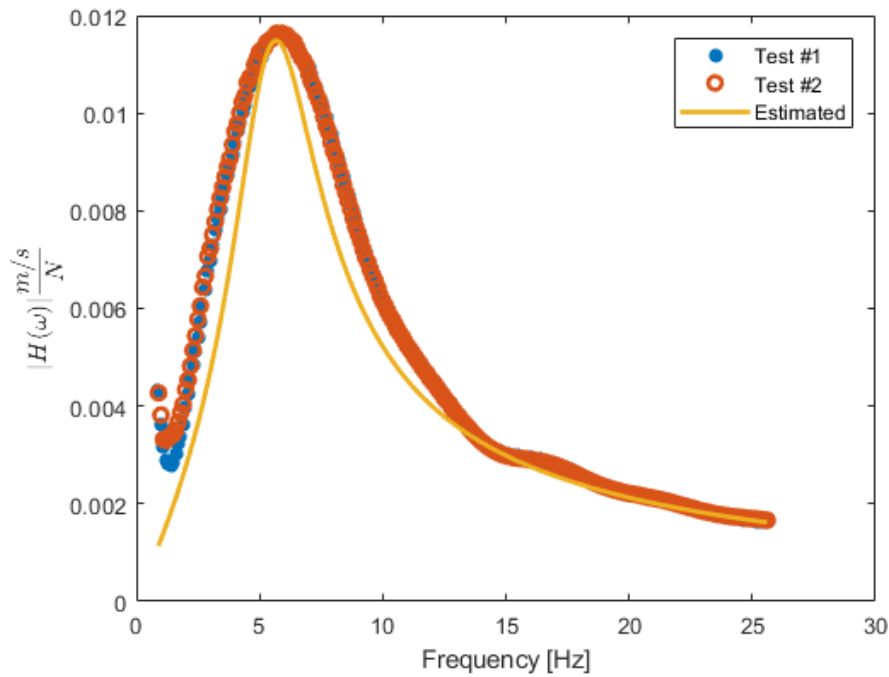Figure 4.28. Experimental and estimated mobility nyquist plot of the configuration X
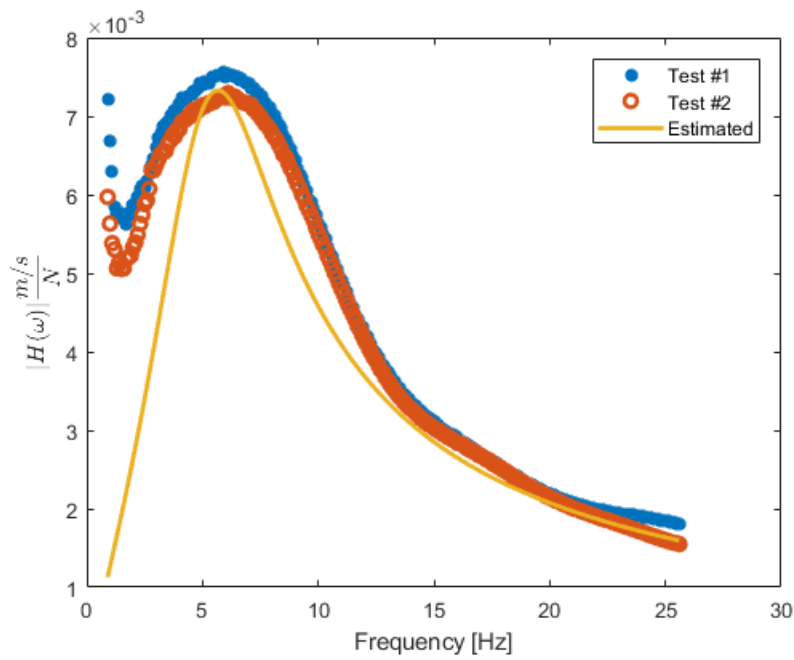
Figure 4.29. Experimental and estimated magnitude mobility frequency response function of the TVA for configuration X

116

4.4.11. Damping Coefficient Of Configuration XI

In this configuration, distance between each magnet block and copper plate is 1 mm. Estimated damping coefficient of the TVA is given in Table 4.9 and it is accepted that damping coefficient of the configuration XI is 162.24 $\frac{N.s}{m}$. Damping of this configuration is the highest because distance between magnets and copper plate is the closest.

Table 4.14. Estimated damping coefficient of configuration XI

	c [$\frac{N.s}{m}$]
Test #1	162.40
Test #2	162.09

Experimental and estimated nyquist plot and magnitude mobility frequency response function of configuration XI are given in Figure 4.30 and Figure 4.31, respectively.
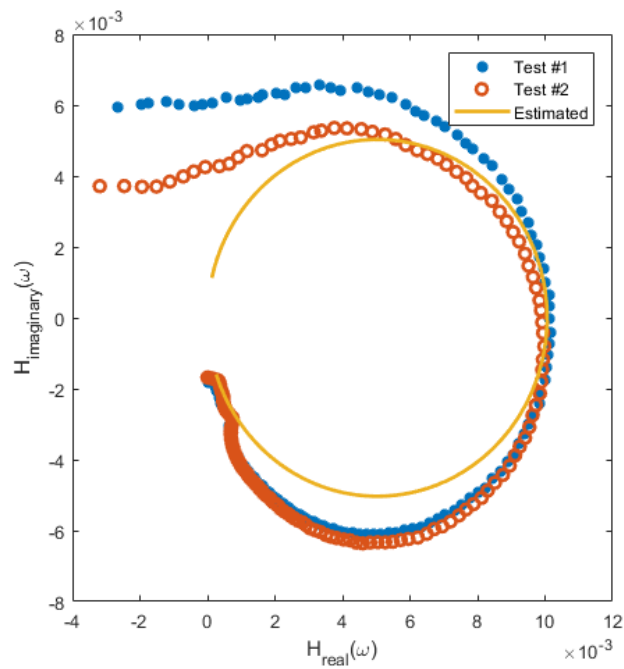

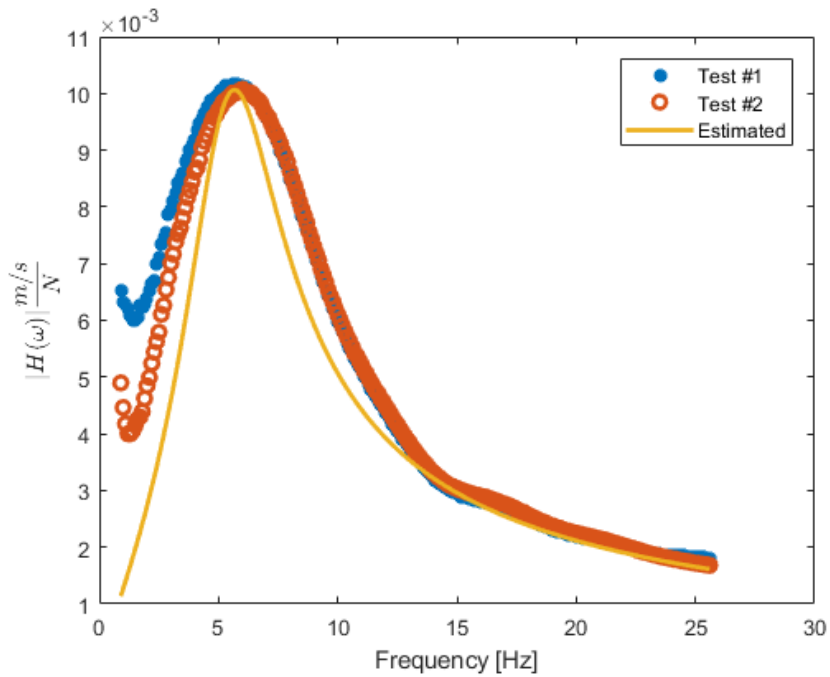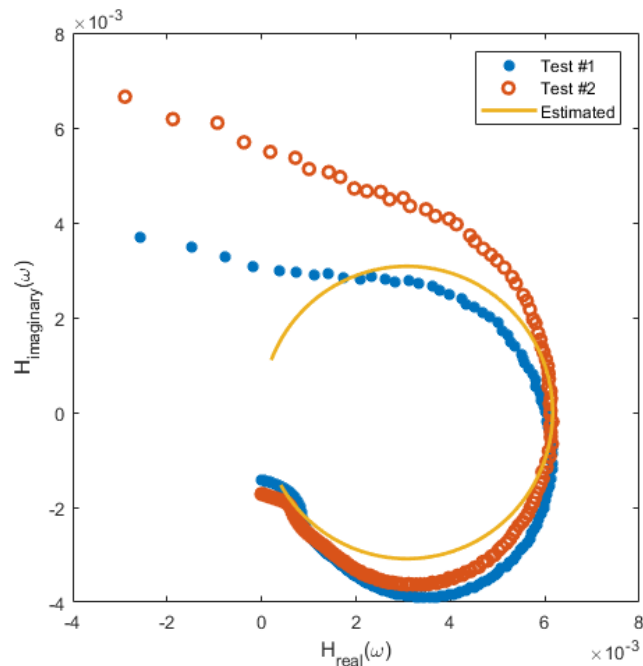Figure 4.30. Experimental and estimated mobility nyquist plot of the configuration XI
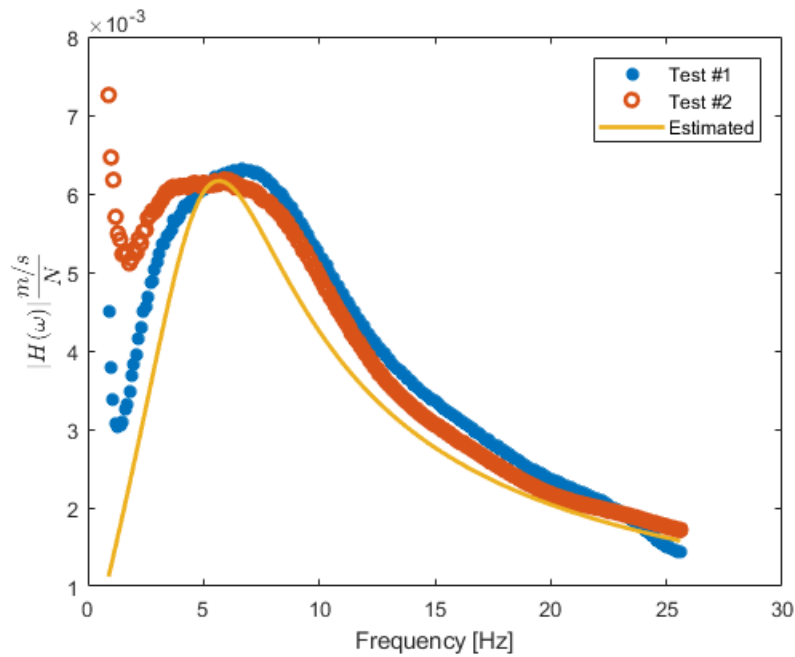
Figure 4.31. Experimental and estimated magnitude mobility frequency response function of the TVA for configuration XI

4.5. Damping Coefficient Of TVA with Different Bearing Types

Friction coefficient of the bearings are not given in their catalogs. To see bearing effect to damping level of the TVA, measurement is repeated for different bearing configuration of Configuration I. These are as follows

- Two ball bearings
- Two plain bearings
- Four plain bearings

Damping level of these cases are estimated as mentioned above, they are given in Table 4.15.

118

Table 4.15. Damping coefficient of the TVA for different bearings

	c $[\frac{N.s}{m}]$
Two ball bearings	5.67
Two plain bearings	12.27
Four plain bearings	24.86

These given damping level show amount of the friction between bearings and rods. As expected, damping level of TVA with ball bearing is the lowest because ball of bearing rotates on the rod. Damping coefficient of four plain bearings are two times more than that of two plain bearings.

4.6. Summary Of Experimental Results

Damping coefficient of the TVA for all configurations obtained via experimental study are given in Table 4.16. For configuration I, damping coefficient is 12.3 $\frac{N.s}{m}$. There is no magnet in this configuration so friction between bearings and rods leads this damping.

Table 4.16. Total damping coefficients of the TVA

Configuration	c $[\frac{N.s}{m}]$	Configuration	c $[\frac{N.s}{m}]$
I	12.3		
II	56.2	VII	87.0
III	63.2	VIII	99.4
IV	76.6	IX	117.9
V	89.3	X	136.5
VI	101.6	XI	162.2

Total damping of the TVA comprises eddy current damping, structural damping and damping due to friction between rods and bearings. Total damping coefficient of the TVA for all configurations is given in Table 4.16. Configuration I does not have any magnet so it is assumed that its eddy current damping is zero. All TVA configurations are similar except number of magnets and distance between magnets and copper plates so damping coefficient of configuration I is accepted as reference damping of the TVA. This reference damping level is subtracted from total damping coefficient of the other configurations to evaluate only eddy current damping coefficient of the other configurations. Eddy current damping coefficient of the TVA are given in Table 4.17.

Table 4.17. Eddy current damping coefficient of the TVA

Configuration	$c\ [\frac{N.s}{m}]$	Configuration	$c\ [\frac{N.s}{m}]$
II	43.9	VII	74.7
III	50.9	VIII	87.1
IV	64.3	IX	105.6
V	77	X	124.2
VI	89.3	XI	149.9

As expected, eddy current damping of the TVA increases while distance between copper plates and magnet are getting closer. Damping coefficient of the configuration XI is 149.9 $\frac{N.s}{m}$ and there are two magnet blocks, distance between copper plates and magnet blocks is 1 mm.

Configuration VII has two times more magnets than configuration II but their rate of damping level is smaller than 2. Using two times more magnet does not mean getting two times damping. It is valid for other configurations.

Estimation of damping is conducted via Equation 2.2. Resistivity and volume of the copper are assumed to constant and magnetic flux density is the only variable. For all configuration, estimated damping coefficient is given in Table 3.9.

Both estimated and experimental damping coefficient for configurations II-XI are given in Table 4.18. Damping estimation is conducted with Equation 2.2 and it is assumed that correction coefficient k is 1. Now, correction coefficient k can be calculated with experimental and estimated eddy current damping coefficients. It is calculated for all for configurations and given in the table.

Table 4.18. Experimental and estimated eddy current damping coefficient of the TVA

| | | Damping ratio | | |
	Configuration	Experimental	Estimated	k
One Magnet Block	II	43.9	59	0.74
	III	50.9	63	0.81
	IV	64.3	67	0.96
	V	77	72	1.07
	VI	89.3	77	1.16
Two Magnet Blocks	VII	74.7	163	0.46
	VIII	87.1	174	0.50
	IX	105.6	185	0.57
	X	124.2	197	0.63
	XI	149.9	210	0.71

Manufactured TVA and its properties are given in Figure 4.32 and Table 4.19, respectively. Damping ratio of the TVA is calculated with Equation 3.4. In this equation, experimental natural frequency and realized TVA mass are used to calculate damping ratio of the configurations.
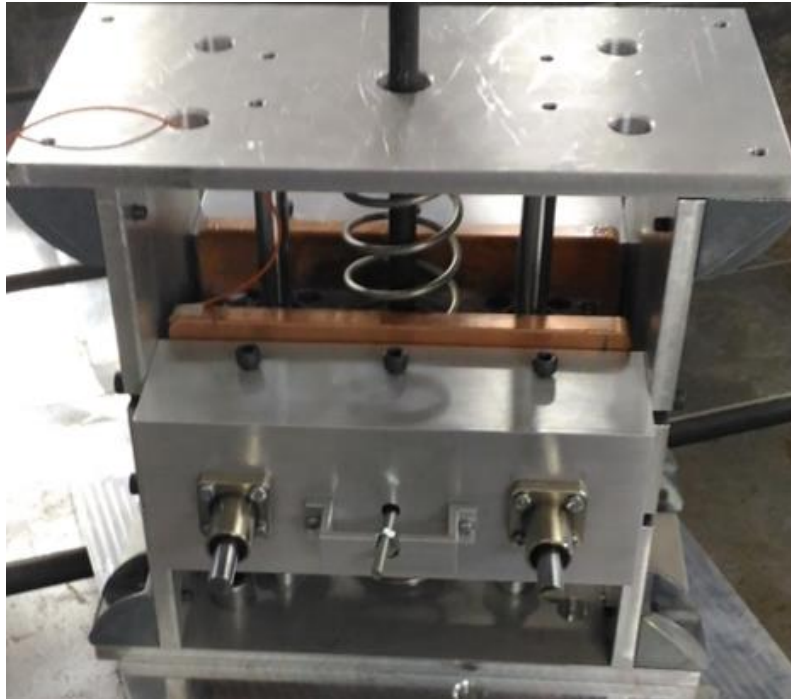
Figure 4.32. Realized TVA

Table 4.19. Specifications of realized TVA

Tuning frequency	5.4 Hz			
TVA Mass	4 kg			
Damping Ratio	Configuration	ζ	Configuration	ζ
	I	0.04		
	II	0.20	VII	0.31
	III	0.23	VIII	0.36
	IV	0.28	IX	0.42
	V	0.32	X	0.49
	VI	0.37	XI	0.58
Dimensions	236mmx123mmx216mm			
Mass	11 kg			
Connection	4 x M12 bolts			
Max. shock	1000g in all direction, half sine, 0.5 ms			
Operation Temperature	Up to 70 °C			
Stroke	30 mm			
Accessories	1-5 mm plate			

CHAPTER 5

CONCLUSION

5.1. Summary

In this study, a passive TVA is designed, manufactured and validated for a tank barrel. A TVA consists of a mass, a spring element and a damping element. Optimum absorber parameters are taken from another study [1]. Type of passive TVA are given in Chapter 2. Details about eddy current damping, spring mounting accessories and linear motion elements are given in same chapter.

Detailed mechanical design process is given in Chapter 3. Tuning frequency depends on TVA mass and properties of spring element. Stiffness and compression length of the spring is the most two important parameters. A design procedure is offered and obtained wire diameter in terms of stiffness and compression length.

Damping level of the TVA is another important parameter. Eddy current damping mechanism is preferred as damping element. Design of eddy current damping element is not straight forward and design step are given here. Damping level of the TVA for all configuration is estimated by conducting magnetic analysis.

Details about other parts of the TVA are given in the same chapter. Several finite element analyses, modal and transient, are conducted to obtained natural frequencies and stress response of TVA under the shock. Finite element result of the TVA under

the defined loads are given lastly. TVA life is also considered to minimum maintance requirement. Fatigue life of TVA is estimated under the defined random vibration.

Tuning frequency of the TVA is directly related with performance. After designed the TVA, shock hammer test is conducted in chapter 4. FRF of TVA is obtained for all configurations. Tuning frequency and damping coefficient are extracted from these FRF. The maximum damping ratio of the TVA is 0.58.

5.2. Future Work

Offered TVA is adjustable which means its damping level can be set with according to customer needs manually. An adjustment mechanism which can change distance between magnets and copper plates can be designed to set damping level of the TVA automatically.

Magnet orientation may change eddy current damping level. In this study all magnet poles are in same direction. A study could be useful with different pole settlement.

Fatigue life of the magnet was not studied in this thesis, fatigue life of magnets can be studied to estimate TVA life.

Validation was performed only by measuring TVA parameters. Structural validation of TVA under defined loads could be performed.

REFERENCES

[1]   Büyükcivelek, F. Analysis and Control of Gun Barrel Vibrations, M.Sc. Thesis, Middle East Technical University, Ankara, Turkey, 2011. http://etd.lib.metu.edu.tr/upload/12613942/index.pdf

[2]   Frahm, H. Device for Damping Vibrations of Bodies, U.S. Patent No. 989958 , 1911.

[3]   Den Hartog, J. P. *Mechanical Vibration*; Dover Publications: New York, 1985.

[4]   Sadek, F.; Mohraz, B.; Taylor, A. W.; Chung, R. M. A Method of Estimating the Parameters of Tuned Mass Dampers for Seismic Applications. *Earthq. Eng. Struct. Dyn.*, 1997, *26*, 617–635. https://doi.org/10.1002/(SICI)1096-9845(199706)26:6<617::AID-EQE664>3.0.CO;2-Z.

[5]   Saidi, I.; Mohammed, a D.; Gad, E. F.; Wilson, J. L.; Haritos, N. Optimum Design for Passive Tuned Mass Dampers Using Viscoelastic Materials. *Aust. Earthq. Eng. Soc. 2007 Conf.*, 2007, 1–8.

[6]   Dayou, J.; Brennan, M. J. Global Controlof Structuralvibration Using Multiple-Tuned Tunable Vibration Neutralizers. *J. Sound Vib.*, 2002, *258*, 345–357. https://doi.org/10.1006/jsvi.5188.

[7]   Tentor L.B., Characterization of an Electromagnetic Tuned Vibration Absorber, Phd Thesis, Virginia Polytechnic Institute and State University, Virgina, USA, 2001.

[8]   Nikooyan, A. A.; Zadpoor, A. A. Mass-Spring-Damper Modelling of the Human Body to Study Running and Hopping-an Overview. *Proc. Inst. Mech. Eng. Part H J. Eng. Med.*, 2011, *225* (12), 1121–1135. https://doi.org/10.1177/0954411911424210.

[9]   Viana, F. A. C.; Kotinda, G. I.; Rade, D. A.; Steffen, V. Tuning Dynamic Vibration Absorbers by Using Ant Colony Optimization. *Comput. Struct.*, 2008, *86*, 1539–1549. https://doi.org/10.1016/j.compstruc.2007.05.009.

[10]   Zuo, L.; Nayfeh, S. a. The Two-Degree-of-Freedom Tuned-Mass Damper for Suppression of Single-Mode Vibration Under Random and Harmonic Excitation. *J. Vib. Acoust.*, 2006, *128* (February), 56. https://doi.org/10.1115/1.2128639.

[11]   Christenson, R. Smart Vibration Absorber For Traffic Signal Supports. U.S. Patent No. 20110193277A1, 2011.

[12]   CSA. (n.d.). Tuned Mass Dampers Datasheet. [Brochure]. USA : Author. Accessed   May   18,   2015,   from

https://www.moog.com/content/dam/moog/literature/Space_Defense/spacelite rature/Vibration_Control/moog-tuned-mass-dampers-m-series-datasheet.pdf

[13]   CSA. (n.d.). Tuned Mass Dampers. [Brochure]. USA.

[14]   Deicon. (n.d.). Viscoelastic Tuned Mass Damper. [Brochure]. USA : Author. Accessed May 12, 2015, from http://www.deicon.com/wp-content/uploads/2014/03/Viscoelastic_TMD.pdf.

[15]   Deicon. (n.d.). Balcony Vibration Control Using Tuned Mass Dampers.[Brochure]. USA : Author. Accessed May 16, 2015, from http://www.deicon.com/wp-content/uploads/2014/03/Viscously_Damped_TMDs.pdf

[16]   Flow Engineering. (n.d.). Tuned Mass Dampers. [Brochure]. USA.

[17]   Fujita. (n.d.). Floor Vibration Control Using Tuned Mass Dampers (TMD). [Brochure]. Japan.

[18]   Gerb. (n.d.). Tuned Mass Dampers for Bridges, Buildings and Other Tall Structures. [Brochure]. USA : Author. Accessed May 20, 2015, from http://www.britec.co.kr/admin/clinic/upload/13-Tuned%20Mass%20Dampers%20for%20Bridges,%20Buildings%20and%20 other%20Tall%20Structures.pdf.

[19]   Maurer Sohne. (n.d.).Tuned Mass and Viscous Dampers. [Brochure]. Germany

[20]   Maurer Sohne. (2011).Maurer Tuned Mass Dampers. [Brochure]. Germany : Author. Accessed April 22, 2017, from https://www.emergo.be/wp-content/uploads/2017/06/maurer_tuned_mass_and_viscous_dampers.pdf.

[21]   Vibratec. (n.d.). Tuned Mass Damper Low Frequency Absorber. [Brochure]. France.

[22]   Leung, a. Y. T.; Zhang, H. Particle Swarm Optimization of Tuned Mass Dampers. *Eng. Struct.*, 2009, *31* (3), 715–728. https://doi.org/10.1016/j.engstruct.2008.11.017.

[23]   Tigli, O. F. Optimum Vibration Absorber (Tuned Mass Damper) Design for Linear Damped Systems Subjected to Random Loads. *J. Sound Vib.*, 2012, *331* (13), 3035–3049. https://doi.org/10.1016/j.jsv.2012.02.017.

[24]   Arfiadi, Y.; Hadi, M. N. S. Optimum Placement and Properties of Tuned Mass Dampers Using Hybrid Genetic Algorithms. *Int. J. Optim. Civ. Eng.*, 2011, *1*, 167–187.

[25]   Dayou, J.; Brennan, M. J. Experimental Verification of the Optimal Tuning of a Tunable Vibration Neutralizer for Global Vibration Control. *Appl. Acoust.*, 2003, *64*, 311–323. https://doi.org/10.1016/S0003-682X(02)00067-1.

[26] Jang, S. J.; Brennan, M. J.; Rustighi, E.; Jung, H. J. A Simple Method for Choosing the Parameters of a Two Degree-of-Freedom Tuned Vibration Absorber. *J. Sound Vib.*, 2012, *331*, 4658–4667. https://doi.org/10.1016/j.jsv.2012.05.020.

[27] Wang, J.; Lin, C.-C.; Lian, C.-H. Two-Stage Optimum Design of Tuned Mass Dampers with Consideration of Stroke. *Struct. Control Heal. Monit.*, 2009, *16* (November 2008), 55–72. https://doi.org/10.1002/stc.312.

[28] Wong, W. O.; Cheung, Y. L. Optimal Design of a Damped Dynamic Vibration Absorber for Vibration Control of Structure Excited by Ground Motion. *Eng. Struct.*, 2008, *30*, 282–286. https://doi.org/10.1016/j.engstruct.2007.03.007.

[29] Gerb. (n.d.). Vibration Control Systems. Vibration Protection for Structures, Buildings, Machinery and Other Equipment with Tuned Mass Dampers. [Brochure]. USA

[30] Sanliturk, K. Y.; Belek, H. T. Design and Implementation of a 2-Dimensional Vibration Absorber on a Pre-Heater Tower at a Cement Factory. In *8th International Congress on Sound and Vibration*; Cheng, C., Ed.; Hong Kong, 2001; pp 2259–2264.

[31] Berşan, A.; Bayık, B.; Çam, E.; Erdoğan, B.; Özcan, A. B.; Güven, C.; Bayız, Y. E.; Erol, F.; Özgen, G. O.; Konukseven, E. İ. Design and Construction of a Tuned Vibration Absorber With Automatically Adjustable Tuning Frequency. In *The 15th International Conference on Machine Design and Production*; Pamukkale, Denizli, Denizli, 2012; pp 1085–1098.

[32] Li, D.; Or, S. W.; Yung, C. S.; Chan, H. L. W.; Choy, P. K.; Liu, P. C. K. A Novel Tunable Mass Damper Based on Giant Magnetostrictive Composite and Piezoelectric Ceramic. In *SPIE*; 2005; Vol. 5760, pp 501–509. https://doi.org/10.1117/12.599566.

[33] Bonsel, J. H. Application of a Dynamic Vibration Absorber to a Piecewise Linear Beam System, M.Sc. Thesis, Eindhoven University of Technology, Eindhoven, Netherlands, 2003.

[34] Hao, K. Y.; Mei, L. X.; Ripin, Z. M. Tuned Vibration Absorber for Suppression of Hand-Arm Vibration in Electric Grass Trimmer. *Int. J. Ind. Ergon.*, **2011**, *41* (5), 494–508. https://doi.org/10.1016/j.ergon.2011.05.005.

[35] Kielb, R. E.; Gavin, H. P.; Dillenbeck, C. J. Tuned Vibration Absorbers : Analysis , Visualization , Experimentation , and Design. 2005, pp 1–10.

[36] Brennan, M. J.; Bonello, P.; Rustighi, E.; Mace, B. R.; Elliott, S. J. Designs of Variable Stiffness Element for a Tunable Vibration Absorber. In *International Congresses on Acoustics*; Kyoto, 2004; pp 2915–2918.

[37] Nashif, A. D.; Jones, D. I. G.; Henderson, J. P. *Vibration Damping*; New York,

1985.

[38] Williams, K.; Chiu, G.; Bernhard, R. Passive-Adaptive Vibration Absorbers Using Shape Memory Alloys. In *Part of the SPIE Conference on Smart Structures and Integrated Systems*; 1999; Vol. 3668, pp 630–641.

[39] Brzeski, P.; Pavlovskaia, E.; Kapitaniak, T.; Perlikowski, P. The Application of Inerter in Tuned Mass Absorber. *Int. J. Non. Linear. Mech.*, 2015, *70*, 20–29. https://doi.org/10.1016/j.ijnonlinmec.2014.10.013.

[40] Bae, J. S.; Hwang, J. H.; Roh, J. H.; Kim, J. H.; Yi, M. S.; Lim, J. H. Vibration Suppression of a Cantilever Beam Using Magnetically Tuned-Mass-Damper. *J. Sound Vib.*, 2012, *331* (26), 5669–5684. https://doi.org/10.1016/j.jsv.2012.07.020.

[41] Chen, W.; Jiang, J.; Liu, J.; Bai, S.; Chen, W. A Passive Eddy Current Damper for Vibration Suppression of a Force Sensor. *J. Phys. D. Appl. Phys.*, 2013, *46*, 075001. https://doi.org/10.1088/0022-3727/46/7/075001.

[42] Ebrahimi, B.; Khamesee, M. B.; Golnaraghi, F. A Novel Eddy Current Damper: Theory and Experiment. *J. Phys. D. Appl. Phys.*, **2009**, *42* (7), 075001. https://doi.org/10.1088/0022-3727/42/7/075001.

[43] Sodano, H. A. Development of Novel Eddy Current Dampers for the Suppression of Structural Vibrations. Phd Thesis. Virginia Polytech. Inst. State Univ., Virgina, USA, 2005.

[44] Sze Kwan Cheah; Sodano, H. a. Novel Eddy Current Damping Mechanism for Passive Magnetic Bearings. *J. Vib. Control*, 2008, *14* (11), 1749–1766. https://doi.org/10.1177/1077546308091219.

[45] Airport. (n.d.). Stock Dashpot. [Brochure]. USA Author. Accessed Nov 22, 2015, from http://www.airpot.com/stock-dashpot-model-p-12-l-en.html.

[46] Schieber, D. Optimal Dimensions of Rectangular Electromagnet for Braking Purposes. *IEEE Trans. Magn.*, 1975, *MAG-11* (3), 948–952.

[47] Cunningham, R. E. Passive Eddy-Current Damping as a Means of Vibration Control in Cryogenic Turbomachinery. NASA Technical Paper 1986.

[48] van Beek, T.; Jansen, H.; Pluk, K.; Lomonova, E. Optimisation and Measurement of Eddy Current Damping in a Passive Tuned Mass Damper. *IET Electr. Power Appl.*, 2016, *10* (7), 641–648. https://doi.org/10.1049/iet-epa.2015.0445.

[49] Huang, Z. W.; Hua, X. G.; Chen, Z. Q.; Niu, H. W. Modeling, Testing, and Validation of an Eddy Current Damper for Structural Vibration Control. *J. Aerosp. Eng.*, 2018, *31* (5), 04018063. https://doi.org/10.1061/(asce)as.1943-5525.0000891.

[50] Tian, H.; Denghong, X.; Xiandong, L.; Yingchun, S. Design and Analysis of a Novel Eddy Current Damper Based on Three-Dimensional Transient Analysis. *J. Vibroengineering*, 2013, *15* (1), 46–64.

[51] Kienholz, D. A.; Pendleton, S. C.; Richards, K. E.; Morgenthaler, D. R. Demonstration of Solar Array Vibration Suppression. In *SPIE*; 1994; pp 59–72.

[52] Pan, Q.; He, T.; Xiao, D.; Liu, X. Design and Damping Analysis of a New Eddy Current Damper for Aerospace Applications. *Lat. Am. J. Solids Struct.*, 2016, *13* (11), 1997–2011. https://doi.org/10.1590/1679-78252272.

[53] Lian, J.; Zhao, Y.; Lian, C.; Wang, H.; Dong, X.; Jiang, Q.; Zhou, H.; Jiang, J. Application of an Eddy Current-Tuned Mass Damper to Vibration Mitigation of Offshore Wind Turbines. *Energies*, 2018, *11* (12). https://doi.org/10.3390/en11123319.

[54] Shi, W.; Wang, L.; Lu, Z.; Gao, H. Study on Adaptive-Passive and Semi-Active Eddy Current Tuned Mass Damper with Variable Damping. *Sustain.*, **2018**, *10* (1), 1–19. https://doi.org/10.3390/su10010099.

[55] Bae, J. S.; Hwang, J. H.; Kwag, D. G.; Park, J.; Inman, D. J. Vibration Suppression of a Large Beam Structure Using Tuned Mass Damper and Eddy Current Damping. *Shock Vib.*, 2014, *2014*. https://doi.org/10.1155/2014/893914.

[56] Chen, F.; Zhao, H. Design of Eddy Current Dampers for Vibration Suppression in Robotic Milling. *Adv. Mech. Eng.*, 2018, *10* (11), 1–15. https://doi.org/10.1177/1687814018814075.

[57] Guo, T.; Li, B.; Zhang, S.; Xu, Y. Using Eddy-Current Vibration Absorbers to Design Locally Resonant Periodic Structures. *J. Appl. Phys.*, 2019, *125* (23). https://doi.org/10.1063/1.5080964.

[58] Ruber, K.; Kanapathipillai, S.; Randall, R. Investigations of Eddy Current Vibration Damping. In *43rd International Congress on Noise Control Engineering*; 2014; pp 1–14.

[59] Sodano, H. A.; Bae, J. S.; Inman, D. J.; Keith Belvin, W. Concept and Model of Eddy Current Damper for Vibration Suppression of a Beam. *J. Sound Vib.*, 2005, *288* (4–5), 1177–1196. https://doi.org/10.1016/j.jsv.2005.01.016.

[60] Bae, J. S.; Hwang, J. H.; Park, J. S.; Kwag, D. G. Modeling and Experiments on Eddy Current Damping Caused by a Permanent Magnet in a Conductive Tube. *J. Mech. Sci. Technol.*, 2010, *23* (11), 3024–3035. https://doi.org/10.1007/s12206-009-0819-0.

[61] Zhihao, W.; Zhengqing, C.; Jianhui, W.; Wang, Z.; Chen, Z.; Wang, J. Feasibility Study of a Large-Scale Tuned Mass Damper with Eddy Current

Damping Mechanism. *Earthq. Eng. Eng. Vib.*, 2012, *11* (3), 391–401.

[62]   Anonymous, (n.d.). Resistivities for common metals. Accessed Dec 9, 2015. http://www.cleanroom.byu.edu/Resistivities

[63]   CDA InterCorp. InterCorp Engineering: Eddy Current Damper Application Data. [Brochure]. USA. Author. Accessed June 5, 2014. from http://www.cda-intercorp.com/PDF/Eddy%20Current%20Damper%20Application%20Data.pdf

[64]   Deicon. (2015). Air Suspended Tuned Mass Damper. [Brochure]. USA

[65]   Anonymous, (n.d.). Steel Holder Accessed Dec 9, 2015. Accessed Oct 12, 2015. http://www.starlineenterprises.in/cased-spring-mount.htm

[66]   Anonymous, (n.d.). Spring Retainer Accessed Dec 9, 2015. Accessed Oct 20, 2015. http://www.racingsprings.com/Beehive-600-Series/sku/165#.

[67]   Anonymous, (n.d.). Spring Adapter Accessed Dec 9, 2015. Accessed Oct 21, 2015. http://www.nolimitmotorsport.com/ferrea/seat-locators.html.

[68]   Robert O. Parmley. *Machine Devices and Components Illustrated Sourcebook*; McGraw-Hill: New York, 2005.

[69]   Anonymous, (n.d.). Bushings . Accessed Oct 12, 2015. http://bearing-solutions.isostatic.com/category/tal-bronze-sae841-flange-bearings-metric-1.

[70]   Anonymous, (n.d.). Selecting Bronze Bearing Materials. Accessed Nov 20, 2015. http://www.copper.org/applications/industrial/bronze_bearing.html.

[71]   Anonymous, (n.d.). Linear Bearing. Accessed Oct 12, 2015. http://www.pbclinear.com.

[72]   Anonymous, (n.d.). SIMO Series Components - GST. Accessed Oct 12, 2015. http://www.pbclinear.com/SIMO-Series-Components---GST?tab=Specifications.

[73]   Anonymous, (n.d.). PBC. Square Bearings and Linear Rails.

[74]   Anonymous, (n.d.). Magnetics, K. Neodymium Magnet Physical Properties Accessed Dec 26, 2016. https://www.kjmagnetics.com/specs.asp

[75]   Lalanne, C. *Mechanical Vibration and Shock Analysis: Mechanical Shock*, 2nd ed.; Wiley & Sons, Inc., 2009.

[76]   SAE Spring Committee. *Spring Design Manual*; Society of Automotive Engineers, 1990.

[77]   Carlson, H. *Spring Designer's Handbook*; L.L. Faulkner, Ed.; Marcel Dekker, Inc.: Ohio.

[78] Brown, A. A. D. *Mechanical Springs / A.A.D. Brown on Behalf of the Spring Research and Manufacturers' Association*; Published for the Design Council, the British Standards Institution, and the Council of Engineering Institutions by Oxford University Press, 1981.

[79] Shigley, J. E.; Mischke, C. R.; Budynas, R. G. *Mechanical Engineering Design*; McGraw-Hill, 2002; Vol. New York,.

[80] Anonymous, (n.d.). Springs Accessed Jun 5, 2015. http://www.learneasy.info/MDME/MEMmods/MEM30009A/lifting_systems/Univ_of_WA.htm.

[81] Anonymous, (n.d.). General Wire Spring Company. Stainless Spring Wire Springs Accessed Aug 7, 2016. https://www.generalwirespring.com/stainless-steel-wire-springs.html.

[82] ASTM A313/A313M-13. *Standard Specification for Stainless Stell Spring Wire*.

[83] Anonymous, (n.d.). Bunting Magnetics Europe Ltd. Characteristics of NdFeB Magnets Accessed Jun 3, 2019. https://e-magnetsuk.com/neodymium_magnets/characteristics.aspx.

[84] Anonymous, (n.d.). Neodymium magnet. Accessed Jun 3, 2019. https://en.wikipedia.org/wiki/Neodymium_magnet

[85] Anonymous, (n.d.). Silver Contract. Accessed May 19, 2019. https://www.investing.com/commodities/silver.

[86] Anonymous, (n.d.). Copper Contract. Accessed May 19, 2019. https://www.investing.com/commodities/copper

[87] Advanced Spring Design User's Manual. Spring Manufactureres Institure. Illinois, USA

[88] Chopra, A. K. *Dynamics of Structure Theory and Applications to Earthquake Engineering*, Third.; Pearson: New Jersey, 2007.

[89] Anonymous, (n.d.). Aluminum 7075-T6; 7075-T651. Accessed May 10, 2019. http://asm.matweb.com/search/SpecificMaterial.asp?bassnum=MA7075T6.

[90] Anonymous, (n.d.). Copper, Cu; Annealed. Accessed May 10, 2019. http://matweb.com/search/datasheet_print.aspx?matguid=9aebe83845c04c1db5126fada6f76f7e

[91] Anonymous, (n.d.). AISI 4140 Steel, oil quenched, 13 mm (0.5 in.) round [845°C (1550°F) quench, 540°C (1000°F) temper]. Accessed May 10, 2019. http://www.matweb.com/search/datasheet.aspx?matguid=423b97220479413cbecf2143727e8b3b&ckck=1.

[92] Customer Training Material Introduction to ANSYS NCode DesignLife (2012). Ansys Inc. PA, USA.

[93] Bishop N. W. M. The Use of Frequency Domain Parameters to Predict Structural Fatigue. Phd Thesis, University of Warwick, Warwick, UK, 1988.

[94] Rice, S. O. Mathematical Analysis of Random Noise. *Bell Syst. Tech. J.*, 1944, *23* (3), 282–332. https://doi.org/10.1002/j.1538-7305.1944.tb00874.x.

[95] Dirlik, T. Application of Computers in Fatigue Analysis. Phd Thesis, University of Warwick, Warwick, UK, 1985.

[96] He, J.; Fu, Z.-F. 2001. *Modal Analysis*; Betterworth Heinemann: Oxford.